Revised: 08_30_02

Chapter 6. A Qualitative Theory of Molecular Organic Photochemistry

6.1 A Qualitative Theory of Organic Photoreactions

Scheme 6.1 shows the global paradigm for organic photochemical reactions that has been employed in earlier chapters and which, together with state energy diagrams, is the starting point for the global analysis of all organic photochemical reactions. Chapters 2 and 3 described theories consisting of conceptual tools and methods required to develop state energy diagrams and to qualitatively express and visualize ***photophysical*** radiative (R + hν ⇔ *R) and radiationless (*R ⇔ R) transitions in terms of electronic configurations, nuclear configurations and spin configurations. Chapters 4 and 5 presented examples of experimental data which could be interpreted in terms of the state energy diagram. In this Chapter we are concerned with extending the state energy diagram and in developing a theory consisting of conceptual tools and methods required to qualitatively express and visualize the two types of ***primary photochemical*** processes (*R→ I and *R → P). A third type of primary photochemical process, *R → *P, converts the excited state of the reactant (R) to an excited state of the product **(**P). This process is rare, but known and is not considered explicitly for simplicity. The primary photochemical process *R→ I involves the conversion of the electronically excited state *R into a conventional reactive organic intermediate, I. In general , I can be trapped and can be detected directly by spectroscopic methods. The primary photochemical process *R → P does not involve a conventional reactive organic intermediate and is not concerted in the sense that the reactant is an excited state and the product is a ground state. What are the typical reactive intermediates formed in the *R→ I process and how do we describe the structural changes occurring in the *R→ P process?

Examination of a wide range of organic reactions have revealed that typically *R = S_1 or T_1 (lowest energy excited singlet or lowest energy triple, Kasha's rule) and that I = D or Z (a diradical like or zwitterions like reactive intermediate, Salem's rule). According to theory, the "direct" process *R → P does not involve a traditional reactive organic intermediate, but instead involves a "funnel" that takes *R to P. Current theory indicates that such funnels may be characterized as "avoided crossings" or "conical intersections", which are not familiar structures to organic chemists and therefore will be considered in some detail in this chapter.

The conceptual tools and methods we shall use require the extension of the ***two dimensional energy curves*** which have been used in earlier chapter to ***three dimensional energy surfaces*** which describe the *R→ I and *R → P processes.

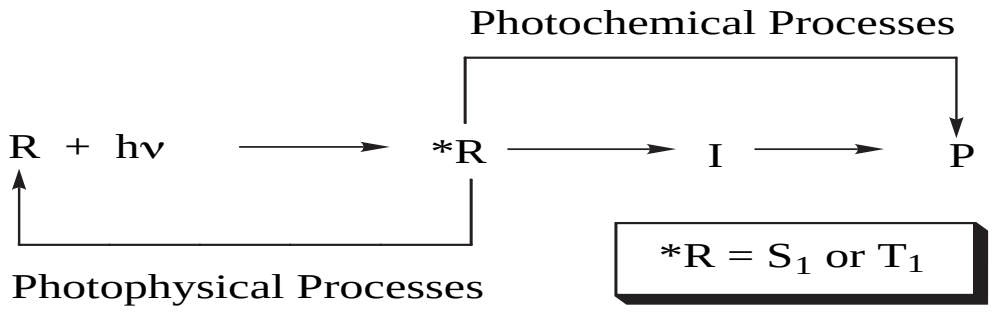

Scheme 6.1. A global paradigm for organic photophysical and photochemical processes.

Towards a General Theory of Organic Photochemical Reactions

A general theory of molecular organic photochemistry is concerned with qualitative and quantitative description of the two key primary photochemical processes *R → I, *R → P of the global paradigm. These two processes involve equilibrium structures, transition structures, barriers and funnels on the excited surface and the barriers on the ground surface associated with the geometry changes associated with the overall photochemical structural changes. Ideally, we such a theory will allow us to visualize the structural and energetic details of the two reaction pathways and how to a priori or a postiori deduce the connections all along the entire photochemical reaction pathway, "from cradle to grave". In addition, the theory should be able to account in a natural way for the photophysical radiationless processes that occur from *R to R, which compete with the primary photochemical processes. There should be no fundamental difference between the way the theory treats radiationless photophysical and photochemical processes since both involve pathways that start on an electronically excited surface and terminate on a ground state surface.

To the organic photochemist, a good theory deals is not only capable of dealing with structural and energetic issues of photochemical reactions, but also is capable of producing simple qualitative exemplars that serve as a starting point for rationalizing the results a spectrum of related reactions. These exemplars will provide a fundamental global understanding and will permit easy visualization of the results of theory. This visualization of the complex set of plausible structures and transitions which occur in an organic photochemical reaction can be achieved through an extension of the ideas of the simple and intuitive two dimensional potential energy curves which served as the basis for understanding the photophysical processes R + hν → *R and *R → R (+ Δ or hν) described in the previous chapters. These energy curves were discussed in terms of an initial (equilibrium) nuclear geometry for R using the exemplar of the behavior of potential energy of a diatomic molecule as a function of the internuclear separation of the atoms of the molecule. For the transitions R + hν → *R and *R → R (+ Δ or hν) the equilibrium geometry of the electronically excited state(s), *R (S_1 and T_1), were considered to be similar to those of the equilibrated ground state, R. It is the fundamental nature of photochemical ***reactions*** that the representative point characterizing the time dependent nuclear geometry of *R will undergo a significant change as it proceeds along an excited (or ground) state surface on the way to I or P. The molecular geometry of the products are different from the molecular geometries of the reactants. We therefore seek in our theory of photochemical reactions an energy surface description of tracking the nuclear geometry changes which occur on the way from *R → I or *R → P. We note that the important energy changes and the positions of maxima and minima during reaction are automatically handled by the fact we are dealing with potential energy ***surfaces*** and not potential energy ***curves***. We need to determine the correspondence between the structural changes that we would consider for a photochemical transformation and how these structural changes are controlled by the electronic energy surfaces.

A theoretical treatment of photophysical (*R → R) and photochemical (*R → I and *R → P) processes requires knowledge of potential energy surfaces of both the ground state and of relevant excited states (starting from S_1 and T_1) and the manner in which these surfaces control the nuclear motion of the system during the radiationless process from *R to I or P. In this Chapter we present a qualitative theory of photochemical reactions based on simple concepts of ***frontier molecular orbital interactions*** which initiate primary photochemical processes and which trigger transitions between electronic states and ***molecular orbital correlation diagrams*** which follow molecular orbitals from the initial to final state of a photochemical reaction. These concepts are then employed to construct a more realistic ***molecular state correlation diagrams*** which describe the electronic pathway of the initial state to the final state. Employing frontier molecular orbital interactions, systems will be described which provide a useful and intuitively pleasing basis for developing and discussing a set of exemplar plausible primary photochemical reactions of the two most important electronic configurations in organic photochemistry, the n,π* and π,π* configurations. It should be noted at this point that the ***secondary*** "thermal" reactions I → P are not a direct concern of a theory of photochemical reactions because the I → P process involves the reaction(s) of ***ground state reactive intermediates***, I. However, the same orbital concepts apply to the secondary processes.

Our qualitative theory of photoreactions will seek and provide useful answers to the two important questions: (a) What are the *plausible* intermediates, I of a primary photoreaction which starts from a particular electronic state, *R? (b) what are the *plausible* pathways that are followed during the primary photochemical reactions *R → I or *R → P? In particular, since the typical reactive intermediate, I, produced in a primary photochemical reaction is a diradical like or zwitterions like species, knowledge of the theory of radical reactivity is crucial for a complete understanding of photochemical reactions. It is assumed that the reader has some familiarity with radical chemistry, but brief discussions and reviews of radical chemistry will be given where appropriate and references to further reading of the review and primary literature will be provided. A more detailed discussion of radical chemistry will be presented in Chapter 8, where the theoretical aspects of photochemical reaction mechanism are connected to experimental observations.

In providing answers to questions of plausibility of intermediates and pathways, we will seek to visualize the energy surfaces which connect the starting molecular structures (*R) to the possible final molecular structures (reactive intermediates, I, and stable products, P). Visualization of these energy surfaces, provides as maps or networks of geometric structures and pathways which would allow us to immediately recognize the following important nuclear geometries involved in organic photoreactions:

1. The plausible nuclear geometries for the ***energy barriers*** on the excited and ground surfaces which must be overcome in proceeding from *R → I or *R → P.

2. The plausible nuclear geometries associated with ***energy minima*** on the excited and ground surfaces which serve as ***funnels*** for the photochemical processes *R → I or *R → P, i.e., which bring the system from an excited state surface to a ground state surface.

3. The plausible "critical" nuclear geometries for which excited surfaces come close to other excited state and either "***touch***" or "***intersect***", and for which an excited surface comes close to the ground state and either "touch" or "intersects" the ground state which serve as ***funnels*** for the photochemical processes *R → I or *R → P.

4. The "critical" nuclear geometries for which excited surfaces come close to other excited state or the ground state and "***avoid***" each other to create relatively stable minima on the excited surface which serve as ***funnels*** for the photochemical processes *R → I or *R → P.

For most organic photoreactions in solution we need consider in detail only the S_1, T_1, and S_0 surfaces corresponding to the *R → I or *R → P processes. These surfaces are the natural extension of the state energy diagrams that we have used in Chapters 3, 4 and 5 to examine photophysical processes (where a single nuclear geometry is assumed adequate to describe S_1, T_1, and S_0). The task of a useful theory of photoreactions is to provide procedures for qualitatively predicting the maxima and minima and the critical geometries of the S_0, T_1, and S_1 surfaces since these features of the energy surface determine the rates and probabilities of the *R → I or *R → P processes. Theory should also allow an evaluation of the "***electronic nature***" of minima and maxima on the various surfaces, e.g., whether or not they are the results of surface crossings or avoided crossings.

We shall first review some important features of ***potential energy curves and potential energy surfaces*** and then develop concepts and methods of a theory of photochemical reactions which will assist in the qualitative understanding of the pathway of photochemical reactions. We shall review how ***frontier orbital interactions*** can "trigger" photochemical reactions and provide the lowest energy barriers for the initial pathways from *R towards I or P. We shall then develop general exemplars for two common ***surface touchings*** which result from the ***stretching of σ bonds or the twisting of π bonds***. Then we will develop specific ***surface crossings*** or ***surface avoidings*** which result from orbital and state correlations of exemplar primary photochemical reactions, based on certain reaction symmetries.

6.2 Potential Energy Curves and Potential Energy Surfaces

A molecule in a particular electronic state may exist with various configurations of its nuclei, each configuration in space corresponding to a particular potential energy of the system. For a diatomic molecule the internuclear separation is the only variable describing the nuclear geometry of the system. A plot of the potential energy of the nuclear geometry of a diatomic molecule is a simple two dimensional ***potential energy curve***, i.e. a parabolic curve of a harmonic oscillator (e.g., Figure 2.3, Figure 3.2). For typical organic molecules the instantaneous nuclear geometry is a much more complicated function of the position of the nuclei in space than the potential energy curve. Indeed, the potential energy of an organic molecule as a function of the nuclear geometry is not a simple two dimensional curve but a complex ***multidimensional surface***. A map of the potential energy of an organic molecule versus nuclear configuration for a given electronic state is called a *potential energy surface for that state*.[1]

Although it is not as accurate representation, a two-dimensional energy curve is much more readily visualized than a three dimensional or multidimensional energy surface. However, the simple potential energy curve of a diatomic molecules contains many if not most of the important surface features that are encountered even for complex organic molecules. Thus, we shall use the potential energy curve and seek to modify it appropriately so that it serves as an appropriate approximation of the more realistic potential energy surface. Simplifying assumptions are therefore required. First.g., we can replace the concept of a single internuclear separation of two nuclei with the notion of a single *center of mass which represents the entire nuclear geometry of an organic molecule*. This center of mass replaces the single geometric coordinate, the internuclear separation, as a ***representative point*** that moves along an energy surface with the same characteristics as a single point or (classically) a single particle. The center of mass of a system is known, from elementary physics, to depend only on the masses of the particles of the system and their positions *relative* to one another. Since the relative positions of the atoms in a structure correspond to the nuclear geometry, we see that the center of mass is an appropriate variable to ***represent*** the nuclear geometry.

When a complicated array of bound particles (the nuclei of a molecule) moves under the influence of external forces, ***the center of mass moves in the same way that a single particle subject to the same external forces would move.*** The concept of the center of mass as a representative point allows us to visualize in a simple way an energy trajectory of a complex system of particles executing very complicated motions. The important topological (i.e., qualitative geometric) features of a potential energy curve may be generalized to deduce the topological features of potential energy surfaces. A potential energy curve or three dimensional energy surface serves as a an approximation to the more complex multidimensional energy surface allows a visualization and provides a insight to many problems of importance in molecular organic photochemistry.

In summary, the readily visualizable *potential energy curves* for a diatomic molecule will be extrapolated to visualization of multidimensional *potential energy surfaces*. We have seen in Chapters 4 and 5 how the simple notion of potential energy curves may be used to unify the ideas of structure, energetics, and dynamics of radiative ($R + h\nu \Leftrightarrow R$) and radiationless photophysical ($^*R \Leftrightarrow R$) transitions between states. Now we shall see how potential energy curves and energy surfaces can provide a general basis for a qualitative visualization of molecular energetics, molecular structure and molecular radiationless transitions corresponding to ***primary photochemical processes***. ($^*R \rightarrow I$ and $^*R \rightarrow P$).

6.3 Movement of a Classical Representative Point on a Surface[2]

The behavior of a representative point on a potential energy curve is analogous to that of a classical marble rolling along a curved surface (Figure 4.1). The point represents a specific instantaneous nuclear configuration. In addition to potential energy (PE) the marble may possess kinetic energy (KE) of motion if it moves along the energy surface. The marble is "held" onto a real surface by the force of Earth's gravitational field; in analogy, the representative point is evidently "held" onto the potential energy surface by some sort of force. If the marble leaves the surface as the result of an impulse (a force delivered in a short time period) from some external force, it makes a momentary departure from the surface, but gravity provides a restoring force which quickly attracts the particle back onto the surface. What is the nature of the analogous restoring force that attracts the representative point the energy curve? That force is the simple result of the Coulombic attractive force of the positive nuclei for the negative electrons. *The*

restoring force of our representative point that keeps it "sticking" to the surface is analogous to the force of gravity which "holds" the particle on a surface.

From elementary physics,[2] the magnitude of the gravitational or Coulombic force acting on the representative point is given by eq. 6.1.

Force acting on the particle at *r*	$F = -dPE/dr$	Slope of the curve at *r*	(6.1)

Equation 4.1 is of great importance for an understanding the behavior of the representative point since it relates the magnitude of the force acting on the representative point to the instantaneous slope or the "steepness" of the potential energy curve at *r*. The steeper the slope the stronger the "pull" of the positive nuclei on the electrons.

The potential energy of the representative point is analogous to the height of a mass of a particle above the earth's surface. Because of the physical requirement that KE - PE > 0, the representative point is not allowed to "drop" below the lowest energy surface. Thus, in Figure 6.1, the shaded region of space forbidden to the representative point corresponds to negative potential energy on the earth. This "impenetrability" of the surface is analogous to a mass moving along a hard crust on the earth.

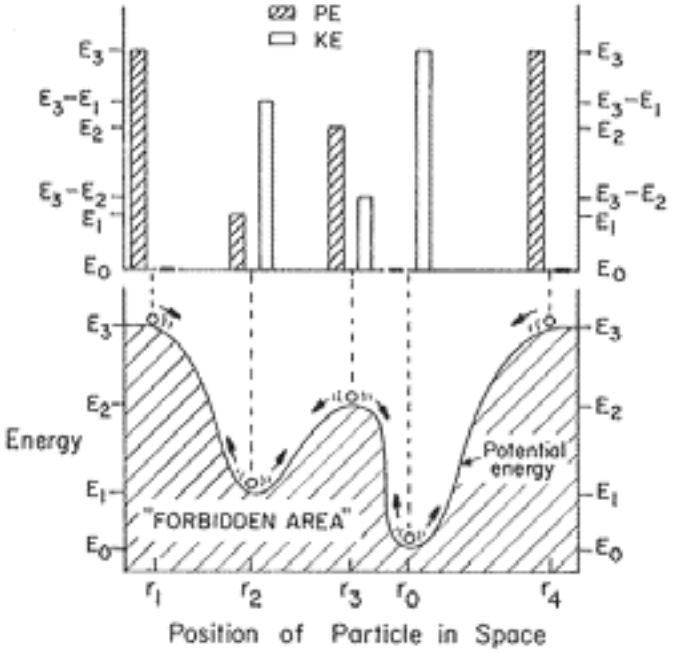

Figure 6.1. Potential energy of a particle (representative point) as a function of a position coordinate. The total energy of the particle is a combination of potential energy and kinetic energy.

6.4 The Influence of Collisions and Vibrations on the Motion of the Representative Point on an Energy Surface

What forces cause the representative point to pick up kinetic energy and to move on a potential energy surface? Why might it prefer to move in one direction rather than another? How is the law of conservation of energy and momentum conserved as the point moves over a surface? In solution, the answers to these questions are available by consideration of the vibrational motions that are available within the molecule and of collisions that occur with other molecules in the environment. Consider the

effect of collisions on a molecule in solution. Such collisions may be considered as impacts (forces delivered in the short periods of contact) which a molecule experiences as a result of interactions with other molecules in its immediate neighborhood. The magnitude of these impacts depends on temperature, varies over a wide distribution of energies, and follows a Boltzmann distribution. Near room temperature the average energy per impact is ~ RT = 0.6 kcal/mole. The energies associated with collisions is nearly continuous. Thus, near room temperature, collisions can be considered to provide a reservoir of coninuous energy which will match, without much difficulty, vibrational energy gaps.

Figure 6.2 schematizes the effects of collisions on movement along a potential-energy surface from one minimum to another. Suppose the reactant starts with a nuclear configuration in which a reacting bond has an internuclear separation equal to R_R. Collisions serve as an kinetic energy source and move the reactant along the energy surface to a maximum (transition state) geometry, R. Further movement along the surface toward the product requires removal of energy, i.e., the collisions serve as an energy sink as the system moves from R_R to R to R_p.

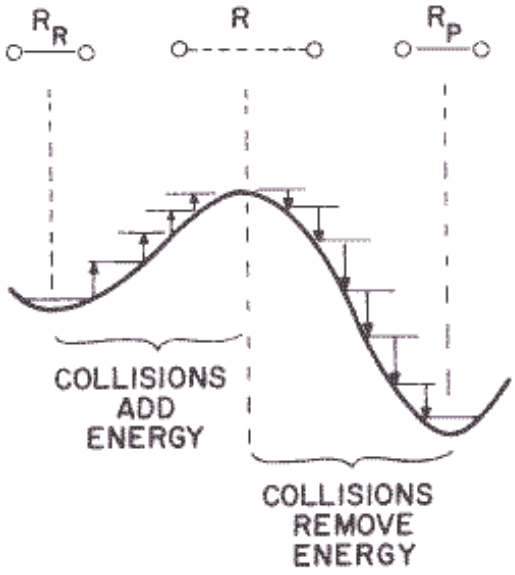

Figure 6.2 Effects of Collisions in Providing and Removing Energy to a Particle Moving Along a Potential Energy Surface

6.5 Radiationless Transitions on Potential Energy Surfaces. Surface Intersections, Minima and Funnels on the Way From *R to Products

The notion of a potential energy surface which controls the motion of the nuclei of a molecular system can take different points of view. From the classical point of view the potential function is the work (force times a distance) which must be done to bring the constituent atoms from infinite separation to specified nuclear geometry. From the quantum mechanical point of view, a potential energy surface, when represented by the appropriate quantum mechanical description of the nuclear motion, reproduces some experimental observations and applies to a wide variety of experiments. Many phenomena are though of as being controlled by a single potential energy surface. For example, reactions in the ground state involve a single electronic potential energy surface. However, molecular photochemistry which involves *R → I (or P) transitions at various stages, must be described in terms of more than one energy surface, i.e., at least one electronically excited surface and one ground state surface.

In ground state chemical reactions the reactant, R, starts in a minimum on the potential energy surface and leads to various reactive intermediates, I, or products, P, via passage through a path-way specific transition structure. On the other hand photochemical reactions start in a Franck-Condon minimum,

*R, on an electronically excited surface and radiationless transitions eventually bring the system to a reactive intermediate, I, or a ground state product, P. Thus, a transition from an excited surface to a ground state surface must occur somewhere along the *R → I (or P) process. Thus, during a photochemical reaction the motion of the representative point is initially on the excited surface, then a transition occurs to the ground surface and the final evolution to products is on the ground state surface. Evidently there is a region of energy and structure for which the system undergoes an electronic transition and "switches" or "jumps" from an excited surface to a ground state surface.

The Fundamental Topologies for "Funnels" from Excited Surfaces to Ground State Surface: Surface Touchings, Surface Intersections and Surface Avoidings

A central mechanistic question associated the determination and description of the location of the "funnel" on the excited surface which separates the part of the reaction that occurs on the excited surface from the part of the reaction path that lies on the ground surface. There are limiting surface topologies (Figure 6.3) encountered in the primary photochemical processes (*R → I and *R → P) of organic molecules: (a) a *surface intersection* for which an excited surface and a lower energy surface cross at a certain point; (b) a surface avoiding which corresponds to a surface intersection of an excited surface and a lower energy surface in a lower approximation but becomes a surface avoiding in a higher adiabatic approximation and (c) a *surface touching* for which an excited surface and a lower energy surface touch at one or more point, but do not cross. The rate of crossing from one surface to another which they possess identical nuclear geometries depends on the interaction of the surfaces at these geometries and the energy gap between the surfaces (Eq. XX). The larger the energy gap the slower the decay and transition from the excited state surface to the ground state surface. For the surface crossing (Figure 6.3a) and surface touching (Figure 6.3c) the energy gap corresponding to the funnel geometry is zero. In such cases the rate of transition between the excited surface and ground state surface may be limited by the rate of vibrational relaxation on the surface. For the case of two avoided surface (Figure 6.3b), the energy gap is finite. The larger the energy gap the slower the decay and transition from the avoided crossing on the excited state surface to the ground state surface. If the gap is large enough, the lifetime of this type of funnel could be quite long and the geometry could be considered to be a true electronically excited state intermediate that is characterizable by direct spectroscopic methods.

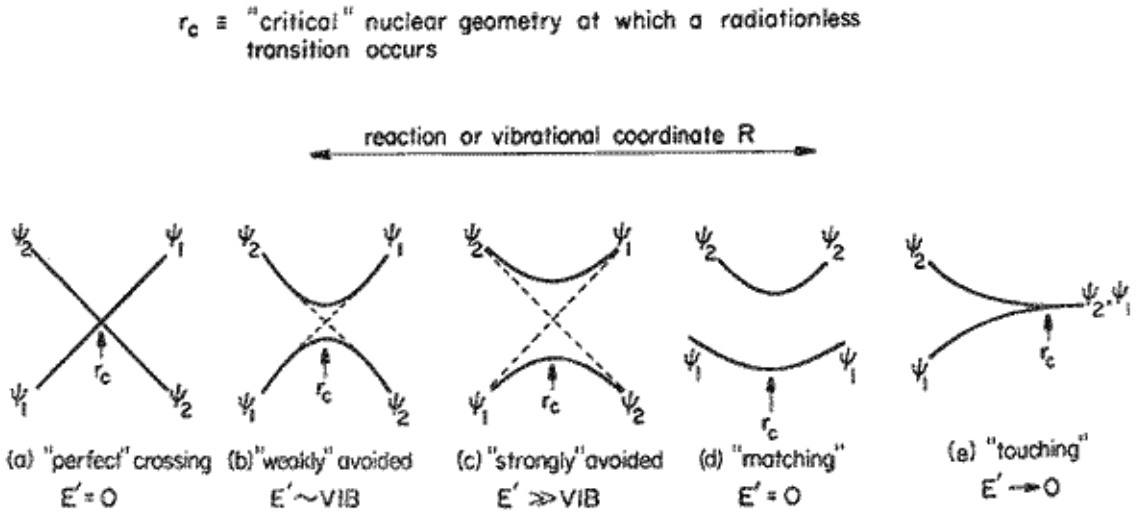

Figure 6.3 Two dimensional otential energy curve descriptions of three limiting cases of funnels leading from an electronically excited surface to a ground state surface: (a) a surface crossing, (b) a strongly avoided surface crossing and (c) a surface touching.

To obtain the "flavor" of added dimensionality to the visualization of energy surfaces, consider Figure 6.4 which provide three dimensional representations of a (a) true surface crossing, (b) an avoided surface crossing and (c) a surface touching.

Figure 6.4 Three dimensional potential energy surface descriptions of three limiting cases of funnels leading from an electronically excited surface to a ground state surface: (a) a surface crossing, (b) a strongly avoided surface crossing and (c) a surface touching.

From this discussion it is clear that it is of greatest interest to molecular photochemistry to be able to identify energy surfaces which cross or intersect at some reasonable level of approximation, since surface intersections often correspond to funnels to the ground state. Such crossings are sometimes predictable based on simple correlation diagrams which assume a certain symmetry for a nuclear configuration change corresponding to an initial and final state and then correlates the initial states with the final states by drawing surfaces which connect states appropriately to general a *state correlation diagram*. Inspection of the state correlation diagram reveals the surface crossings (intersections). Next it is of interest to determine whether the surface crossing holds up in higher degrees of approximation of the energy surface. Finally it is of interest to determine what sorts of nuclear geometry changes might generally correspond to each of the situations in Figure 6.3. We shall address these points in the remainder of the chapter.

The Nature of Funnels Corresponding to Surface Crossings, Surface Avoidings and Surface Touchings.

Minima on excited state surfaces which possess geometries similar to those on the ground state surface are termed *spectroscopic or photophysical minima* and have been discussed in Chapter 3 and 4. These minima correspond to the geometries of electronically excited states, *R, which have similar geometries to the ground state minimum for R. Both radiative and radiationless transitions may take place from these minima are constrained by the Franck-Condon principle. These minima serve as relatively stable "funnels" which bring excited states to the ground state. Transitions from these minima are considered "vertical" transitions in the sense that the transition does not involved a significant change in the nuclear geometry. These minima may be considered as the initial states of all photophysical processes (fluorescence, phosphorescence, internal conversion and intersystem crossing) and the excited state *R ($S_)$ or T_1) ends up in the original minimum from which light absorption occurred, i.e., R. Photochemical reactions involve *minima which are "funnels" that take an excited state to a ground state reactive intermediate, I, or isolable product, P (*R → I or *R→ P).* These minima, in contrast to photophysical minima, will possess geometries very different from those on the ground state surface for R since both I and P are difference chemical species.

Surface touchings and surface crossings are common topologies for primary processes which produce radical pairs and biradicals as the primary products in the *R → I step. Surface crossings and avoided crossings are common topologies for primary photochemical reactions involving a *R → P step. Since most isolable products, P, are singlets, this means that *R will generally be a singlet state, i.e., S_1. In the following sections we shall describe examples of each of these topologies.

The Non-Crossing Rule. Conical Intersections.

The "non-crossing rule" for two energy curves states that if there is a geometry for which two electronic curves possess the same energy and nuclear geometry, the curves do not cross but "avoid" each other as the result of quantum mechanical mixing. The idea behind the rule is that for an adiabatic surface (one that follows the Born-Oppenheimer approximation) when two states have the same energy and same geometry there will always be some "mixing" of the states to produce two adiabatic surfaces, one of higher energy and one of lower energy, i.e., the surfaces "avoid" each other as the result of the mixing. This rule applies strictly to molecules possessing high symmetry such diatomic molecules. However, for polyatomic molecules which generally possess little or nosymmetry with respect to local geometries, the non-crossing

rule is no longer a strict selection rule and two electronic states of the same spatial/spin symmetry may turly cross (Teller, E. J. Phys. Chem. **1937**, *41*, 109; Kauzmann, W. *quantum Chemistry; Academic Press: New York, 1957, 696*). The occurrence of true surface intersections between singlet state surfaces in organic photochemistry was suggested by early computations of excited state surfaces in the 1970s (3-6 Spectrum). The concepts developed can be applied to a visualization of vibrational relaxation, radiationless internal conversion and radiationless photochemical reactions involving singlet states. Crossings of triplet states and singlet states presents no conceptual problems since the crossing states are of different spin symmetry. Crossings of two triplet surfaces may be treated in the same manner as the crossings between two singlet surfaces.

In the 1990s more advanced computations were possible because of advances in software and development of algorithms for computing energy surfaces, coupled with increased efficiency of computers (Michl book, reviews) showed convincingly that the intersections of two potential energy surfaces and showed that the in 3 D the energy surface that in the immediate vicinity of the touching point the surface crossings have the form of a double cone which has been termed a "*conical intersection*" (Figure 6.4a). A conical intersection is defined as the touching of two electronic potential energy surfaces when plotted along two coordinates. It is now widely accepted by theorists that real crossings between singlet surfaces and associated conical intersections are ubiquitous and often accessible from *R.

The generation of the conical intersection can be visualized as resulting from sweeping of the intersection in 2D about the symmetry axis (figure 6.4a). An important feature of conical intersections is that they serve as very efficient "funnels" which take the representative point rapidly from an excited surface to the ground state surface. Movement along the "wall" of a conical intersection is essentially a vibrational relaxation of the system and therefor provides a very efficient pathway from an excited surface to a ground surface and as such is the ultimate "funnel" leading form an excited state to the ground state. The notion is that trajectories of the representative point through the tip of the cone follow a steep slope of the cone wall and effectively convert electronic energy into nuclear motion (vibrations). Thus, a conical intersection presents no rate determining bottleneck in a radiationless pathway. The return to from a conical intersection can occur with unit efficiency when the representative point enter the region of the intersection.

The conical intersection concept may also be associated with fast motion of the representative point on a surface. In the case of fast motion the Born-Oppenheimer approximation may break down so that there is no time for electronic wavefunctions to react to nuclear motion and mix in regions where surface crossings occur in Zero Order. In other words in such situations the surface crossings are maintained. In this case the representative point stays on the same electronic surface and the concept of a "jump" between adiabatic surfaces loses its meaning. In effect the same wavefunction may be classified as an excited state wavefunction (Ψ^*) in the region of energies higher than the crossing point and a ground state wavefunction (Ψ) in the region of lower energies than the crossing point. The path through a conical intersection is so rapid that the representative may preserve a memory of its initial trajectory from *R. The reaction path is essentially "concerted" in the sense that no reactive intermediates (I) are involved and that the flight through the conical intersection is so fast that stereochemical information, even with respect to rotations about single bonds, is conserved. The term "funnel" is used to describe regions of a surface for which passage to another (adiabatic) surface is so fast that there is not time for vibrational equilibration which is required for a surface to be considered adiabatic. Thus, a true surface crossing or a weakly avoided surface crossing serve as funnels for bringing higher energy electronically excited states to lower energy excited states and to the ground state for both photophysical and photochemical radiationless processes.

If, for example, the S_1 and S_0 states actually touch they are energetically degenerate at the conical intersection, the return to S_0 will be very efficient and it is considered that the transition S_0 to will occur as soon as the intersection is reached from S_1. When this is the situation, the transition from $S_1 \rightarrow S_0$ will not be controlled by the energy gap between the surfaces undergoing transition. But by the features of either the ground or excited state surface. The notion of a conical intersection is quite different from a strongly avoided crossing which corresponds to a short lived intermediate on the excited surface. For example, if a biradical with stereochemistry is formed at an avoided crossing, there is a chance that the biradical will lose it's stereochemistry during the time the species spends in the avoided crossing region. On the other hand if the biradical structure corresponds to a conical intersection, passage through the biradicaloid region will be

so fast that stereochemistry will not be lost. Indeed, computation and experimental data indicate that the representative point passes through the conical intersection so rapidly that the rate is competitive with that of a vibrational period. In other words, passing through a conical intersection is a form of vibrational relaxation.

In the classical expression for the probability, P, from n an excited state to a ground state is proportional to the negative exponential of the energy gap between the two states undergoing transition. Since the energy gap is 0 for a conical intersection, the probability, P = 1. Let us consider a computation (Fuss, et al, Chem. Phys. **1998**, *232*, 161-174) to see how this classical probability decreases as the energy gap increases. For an energy gap of ~ 23 kcal/mole (one electron volt) for *maximal* values of $v = 10^{13}$ Å/s and Δs = ~ 30 kcal/moleÅ, P decreases from 1 to ~ 10^{-21}! On the other hand, internal conversion from the S_1 of ethylene can be computed to take place on the order of tens of femtosec (~ 10^{-14} s) from the broadening of the bands of ethylenes UV spectrum (internal conversion is so rapid that fluorescence in not detectable). This time is of the order of a torsional vibration about the C=C bond in the ground state. Since the C=C bond is much weaker in $S_1(\pi,\pi^*)$ state because of the π^* electron, it can be concluded that internal conversion takes place in the first twisting attempt on the singlet surface.

A difficulty with the distinguishing conical intersections from avoided crossings is that determining their occurrence requires a rigorous theoretical computation. However, in this chapter we shall show that the *plausible* existence of a conical intersection or avoided crossing can be inferred from inspection of orbital correlation and electronic state correlation diagrams.

.

An interesting theoretical feature of both conical intersections and avoided crossings is that they may provide access to a number of reactive intermediates (I_n) or products (P_n) from a single conical intersection (Figure 6.5a) or avoided crossing (Figure 6.5b), i.e., $^*R \rightarrow I_1 + I_2 + I_3$, etc or $^*R \rightarrow P_1 + P_2 + P_3$, etc. However, the theoretical pictures are distinct for the two types of transitions although the final result is similar. In the case of an avoided crossing (Figure 6.5b), since the representative point is in a quasi equilibrium on the excited surface it make wander about in the minimum for a period of time and when it crosses to the ground surface, the trajectory of the point may be toward a product which depends on the details of nuclear motion at the instant the crossing occurs. In this case we suppose that there are several ground state products ($^*R \rightarrow I_n$ or P_n) towards which the varying trajectories of the representative point is carried once it leaves the excited state surface.

Figure 6.5 Passage through conical intersection and avoided crossing.

In the case of product formation through a conical intersection (Figure 6.5a) the picture is quite different. The representative point is viewed as entering the region of the conical intersection from an initial geometry of, say, P_1. As the representative point approaches the immediate apex of the of the conical intersection (bottom of excited state portion of the cone) its detailed trajectory is determined by two independent forces which operate on the representative point: (1) the gradient of the energy change as a function of nuclear motion and (2) the direction of nuclear motions which best mix the adiabatic wavefunctions)which determine its motion. The simple qualitative model presented in Figure 6.5 does not consider these specific features of the conical intersection, but these forces can be computed. The concept is that as the representative point approaches the conical intersection the Born-Oppenheimer approximation begins to break down and the motion of the representative point is determined by a combination of the original momentum of the point on the excited surface as it approaches the conical intersection and the momentum associated with the forces of the various nuclear geometries which are competing for control of the motion of the representative point once it drops to the ground state. Depending o the way the classical trajectories enter the conical intersection region, different product may be produced.

In conclusion, conical intersections (surface touchings and avoided crossings) may correspond to nuclear geometries which are far removed from initial minima on an excited surface. If the representative point, in exploring an excited surface, falls into a conical intersection, its rate of passage from the excited surface will be of the order of vibrational relaxation and because of the competing forces the representative

point experiences when it approaches the apex of the conical intersection, its trajectory is easily directed towards more than one product on the ground state surface. When a conical intersection is involved in a photochemical process, the rate determining step is exploration of the excited surface by the representative point before it finds and falls into the conical intersection. The process *R → (conical intersection) → P is the excited state equivalent of a concerted reaction, i.e., one in which there is no true reactive intermediate involved on the path from *R to P. Thus, from a mechanistic point of view, a conical intersection which serves as a funnel on the excited surface plays a similar role to a transition state on the ground state surface Both describe the nuclear geometry of a transition structure. In a thermal reaction, the ground transition state corresponds to the point of potential energy for which the probability of passage from the reactant to the product is maximal. In a photochemical reaction, the conical intersection corresponds to the point where the probability of transition to the ground state is maximal.

We now consider the case of surface touchings (Figure 6.3c and 6.4c).

6.6 Diradicaloid Geometries from Stretching σ Bonds and Twisting π Bonds

When a pair of degenerate or nearly degenerate non-bonding orbitals are occupied by a total of only two electrons, a very important and simple orbital situation results (Figure 6.6). The geometry of a molecule which corresponds to such a situation is termed diradicaloid geometry and may correspond to a reactive intermediate or to a transition structure. Radical pairs and diradicals are common examples of diradicaloid geometries. Diradicaloid geometries often correspond to touchings or minima on electronically excited surfaces. As such these geometries are important because they are both inherently chemically reactive and because they serve as "funnels" from electronically excited state to lower excited states and to the ground state.

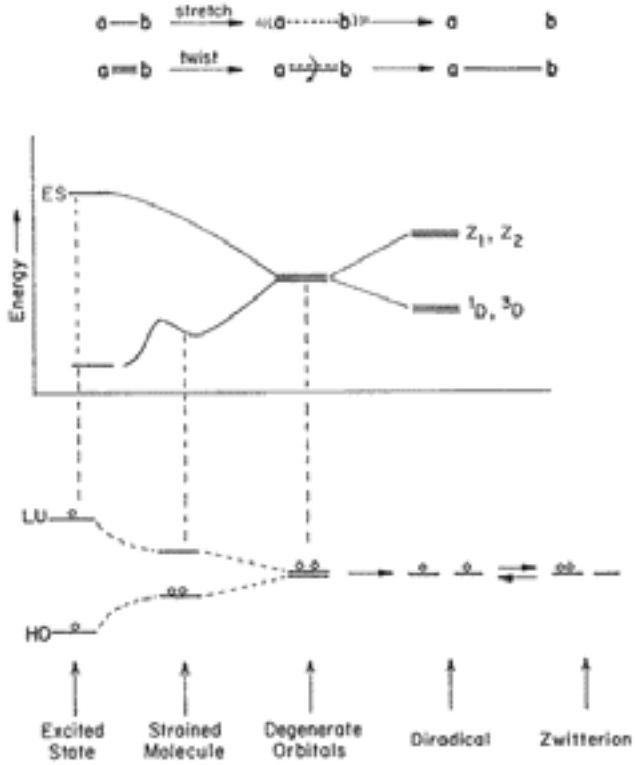

Figure 6.6 Schematic description of the surface relationships of excited states, strained ground state molecules, diradicals, and zwitterions.

Many photoreactions produce diradicals or "diradicaloid" structures as primary photochemical products, i.e., conform to a *R → I primary photochemical process, where I is a radical pair or a diradical reactive intermediate (we will use the term “diradicaloids” to characterize such geometries). Two of the simplest and most fundamental exemplars of the geometries (Figure 6.6 top) which correspond to such diradicaloid may be reached from normal equilibrium geometries by: (a) the stretching and breaking of a σ bond, and (b) the twisting and breaking of a π bond. In spite of their simplicity, these two exemplars provide a conceptual basis for the interpretation of an enormous number of organic photochemical reactions. Diradicaloid geometries are common minima for excited surfaces. Since these geometries are minima that correspond to structures possessing two degenerate or nearly degenerate orbitals they are reactive minima and are therefore generally short lived. (Relevance of biradicaloid minima for photoreactions:
Zimmerman, 1966, 1969. Oosterhoff, 1969, Michl, 1972, 1974a.)

An Exemplar for Diradicaloid Geometries Produced by σ Bond Stretching and Bond Breaking. The Hydrogen Molecule

The stretching and breaking of the hydrogen molecule (H-H) into two hydrogen atoms (H + H) is an exemplar for the diradicaloid geometry produced by stretching and breaking a σ bond. As the H-H bond stretches (eq. 7.10) it eventually reaches a geometry for which the bond is completely cleaved a radical pair (Eq. 6.2) will be produced.[5,6,7]
On the ground state surface this corresponds to a thermal R → I process and on the excited state surface this corresponds to a photochemical *R → I process.

H-H	→	H--------H	→	H + H (6.2)
		stretched		cleaved
		diradicaloid		diradical

At the nuclear geometry at which the σ bond is nearly broken, two degenerate 1s orbitals result and four electronic states are possible. This geometry corresponds to the “diradicaloid” geometry. A simple description of the process is shown in Figure 6.7 in terms of (a) the behavior of the orbitals; (b) the possible orbital configurations and state, and (c) the surfaces corresponding to the four electronic configurations as the bond is stretched and broken.

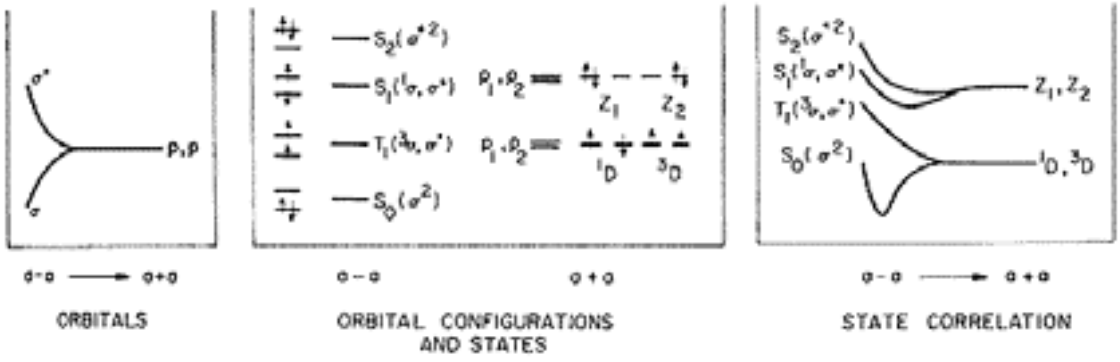

Figure 6.7 Orbitals, orbital configurations, and state correlation diagrams for stretching and breaking of a σ bond.

First let us consider the behavior of the σ and σ* orbitals behavior as the H-H bond stretches. When the H nuclei are close together (close to their equilibrium separation of ca 1Å) the σ orbital is very low in energy relative to the σ* orbital (Figure 6.7a, left). The electronic states which can be derived for this nuclear geometry (H-H) are $S_0(\sigma)^2$, $T_1(\sigma,\sigma^*)$, $S_1(\sigma,\sigma^*)$, and $S_2(\sigma^*)^2$ (Figure 6.7b). As the bond

stretches, the energy of the σ orbital increases and the energy of the σ* orbital decreases. When the H nuclei are far apart (ca 2-3 Å), both the σ and σ* orbitals will approach the same energy and correlate with a pair of nonbonding 1s orbitals, one on each H atom (Fig. 7.10a, left). The electronic states (Figure 6.7b and c) which can be derived from completely separated atoms H + H are $^1D(1s_1,1s_2)$, $^3D(1s_1,1s_2)$, $Z_1(1s_1)^2$, and $Z_2(1s_2)^2$. In the terminology employed here, D stands for a general *diradicaloid geometry* (and may be a radical pair or diradical reactive intermediate, I) and will always refer to a state in which two orbitals of comparable energy are half-filled (Figure 6.7b); Z stands for *zwitterion* and will always refer to a state in which two orbitals of comparable energy have their electrons all *spin-paired* and one of the two orbitals is doubly occupied (Fig. 6.7b). There are two possible D states, a singlet (^1D) and a triplet (^3D) and they will always be similar in energy because they correspond to weak overlap or orbitals in space and do not mix because they possess different spin multiplicities. The Z states are always singlets. Although in the example given for a hydrogen molecule, the two Z states would be of identical energy at the diradicaloid geometry, for any asymmetric bond cleavage, one Z state (defined as Z_1) will be lower in energy than the other Z state (defined as Z_2), because one of the orbital occupancy possibilities will generally be of lower energy when the atoms making up the bond are different.

A simple state correlation diagram[5] for breaking a H-H bond is shown in Figure 6.7c. It is clear that the σ orbital will correlate with a 1s orbital on each of the atoms and lead to a $D(1s_{1,}1s_2)$ state in the product. Since S_0 is a singlet, it must correlate with the $^1D(1s_1,1s_2)$ state. The $T_1(\sigma,\sigma^*)$ state must correlate with $^3D(1s_1,1s_2)$ since the latter is the only triplet state of the product. By exclusion, *both* $S_1(\sigma,\sigma^*)$ and $S_2(\sigma^*)^2$ must correlate with Z_1 or Z_2.

The state correlation diagram shown in Figure 6.7c is an exemplar for the behavior of the energy of a surface that tracks the cleavage of a σ bond and in fact corresponds closely to the actual surfaces for the hydrogen molecule, where it is known from experiment and computation that the surface along the S_1 and S_2 possess shallow minima just before the diradicaloid geometry is reached. This minimum represents an energetic compromise arising from the competing tendency of to minimize the energy between the σ and σ* orbitals as the bond stretches and to minimize the energy required for charge separation in the zwitterionic states, which are favored by a small nuclear geometries. Such shallow minima will be assumed to be general for a simple σ bond cleavage. On the other hand, the triplet state does not possess a minimum for any geometry, but eventually "flattens out" energetically for large separations for which the triplet surface "touches" the ground-state surface. S_0, of course, possesses a deep minimum corresponding to the stable ground state geometry of the molecule, which corresponds to a much shorter internuclear distance than the diradicaloid geometry.

In summary, the exemplar for a the surface behavior corresponding to a simple σ bond cleavage (Figure 6.7) possesses the following surface characteristics:

1. Along the ground surface, S_0, the bond is stable except for large separations and a large activation energy is required for stretching and cleavage.

2. Along the triplet surface, T_1 , the bond is unstable at all geometries and little or no activation energy is required for cleavage.

3. The products of cleavage along the S_0 or T_1 surface are radical pairs or diradicals.

4. Along the S_1 and S_2 surfaces the bond is unstable, but possess a shallow minimum for geometries for a very stretched but not completely broken bond; from this diradicaloid geometry only a small amount of energy is require for complete cleavage.

5. The products of cleavage along S_1 or S_2 are zwitterions.

An Exemplar for Diradicaloid Geometries Produced by π Bond Twisting and Breaking. Ethylene

Let us now consider the behavior of the energy surfaces which track the twisting and breaking of a π bond. Imagine the twisting of the π bond of an ethylene molecule (CH_2=CH_2), which provides an

exemplar for twisting and breaking a π bond. As the ethylene molecule is twisted it eventually arrives at a nuclear geometry for which the two methylene groups are mutually perpendicular (90° geometry):

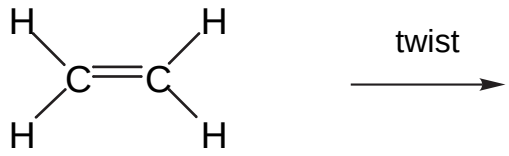

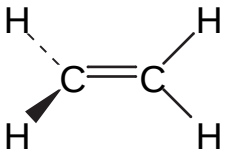

(6.3)

Planar geometry Both CH_2 groups in the same plane.

CH_2 groups are mutually perpendicular

At the 90° geometry, the π bond is broken, two degenerate non-bonding p orbitals are produced so that this structure corresponds to a diradicaloid geometry, and a 1,2-diradical is produced. In terms of a standard structure equation we might write:

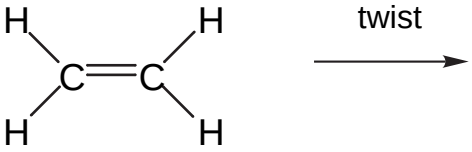

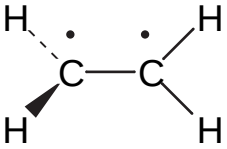

(6.4)

Diradicaloid geometry at 90°

Since two non-bonding orbitals are produced at the 90° geometry, at this diradicaloid geometry, as in the case of a highly stretched σ bond, four electronic states are possible. Again, two diradicals and two zwitterions result (Figure 6.8). As the π bond twists, the energy of the π orbital sharply increases, and the energy of the π* orbital sharply decreases (Figure 6.8a). At 90° of twist (the perpendicular configuration) the π and π* orbitals have transformed into two non-bonding p orbitals, one on each carbon.

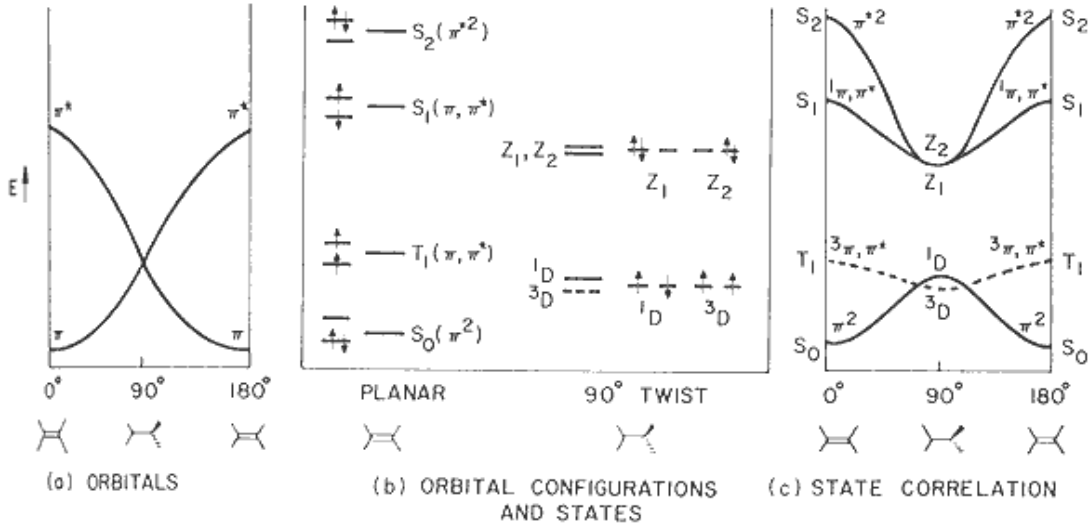

Figure 6.8 Orbitals, orbital configurations, and state correlation diagrams for twisting a π bond.

The electronic states derived from the possible orbital configurations for the planar and twisted geometries are given in eqs. 6.5 and 6.6.[4]

Planar ethylene: $S_0(\pi)^2$, $T_1(\pi,\pi^*)$, $S_1(\pi,\pi^*)$, and $S_2(\pi^*)^2$ (6.5)

90^o Twisted ethylene: $^3D(p_1,p_2)$, $^1D(p_1,p_2)$, $Z_1(p_1)^2$, and $Z_2(p_2)^2$ (6.6)

Twisting about the carbon-carbon bond of an electronically excited ethylene sharply relieves electron-electron repulsion resulting from the π* electron. Thus, ***twist about the carbon-carbon bond will tend to lower the energy of all of the excited states of ethylene***. Thus, the electronic energies of S_2, S_1, and T_1 drop rapidly as a function of the ethylene twisting, because electronic excitation has effectively broken the π bond and the bonding between carbon atoms is similar to that of a carbon-carbon single bond. In contrast, the electronic energy of S_0 *increases* as the molecule is twisted because the π bond is being broken.

The state correlations $S_0 \rightarrow {}^1D$, $T_1 \rightarrow {}^3D$, $S_1 \rightarrow Z_1$, and $S_2 \rightarrow Z_2$ may be made on the basis of orbital symmetry considerations. The symmetry element which brings the starting planar geometry into the twisted (diradicaloid) geometry is a rotation of one CH_2 group.[4] The overall state symmetries must be definable in terms of this symmetry element. Although the rigorous state correlation is best done by use of group theory and point-group analysis, the following qualitative description will indicate the basis of the correlation.

The wave function for the $S_0(\pi)^2$ configuration (Fig. 6.8b) at the planar geometry is essentially covalent (one electron on each carbon atom) in character,[5] i.e., there is very little ionic character to planar ethylene, and the wave function for π^2 has (in terms of atomic orbitals) the form $p_1(\uparrow)p_2(\downarrow)$. This means that for $S_0(\pi)^2$ at all times there is always only one p electron near carbon 1 and one near carbon 2, and these electrons have paired spins. For the $T_1(\pi,\pi^*)$ configuration at the planar geometry there can never be two electrons on one carbon in the same p orbital (violation of the Pauli principle), since the electrons have parallel spins. The T_1 state is thus purely covalent and has no ionic character, and its wave function has the form $^3(\pi,\pi^*) = p_1(\uparrow)p_2(\downarrow)$.

The wave functions for $S_1(\pi,\pi^*)$ and $S_2(\pi^*)^2$ must differ from that of $S_0(\pi)^2$ and must reflect the basis for the high energy content of the state. It is found from computation that the former two states are best described by zwitterionic wave functions. We shall see in Chapter 10 that there is considerable experimental evidence that this simple picture is consistent with the know photochemistry of ethylenes and their derivatives.

In summary, the important qualitative features of the state correlation diagram for a twist about the ethylene double bond (Fig. 6.8c) are:

1. The occurrence of *minima* in the $S_2(\pi^*)^2$, $S_1(\pi,\pi^*)$, and $T_1(\pi,\pi^*)$ surfaces at the 90^o geometry which correspond to Z_2, Z_1, and ^3D respectively.

2. The occurrence of an *avoided crossing nature* of the minimum at Z_2, i.e., the Zero Order $S_0(\pi)^2$ and $S_2(\pi^*)^2$ surface correlation is strongly avoided and the adiabatic surfaces show a minimum in $S_2(\pi^*)^2$ and a maximum in $S_0(\pi)^2$ as the result of the avoiding.

3. The occurrence of a geometry corresponding to a maximum in the $S_0(\pi)^2$ surface which also corresponds to the ^1D geometry.

4. The $S_0(\pi)^2$ and $T_1(\pi,\pi^*)$ in addition the S_2 and S_1 state touch at the diradicaloid 90^o geometry. Importantly, at the diradicaloid geometry the $S_2(\pi^*)^2$ state is degenerate with the $S_1(\pi,\pi^*)$ state.

5. The zwitterionic (closed shell) behavior of $S_2(\pi^*)^2$ and $S_1(\pi,\pi^*)$ for all geometries.

6. The diradical behavior of $T_1(\pi,\pi^*)$ for all geometries.

We shall see later in this Chapter that the state correlation diagrams for *thermally forbidden* ground-state pericyclic reactions have the general form of those for twist about the double-bond of ethylene (see Fig. 6.8). Thus, the exemplar for twisting about a simple π bond has far reaching utility in the interpretation of photochemical reactions of systems containing C=C bonds.

6.7 Orbital Interactions as A Guide to the Lowest Energy Pathways on Energy Surfaces

The simple energy surfaces (Figures 6.7 and 6.8) based on the stretching of σ bonds and the twisting of π bonds provide qualitative exemplars of how energy surfaces behave for two important geometry changes which are common for organic molecules. We now develop a more general approach to examine how energy surfaces behave as a function of reaction path geometries for the two primary processes $^*R \rightarrow I$ and $^*R \rightarrow P$. We shall start with a description of how the use of orbital interactions can provide selection rules for the lowest energy pathways for photochemical reactions of electronically excited states of organic molecules. This will create for us a set of "plausible" or "allowed" primary photochemical reactions. We will then analyze some exemplars for $^*R \rightarrow I$ and $^*R \rightarrow P$ processes in terms of orbital and state surface energy correlation diagrams which will serve as a basis for describing the reaction pathways and the occurrence of energy maxima and minima along the primary photochemical reaction pathway.

A qualitative, *a priori* "feeling" for the occurrence of energy barriers and energy minima on electronically excited surfaces may be obtained by starting with the concepts of initial orbital interactions[1] to deduce the lowest energy pathways of reaction and then using an idealized symmetrical representation of this pathway to generate an orbital or state correlation diagram.[2,3] The theory of frontier orbital interactions assumes that the reactivity of organic molecules is determined by the very initial charge transfer interactions which result from the electrons in an occupied orbital to an unoccupied (or half occupied) orbital. The most important orbitals in the frontier orbital analysis are the highest occupied (HO) orbital and lowest unoccupied orbital (LU) of the ground state of an organic molecule. Two features of the interacting frontier orbitals determine the extent of favorable charge transfer interaction from the electrons in the HO to the vacant LU orbital: (1) the energy gap between the two orbitals and (2) the degree of positive orbital overlap between the two orbitals. For a comparable energy gap between the orbitals, significant positive (in phase) overlap of the interacting highest occupied (HO) and lowest unoccupied (LU) orbitals of reactants signals a small energy barrier to charge transfer and to reaction. On the other hand, negative (out of phase), or zero, net overlap of the HO and LU orbitals signals a large energy barrier to charge transfer and a large barrier to charge transfer and reaction. If we start on a given electronically excited surface from *R along which there are two reaction pathway choices (say $^*R \rightarrow I_1$ and $^*R \rightarrow I_2$), we may call the pathway with the smaller energy barrier "allowed" and the pathways with the larger energy barrier "forbidden." In effect, we postulate that reactions prefer to proceed via transition structures that have obtained the most favorable positive orbital overlap and the smallest energy gap between the interacting orbitals. Thus, consideration of initial or frontier orbital interactions provide a basis for "selection rules" for possible reaction pathways.

After determining (or assuming) a reaction pathway, further information concerning the maxima and minima on excited surface can be obtained from orbital and state correlation diagrams, which require a model with a certain level of symmetry in order to determine the correlations. Within the framework of correlation diagrams, if an initial orbital (or state) makes an endothermic ("uphill") correlation with a high-energy product orbital (or state) along one reaction coordinate but an exothermic ("downhill") correlation with a low-energy product orbital (state) along another coordinate, we may say that the former experiences a state correlation-imposed energy barrier, whereas the latter does not. The uphill process is termed "forbidden" and the downhill correlation is termed "allowed". We in effect have created a selection rule that the movement of the representative point along a surface that corresponds to a reaction coordinate which possesses *an orbital* (*state) correlation-imposed energy barrier* will be less probable (forbidden reaction) than movement along a surface which does not possess correlation-imposed barriers (allowed reaction).

The Principle of Maximum Positive Orbital Overlap[1]

Now let us consider how the principle of *maximum positive overlap* allows the prediction of a *plausible* set of (low energy) reaction pathways from an initial state (R or *R). According to quantum theory, molecular orbitals have spatial directiveness associated with them. As a result, if a reaction is to be initiated by orbital overlap, certain spatial geometric positions of nuclei (and their associated electron clouds) will be favored over others if they correspond to a greater degree of positive orbital overlap (for comparable energy gaps between the orbitals). The principle of stereoelectronic control of reaction pathways postulates that reaction rates are controlled by the degree of positive overlap of orbitals in space, i.e., certain nuclear geometries are easier to achieve then others during a reaction because of the greater positive orbital overlap accompanying one nuclear motion relative to another. In summary, the principle of maximum positive overlap postulates that the reaction rates are proportional to the degree of positive (bonding) overlap of orbitals. Although qualitative in nature, this principle is a powerful basis for analyzing photochemical reactions and for quickly sorting out plausible and implausible reaction pathways.

In the application of the principle of maximum positive orbital overlap, we must also consider the energies of the orbitals involved, since only the higher-energy filled orbitals (i.e., valence orbitals) and lower-energy (vacant) orbitals are likely to be involved in reactions at ordinary temperatures. Recall (perturbation theory, eq. 3.5) that quantum mechanics postulates that the interactions between two orbitals is inversely related to the energy gap between the orbitals involved. Thus, the smaller the energy gap between the HO and LU the greater the energy lower resulting from a given degree of positive overlap of the orbitals. We shall employ the frontier molecular orbital approximation[1] in analyzing orbital interactions for photochemical reactions, i.e., the orbital interactions which determine the nature of reactions from *R. As for ground state reactions, this approximation postulates that chemical reactivity may be gauged by the overlap behavior of "frontier molecular orbitals" (FMO's) corresponding to the electronic configuration of *R. In this case, the key orbitals often correspond to the highest-energy orbital filled in the ground state (the HO orbital) and the lowest-energy orbital unfilled in the ground state (the LU orbital). Since the HO, has the highest energy of all of the occupied in the ground state, it is most readily deformed, and most readily gives up electron density to electrophilic sites in the environment, i.e., the HO generally possesses the highest polarizability and the smallest ionization potential of any orbital that is occupied in the ground state. The LU, which is unoccupied in the ground state, is capable of accepting an electron (is electrophilic) and is most capable of accepting electron density with minimum increase in the total molecular energy. If the initial perturbation is assisted by movement of the HO electrons toward a LU, we can readily visualize how the transfer of charge from one orbital to another actually occurs.

The fundamental underlying principle of HO-LU interactions as a means of understanding chemical reactivity of ground state reactions is the assumption that a majority of chemical reactions should take place most easily (lowest activation enthalpy) at the position of and in the direction of maximum positive overlap of the HO and the LU of the interacting species. Although the same basic principle applies for reactions of excited states, for *R (S_1 or T_1) it is important to note that the HO and LU are half filled, i.e., singly occupied. A singly occupied molecular orbital (termed SO) produced by electronic excitation may play the role of HO or LU, or both.

Stabilization by Orbital Interactions. Selections Rules Based on Maximum Overlap and Minimum Energy Gap.[1]

Perturbation theory predicts that the "stabilization" energy E_{stab} due to overlap of frontier orbitals (FMO's) is given qualitatively by

$$E_{stab} \sim \langle \text{positive overlap of FMO's} \rangle^2/\Delta E \qquad (6.5)$$

The magnitude of in the stabilizing sense will depend directly on the square of the magnitude of the net positive overlap of the FMO's and inversely on the term ΔE, which measures the energy difference between the pertinent interacting FMO's. Because *R possess two SO (half filled HO and half filled LU), a number of possible charge transfer interactions are possible from or to the HO or LU of another molecule (or some other groups in the same molecule).

Consider Figure 6.9 which schematically shows the *apriori* possible SO → LU and HO → SO interactions. The Pauli principle strictly forbids charge transfers from the SO → HO because such an interaction places more than two electrons in a single orbital. Whether charge flows from or to a SO, will depend on the energy differences between the interactions SO and LU (or HO) and the degree of positive overlap. In the case of flow to the SO, the charge flow from HO → SO is generally the most energetically feasible pathway. In the case of flow from the SO, charge flow from SO → LU is preferred.

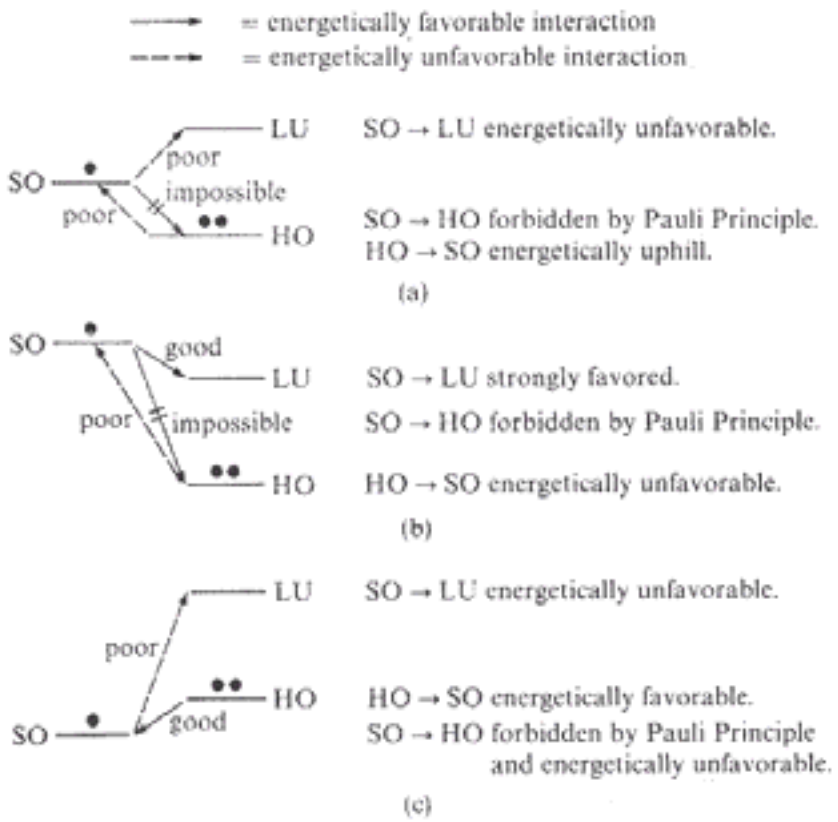

Figure 6.9 Some examples of possible SO-HO and SO-LU interactions. The solid circles represent electrons and orbital occupancy.

Commonly Encountered Orbital Interactions in Organic Photoreactions.

Figure 6.10 shows two commonly orbital interactions that are encountered in the most important primary photochemical reaction steps. By inspection of all of the possible orbital interactions (Pauli violations are not considered) between *D(or D) and A(or *A), we can employ a selection rule based on eq. 6.5: Favored interactions are those which have maximum positive overlap of the interacting orbitals and for which the energy gap between the interacting orbitals is small. Although the overlap depends on the specific system under analysis, we can generalize how the energy gap favors some orbital interactions over others. We start with a general rule that the energy gap between the D(HO) and A(HO) will be smaller than the energy gap between the D(HO) and the A(LU). When this is the case the selection rule based on the energy gap is: in case (Figure 6.10a) the charge transfer D*(LU)→ A(LU) orbital interaction dominates, whereas in case (Figure 6.10b) the charge transfer interaction D(HO) → A*(HO) orbital interaction dominates. The other possible interactions between HOs and LUs are considered relatively weak in Zero Order. As a subselection rule, we assume that all other factors being equal, it is more favorable for the charge transfer to flow to an orbital of lower energy than an orbital of higher energy (Figure 6.10b). The latter subselection rule assumes that there is a thermodynamic aspect to orbital

interactions and that the reaction which is downhill thermodynamically is favored over a reaction that is uphill thermodynamically.

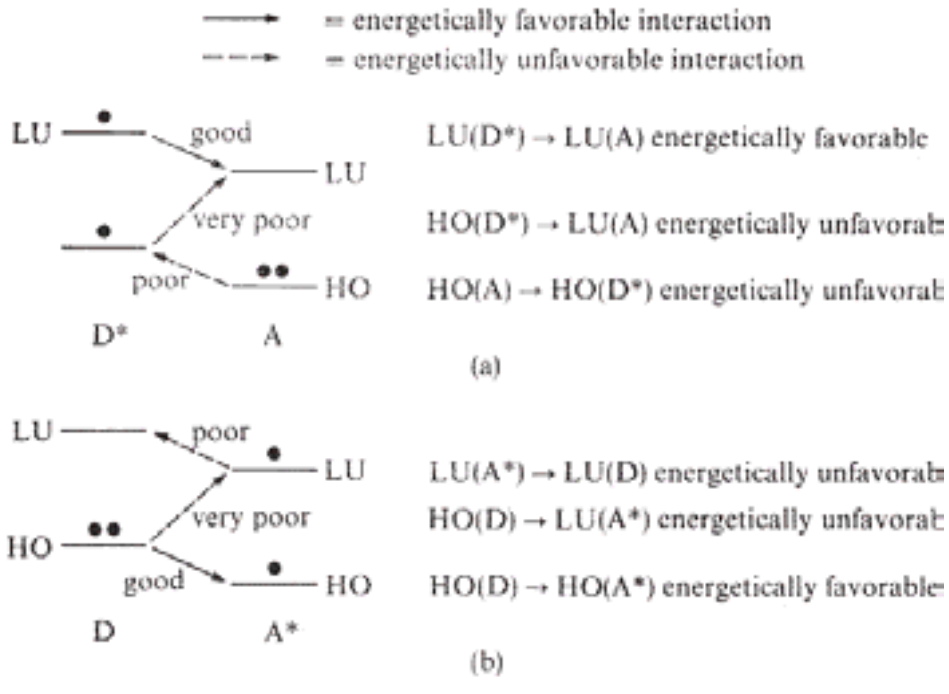

Figure 6.10 Schematic representation of two important orbital interaction types: (a) Dominant D*(LU)—> A(LU) interaction and secondary A(HO) —> D*(HO) and D*(HO) —> A(LU) interactions and (b) Dominant D(HO) —> A*(HO) and secondary D(HO) —> A*(LU) and A*(LU) —> D(LU) interactions.

From Figures 6.9 and 6.10 and the criteria of maximum positive overlap and minimum energy gap, we can postulate the following recipe for deciding how orbital interactions will determine the favored nuclear motions for a given set of photochemical reaction pathways:

1. After setting up the molecular orbitals of the reactants according to their relative energies, identify the FMO's and the half-filled SO's of the electronically excited moiety and the filled HO and unfilled LU of the unexcited moiety.

2. Draw the possible orbital interactions between an SO of the electronically excited moiety and a HO or LU of the unexcited moiety.

3. Determine which orbital interactions lead to the best positive overlap and whether the interaction arrow for these orbital interactions points up (thermodynamically unfavorable) or down (thermodynamically favorable).

4. Evaluate the positive orbital overlap and thermodynamic factors to determine qualitatively the more favorable reaction pathways.

This information provides a qualitative guide to the most favored pathways of reaction from *R → I or *R → P.

6.7 Selection of Reaction Coordinates from Orbital Interactions for *R → I or *R → P Reactions. Exemplars of Concerted Photochemical Reactions and Photochemical Reactions Which Involve Diradicaloid Intermediates

We now consider the two most important classes of photochemical reactions: the *R → P or *R → I processes. Examples of the *R → P reaction are the ***set of plausible photochemical "concerted" pericyclic reactions*** initiated from $S_1(\pi,\pi^*)$ states of ethylenes and conjugated polyenes (electrocyclic ring openings and ring closures, cycloaddition reactions, sigmatropic rearrangements) which follow the Woodward-Hoffmann rules for photochemical. Concerted photochemical pericyclic reactions must be initiated from $S_1(\pi,\pi^*)$ since a spin change is required if the reaction is initiated in $T_1(\pi,\pi^*)$ and the reaction cannot therefore occur in a concerted manner. Examples of the *R → I process is the ***set of plausible photochemical reactions*** of the $S_1(n,\pi^*)$ ***or*** $T_1(n,\pi^*)$states of ketones (hydrogen atom abstraction, electron abstraction, addition to ethylenes, α-cleavage reactions, β-cleavage reactions). We shall see that consideration of orbital interactions creates selection rules such that the set of plausible photochemical reactions of n,π* states are the same and independent of spin. However since the $S_1(n,\pi^*)$ state possesses a higher energy than the $T_1(n,\pi^*)$ state, there is generally greater thermodynamic driving force for reaction from $S_1(n,\pi^*)$ than for $T_1(n,\pi^*)$.

In analyzing a photochemical reaction such as *R → I or *R → P theoretically, one must select the particular reaction coordinate or coordinates which describe the nuclear geometry changes accompanying the transformation of reactants to products. In principle, all possible reaction coordinates might be analyzed. In practice, we seek to select only the lowest-energy reaction pathways from a given initial excited state. These pathways may be qualitatively identified by the use of orbital interactions.

An Exemplar for Photochemical Concerted Pericyclic Reactions.
The Electrocyclic Ring Opening of Cyclobutene and Ring Closure of 1,3-butadiene

As an exemplar of concerted pericylic reactions we consider the photochemical electrocyclic ring opening of cyclobutene and the photochemical electrocyclic ring closure of 1,3-butadiene. The concepts developed from this exemplar can be readily extended to other examples of photochemical electrocyclic reactions and to other photochemical pericyclic reactions.

Consideration of orbital interactions leads to the well-known selection rules for pericyclic reactions.[3] For example the key aspect of concertedness for an electrocyclic reaction is the selective stereochemistry associated with the ring opening and ring closing, which follow the Woodward-Hoffmann rule (see Fig. 6.11). According to the positive overlap and energy gap selection rules of orbital interactions, we are led to the prediction that for reaction initiated from the $S_1(\pi,\pi^*)$ states of cyclobutene both $\sigma \rightarrow \pi$ and $\pi^* \rightarrow \sigma^*$ charge transfers should contribute most significantly.

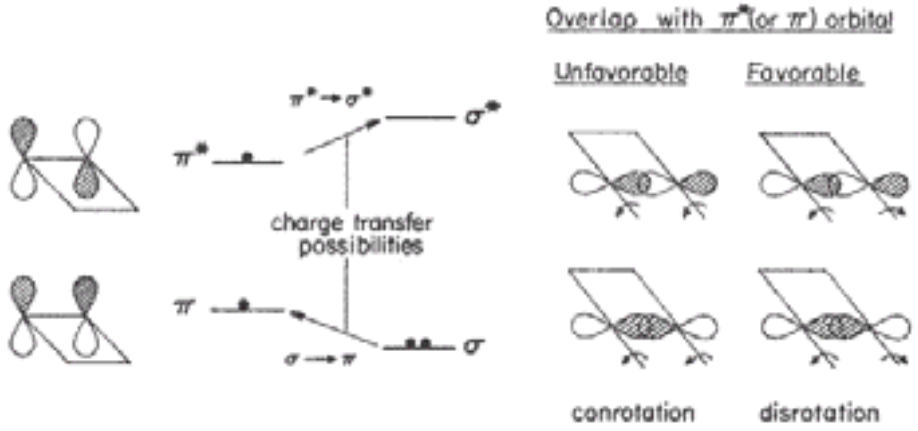

Figure 6.11 Orbital interactions for the conrotatory and disrotatory ring opening of the π,π• state of cyclobutene to form 1,3-butadiene.

Inspection of the orbital symmetry for disrotatory and conrotatory processes[3] shows that the former is favored by the rule of maximum positive overlap:

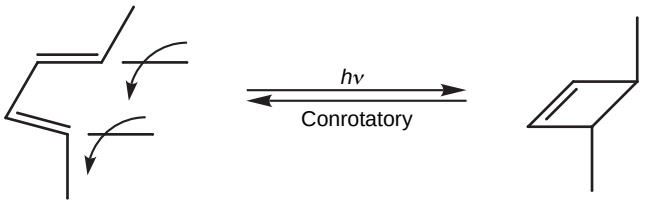

"Forbidden" by orbital interactions (6.6)

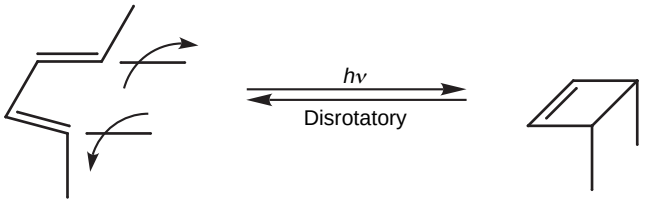

"Allowed" by orbital interactions (6.7)

Thus, simply from a consideration of orbital interactions we expect that for this four-electron system the *disrotatory interconversions are photochemically allowed* (favorable orbital interactions), whereas the *conrotatory interconversions are photochemically forbidden* (unfavorable orbital interactions). These rules assume that the processes are thermochemically allowed. These conclusions are important since they allow a theoretical process for selecting a small set of plausible *initial* interactions of π,π* states which determine the stereochemistry of concerted pericyclic reactions. To confirm that these initial interactions are carried over in the *R → P reaction, we will need to generate orbital and state diagrams for the overall process, which will be done in the next section of this Chapter.

An Exemplar for Photochemical Reactions Which Produce Diradical Intermediates

As an exemplar of photochemical reactions which produce a diradical as the primary photochemical product we shall examine the photochemistry of the n,π* states of ketones. In this case we are concerned not with the stereochemical characteristics of a given class of reactions (as was the case for the pericyclic reactions discussed in the previous section) but with determine the set of plausible reactions from a specific excited state electron configuration based on an analysis or orbital interactions.

The objective again is to develop a plausible set of primary photochemical processes of a n,π* state of a ketone. Thus one needs to survey all of the SO orbital interactions that are possible from a n,π* state with the HO and LU of other species (intermolecular reactions) or with groups within the molecule possessing the electronic excitation. Figure 6.12 lists these possibilities: (1) charge transfer interactions in which one of the electrons from the HO of a nucleophilic species is transferred to the electrophilic half filled n_o SO of the n,π* state and (2) charge transfer interactions from the nucleophilic half filled π^*_{CO} SO of the n,π* state to a vacant LU of an electrophilic species. What are the common orbitals that correspond to the nucleophilic HO and to the electrophilic LU? For organic molecules the three most common HOs correspond to σ orbitals, π orbitals and n orbitals and the two most common LUs correspond to π* and σ* orbitals. An example of a σ HO orbital is the σ_{CH} orbital associated with a CH bond; an example of a π HO bond is the $\pi_{C=C}$ orbital of a C=C bond; an example of a n HO orbital is the n_N HO orbital associated with an amine. An example of a π* LU orbital is the $\pi^*_{C=C}$ associated with a C=C bond; An example of a σ* LU orbital is the σ^*_{C-X} associated with a C-X (carbon halogen) bond.

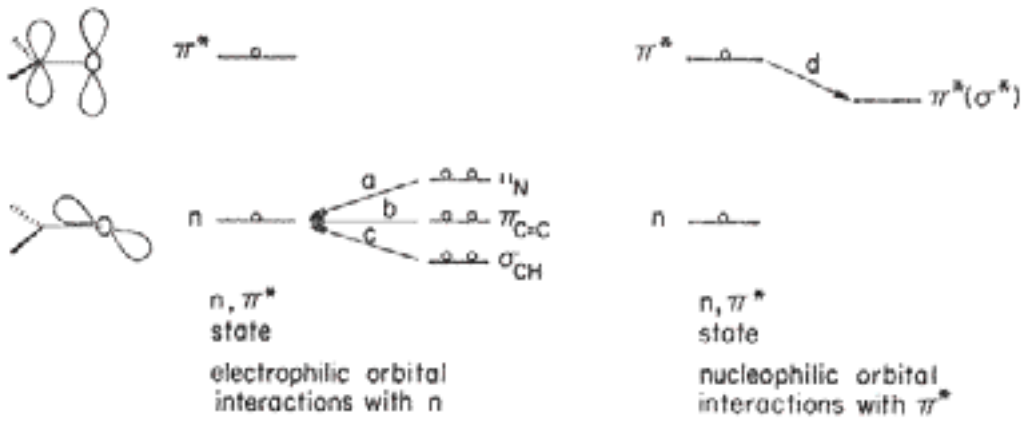

Figure 6.12 Orbital interactions of the n,π* state with substrates.

According to the selection rules for orbital interactions, we expect the low energy or allowed reaction pathways for the n_o orbital to be $\sigma_{CH} \rightarrow n_o$, $\pi_{C=C} \rightarrow n_o$, and $n_N \rightarrow n_o$ and for the $\pi^*_{C=C}$ orbital to be $\pi^*_{C=O} \rightarrow \pi^*_{C=C}$ and $\pi^*_{C=O} \rightarrow \sigma^*_{C-H}$. These interactions define the orbital requirements which must be met for a reaction to be considered as a member of the plausible set of photochemical reactions of an n,π* state (assuming that the overall reaction, *R → I is thermochemically allowed). This is a rather important conclusion since it allows a theoretical process for selecting a small set of plausible *initial* interactions of n,π* states with potential reagents, both intermolecular and intramolecular. To confirm that these initial interactions are carried over in the *R → I reaction, we will need to generate orbital and state diagrams for the overall process, which will be done in the next section of the Chapter.

6.9 Orbital and State Correlation Diagrams

After orbital interactions have been utilized to allow us to postulate the lowest-energy reaction coordinates, we can then employ orbital and state correlation diagrams to deduce the nature of the energy surfaces which connect reactants to primary photochemical products (i.e., deduce the surface topology) and determine whether the reactions are “allowed” or “forbidden”.

The protocol for the generation of orbital and state correlation diagrams depends heavily on the concept of molecular and electronic symmetry (either for the complete molecule or a portion of it). It is assumed that the reader is somewhat familiar with this concept, and only a brief review of the terms used to describe orbital and state symmetry will be given here.[2,3]

Consider the symmetry properties of orbitals which are possible with respect to a plane.[6] If a molecule possesses a plane of symmetry, all of its MO must be either symmetric (**s**) or antisymmetric (**a**) with respect to reflection through the symmetry plane. For example, for the formaldehyde molecule (Fig. 6.13), the n orbital has **s** symmetry (the wave function does not change sign within the molecular plane) and the π (and π*) orbital has **a** symmetry (the wave function changes sign above and below the molecular plane) with respect to reflection through the plane. In other words, reflection of the n orbital through the plane does not change the sign of the wave function (**s** symmetry) but reflection of the π (or π*) orbital through the plane does change the sign of the wave function (a symmetry).

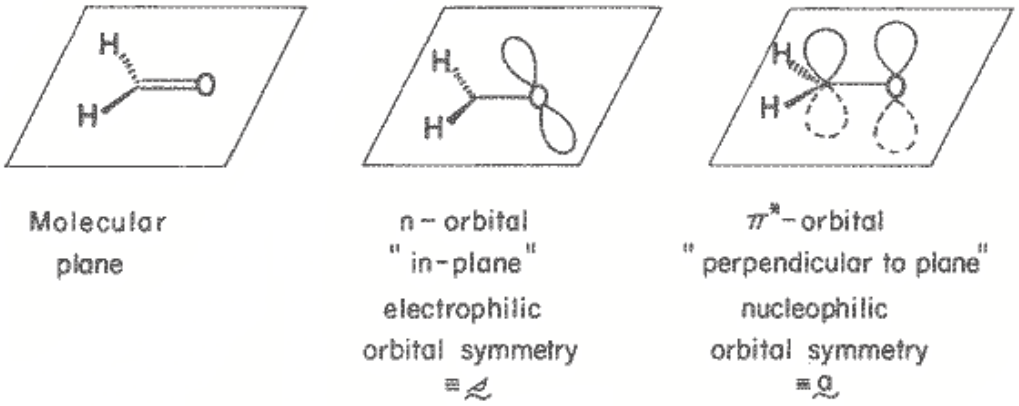

Figure 6.13 The symmetry plane of formaldehyde. The n_0 orbital lies in the symmetry plane and is termed symmetric (s) with respect to reflection through the symmetry plane. The π* (and the π) orbital lies above and below the symmetry plane and is termed anti-symmetric (a) with respect to reflection through the symmetry plane.

Electronic *state* symmetry is a composite or mathematical *product* of orbital symmetries.[2] If we know the orbital symmetries relative to a symmetry element and if we know the orbital electron occupations, we can immediately deduce the state symmetries. The protocol for classification of state symmetries is as follows:

1. If only doubly occupied orbitals occur in a configuration, the state symmetry is automatically **S** (totally symmetric because the mathematical product of minus times minus or plus time plus is positive).

2. If two (and only two) half-occupied orbitals ϕ_i and ϕ_j occur in a configuration, the state symmetry is given by the following rules:

Orbital symmetry		State symmetry
ϕ_i	ϕ_j	$\Psi_{ij} = ---\phi_i\phi_j$
a	**a**	**S**
a	**s**	**A**
s	**a**	**A**
s	**s**	**S**

Similarly, the symmetry of orbital changes associated with disrotatory and conrotatory motion of the ring openings and ring closings in electrocyclic reactions may be classified as **a** or **s** and the state configurations associated with these motions may be classified as **A** or **S**. The interested reader is referred to any one of a number of texts dealing with the orbital and state symmetries associated with concerted pericyclic reactions.

The Construction of Electron Orbital and State Correlation Diagrams for a Selected Reaction Coordinate

In an orbital correlation diagram (e.g., *vide infra*, Figure 6.14) a *straight line* between an orbital of the initial state and an orbital of the final state means that there is a direct electronic correlation between the orbitals. This means that the correlated orbitals "look alike" and are smoothly transformed throughout the

orbital correlation. Likewise, a straight line between an initial state and a final state means that the initial state and final states look alike and there is a direct electronic correlation between the states. A direct orbital or state correlation means that there is no *electronically* imposed energy maximum or minimum on the potential energy surface which links the tow corresponding orbitals or states. A *curved line* between two orbitals (or states) means that the correlation between these state results form an (possible) avoided crossing somewhere between the initial and final orbitals (states). It should be noted that the correlation diagrams are qualitative and need to be calibrated energetically for quantitative comparisons and predictions. In particular, thermodynamics of the reaction (enthalpies and entropies of initial and final states) must be considered in order to quantitatively determine plausibility and probability of primary photochemical processes. For example, if a state diagram indicates a direct correlation between the initial and final state, but if the energy of the final state lines at an unattainably high energy, the reaction is unambiguously electronically allowed, but is also thermodynamically forbidden in the kinetic sense, i.e., the rate will be extremely slow. The role of thermodynamic calibrations and control of photochemical reactions will be considered explicitly in Chapter 8.

The construction of electronic orbital or state correlation diagrams starts with the selection of a chemical reaction coordinate. This selected coordinate is based on consideration of orbital interactions, computations or experimental data, and describes the nuclear motions and geometry changes that transform the initial reactant into a primary photochemical product (*R → I or *R → P). First a Zero Order correlation of the orbitals of the reactant with the orbitals of the primary product is made.[6,7] Next the non-crossing rule is applied in order to set up the First Order *adiabatic* orbital correlation diagram. (Recall that the non-crossing rule is not mandatory for organic molecules, so that it is not mandatory in an orbital and state correlation diagram). The state correlation diagram is then generated by connecting the states of reactants to the states of the primary product. This First Order state correlation diagram is considered to be a *working* set of surfaces, which should have the correct general topology for discussion of the possible mechanisms. Now let us list a specific protocol, or set of general rules, for the construction of an electronic state correlation diagram for a given reaction coordinate:

1. Enumerate and rank energetically the reactant and primary product electronic states (generate a reactant and primary product state energy diagram), using any pertinent theoretical, semi-empirical, or experimental evidence available. A basic goal of the correlation diagram is to determine the connectivity relations of the S_0, S_1, and T_1 states of the reactant to the states of the primary product, and to determine the connectivity relations of the corresponding lowest states of the primary product with the appropriate states of the reactant.

2. Determine the symmetry elements common to the reactant and primary product. Deduce the molecular symmetry in terms of the implied reaction coordinate. Search for symmetry elements which persist throughout the course of the reaction and bisect or contain the bonds being made or broken during reaction. To each orbital assign a symmetry type (symmetric, **s**, or antisymmetric, **a**).

3. In order to be useful, a symmetry element selected for correlation must be relevant to the actual chemistry which is occurring. Therefore, the appropriate elements must relate to the bonds being made or broken during the course of reaction. If no such symmetry element exists, it will usually not be possible to construct a meaningful correlation diagram.

4. The *orbitals* of the reactant are now correlated in Zero Order (crossings ignored) with the orbitals of the primary product. The correlation proceeds by the rule that the lowest-energy orbital of reactant of a given symmetry is connected directly to the corresponding orbital of the product.

5. The orbital correlation diagram is inspected for orbital crossings in Zero Order. If these crossings correspond to orbitals of the same symmetry, the crossing is replaced by an avoiding (i.e., the non-crossing rule is applied). The resulting diagram is a First Order (working) *adiabatic* orbital correlation diagram.

6. One now returns to the state energy diagram which displays the electronic configurations and relative energetic rankings of the reactant and product states. To each reactant and product state (usually

only the lowest-energy states need be considered explicitly) a characteristic electronic orbital configuration is assigned.

7. Based on the orbital correlation diagram, an orbital symmetry is associated with each orbital of a characteristic orbital configuration, and the state symmetry is deduced for each electronic state. Corresponding states of the same symmetry are now connected. The connections are continued until the lowest lying states of reactants and the lowest lying states of the primary products have all been correlated. An important rule of making connections between states is that only one connection may be made between any given individual reactant state and any product state. In other words, two product states may not correlate with the same reactant state and vice versa.

8. The *non-crossing rule* is now applied to the state correlation diagram. All curve crossings of states of the same symmetry are replaced by avoidings. The resulting diagram is a First Order adiabatic state correlation diagram.

With the First Order state correlation diagram in hand we have a means of quickly enumerating possibilities of reaction pathways, and by using the theory of radiationless transitions we can judge reactivities and probabilities (efficiencies) of various reaction pathways.

To summarize, to create an adiabatic state correlation diagram, first an orbital correlation diagram is generated (orbital symmetry determines connectivity relationships), then orbital configurations are assigned to the lowest energy reactant and product states in the state energy diagram. Finally, an adiabatic state correlation diagram is generated by identifying all surface crossings and assume that they correspond to avoided crossings.

6.10 Typical State Correlation Diagrams for Concerted Photochemical Pericyclic Reactions[3,8]

Let us demonstrate the construction of electronic state energy correlations diagrams for an the exemplar of concerted pericyclic reaction discussed in Section XX: electrocyclic ring opening of cyclobutene and the electron cyclic ring closure of 1,3-btadiene (eq. 6.8).[3,8] The ideas presented here are readily extendable to other types of concerted pericyclic reactions (sigmatropic rearrangements and cycloadditions).[3a]

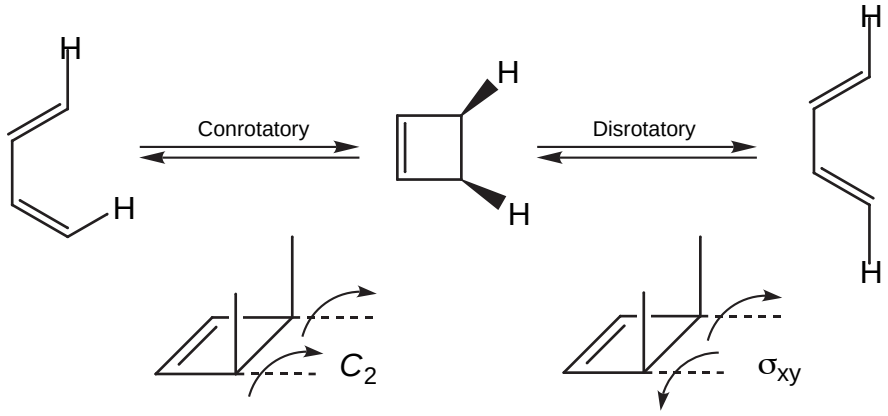

(6.8)

Under the three assumptions (1) that the starting carbon framework of both cyclobutene and 1,3-butadiene are planar, (2) that the carbon framework is still planar in the transition state and (3) that the 1,3-butadiene is formed as a *primary product* in the s-cis-conformation, we deduce two main symmetry elements for the reaction:

1. A twofold axis which bisects the cyclobutene 1,2- and 3,4-bonds and the butadiene 1,2-bond. We call this a C_2-axis. A ring opening or closing which preserves this symmetry element is termed conrotation (eq. 6.9).

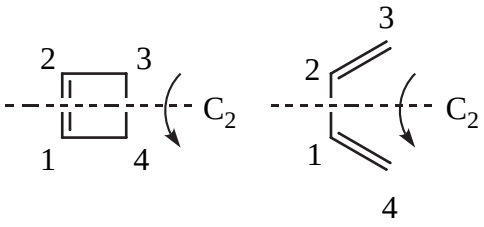

C_2-axes (6.9)

2. A mirror plane of symmetry perpendicular to the molecular plane and bisecting the cyclobutene 1,2 and 3,4 bonds. We call this plane σ_{xy}. A ring opening or closing which preserves this symmetry element is called a *disrotation* (eq. 6.10).

Reflection plane σ_{xy}

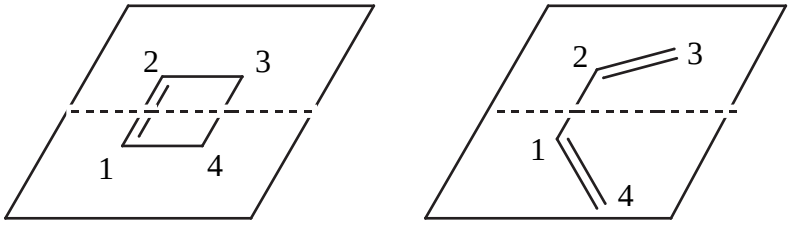

(6.10)

(7.9)

If the cyclobutene to 1,3-butadiene process occurs with the maintenance of a C2 or σ_{xy} symmetry element, we can construct a state correlation diagram for both reaction pathways.

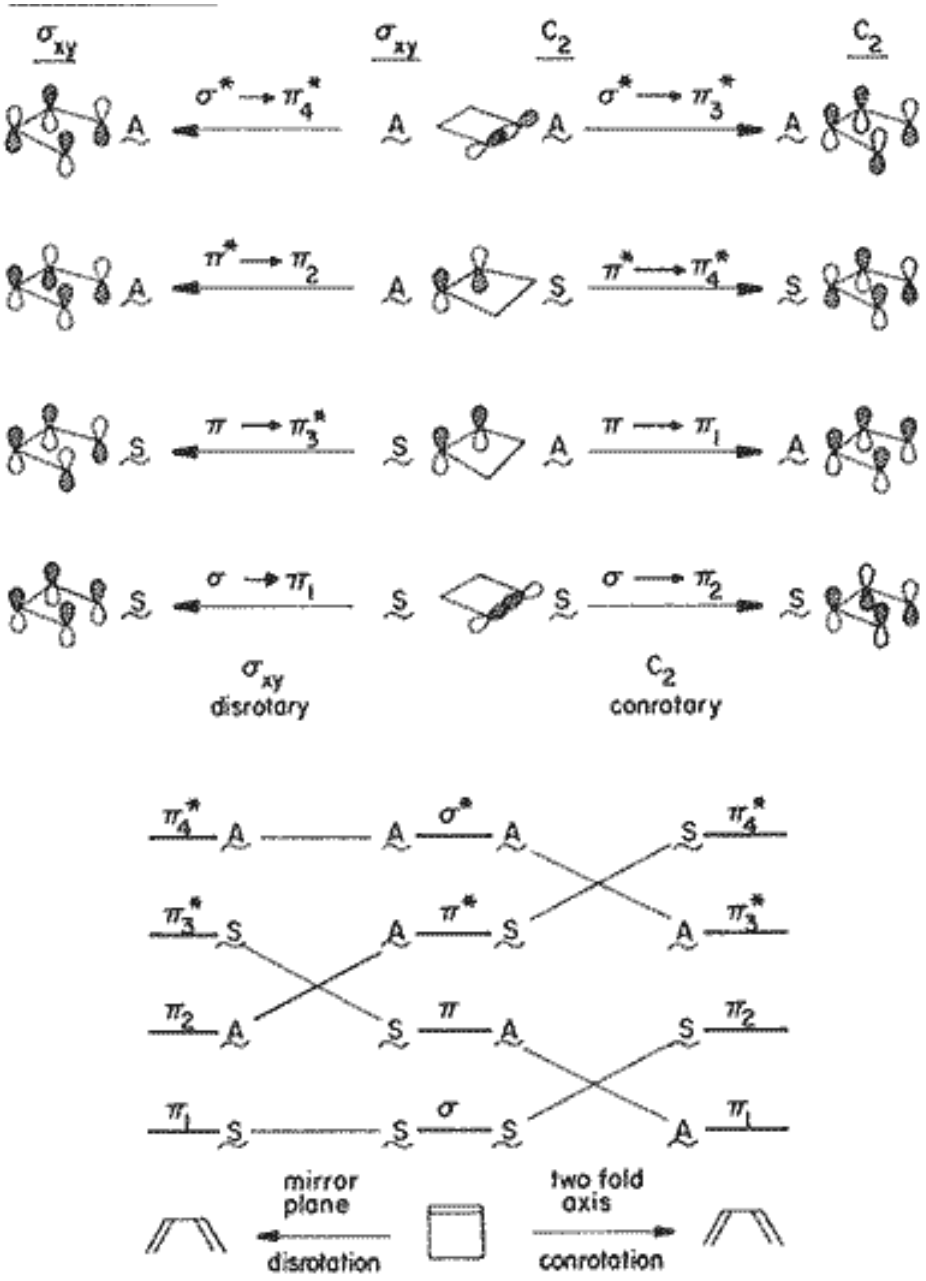

Figure 6.14 Transformation of the four key orbitals of cyclobutene into those of butadiene (top) and orbital correlation diagram (bottom) for the C_2 operation (conrotation) and σ_{xy} operation (disrotation).

An Exemplar Concerted Reaction. Classification of Orbitals and States for the Electrocyclic Reactions of Cyclobutene and 1,3-Butadiene

The orbitals of 1,3-butadiene and cyclobutene may now be classified as **a** or **s** for the conrotatory and disrotatory reactions. The results are given in Figure 7.6.[3] From the information in Figure 6.14, the state correlations for the conrotatory and disrotatory reactions can be deduced. For example, S_0 (cyclobutene) = $\sigma^2\pi^2$. From Figure 7.6 for a conrotatory motion, σ(cyclobutene) → π_2(butadiene) and

π(cyclobutene)$\rightarrow$ π_1(butadiene). Thus, S_0(cyclobutene) = $\sigma^2\pi^2$ correlates with a $(\pi_1)^2(\pi_2)^2$ configuration of butadiene. The latter corresponds to S_0 of butadiene. For a disrotatory motion, S_0(cyclobutene) = $\sigma^2\pi^2$ correlates with a $(\pi_1)(\pi_2)^2(\pi^*_4)$ configuration of butadiene for a conrotatory motion but correlates with a $(\pi_1)^2(\pi_2)(\pi^*_3)$ configuration for a disrotatory motion.

Thus, S_0(cyclobutene) goes uphill in energy during a disrotatory motion but downhill in energy during a conrotatory motion.[9] The reverse is true for a conrotatory motion. From the qualitative Zero Order state correlation diagram one expects a small activation energy for the thermal conversion of S_0(cyclobutene) to butadiene via the conrotatory pathway. In fact, an activation energy[10] of only 3 kcal/mole is observed for this reaction. The simple interpretation of the Zero Order state correlation diagram is that ***there is no state-correlation-imposed barrier for the thermal conrotatory reaction*** but ***there is a state-correlation-imposed barrier for the thermal disrotatory reaction***. Recall that the spirit of "allowed" and "forbidden" is really "faster" and "slower" in the sense of reaction rate or probability. In this sense, to the extent that both conrotatory and disrotatory reaction paths are otherwise comparable, the thermal disrotatory pathway is slower ("forbidden") relative to the faster thermal conrotatory pathway ("allowed") because the former automatically experiences a state-correlation-imposed energy barrier. It should be remembered that this discussion presumes *concerted* reactions.

By a similar line of reasoning, it follows that S_1(cyclobutene) should follow the disrotatory pathway preferentially to the conrotatory pathway. It should also be noted that butadienes should undergo favored conrotatory ring closure on S_0 and favored disrotatory ring closure on S_1.

We can complete the diagram (for the singlet states) by adding the correlations of butadiene: for the disrotatory motion $S_0(\pi_1^2\pi_2^2) \rightarrow S_m(\sigma^2(\pi^*)^2)$, and for the conrotatory motion $S_1(\pi_1^2\pi_2\pi^*_3)\rightarrow S_n(\sigma\pi^2\sigma^*)$.

If we assume that the shape of the T_1 energy surface parallels the S_1 energy surface, we produce a working *adiabatic* (appropriate crossings are avoided) state correlation diagram as shown in Figure 7.8.

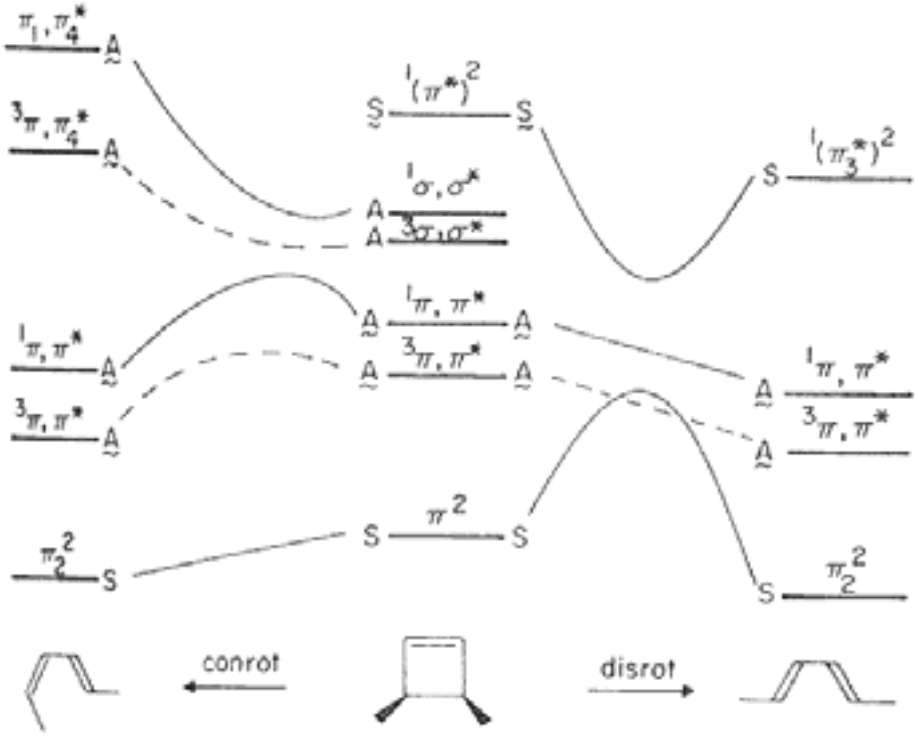

Figure 6.15 Simplified state correlation diagram for the concerted ring opening of cyclobutene to 1,3-butadiene.

The topology of these surfaces, derived for the specific example of an electrocyclic reaction, has been shown to be general for concerted pericyclic reactions.[3,6] Thus, all ground state forbidden pericyclic reactions can be expected to have a surface topology qualitatively equivalent to the disrotatory ring opening of cyclobutene to butadiene; all ground-state-allowed pericyclic reactions may be expected to have a surface topology qualitatively equivalent to the conrotatory ring opening of cyclobutene to butadiene.

The important features of these surfaces are: (a) the occurrence of a maximum on the S_0 surface (for the forbidden ground-state reaction) which comes close in energy to the S_1 surface and T_1 surface; and (b) the occurrence of a barrier on the S_1 surface (for the allowed ground-state reaction) and (c) the absence of close approach of the excited surfaces and S_0 at any point along the reaction pathway.[9] Notice the relationship of the topologies of the energy surface for the forbidden ground state disrotatory reaction and the forbidden ground state twisting of a π bond. Also notice that the minima in the excited singlet surface and the maximum in the ground state surface are the result of an avoided crossing.

The geometry for the transition state for a *forbidden* ground-state reaction, like the 90° geometry in twisting a π bond, to correspond to a diradicaloid structure.[5,6] From the general rules for radiationless transitions such a structure corresponds to a "critical" geometry so that a jump from the S_1 surface to S_0 should be favored from the minimum on the S_1 surface, because the S_1 and S_0 surfaces are very close at this geometry (Fig. 6.16).

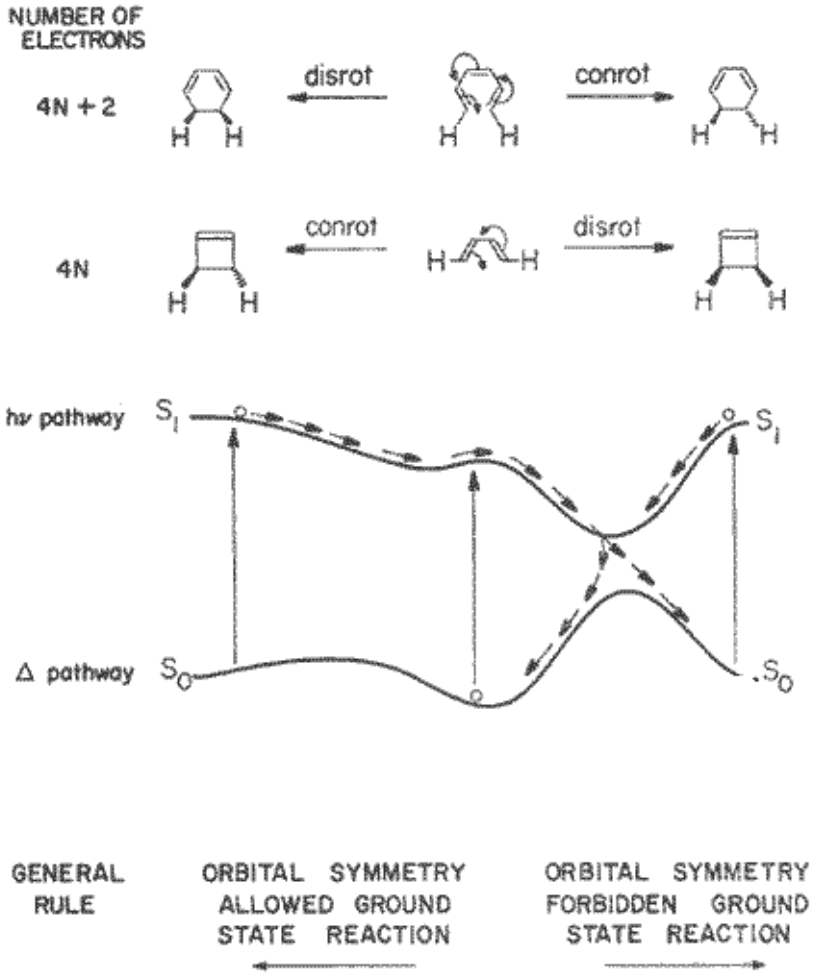

Figure 6.16 A simplified, general schematic description of the two lowest singlet surfaces for a concerted pericyclic reaction. The selection rules are shown for 4N electron and for 4N + 2 electron

reactions (N = 0 or an integer and 4N or 4N + 2 is the number of electrons involved in bond making or bond breaking).

To a first approximation the topology state correlation diagram shown in Figure 6.16 below may be extended to all concerted pericyclic reactions. For four (or more generally 4N) electron concerted pericyclic reactions the disrotatory (or stereochemically equivalent) pathway corresponds to motion from the center of the diagram to the right and the conrotatory (or stereochemically equivalent) pathway corresponds to motion from the center of the diagram to the left. We see that this means that four (or 4N) electron concerted pericyclic reactions are generally photochemically allowed.

For six (or more generally 4N + 2) electron concerted pericyclic reactions the disrotatory (or stereochemically equivalent) pathway corresponds to motion from the center of the diagram to the left and the conrotatory (or stereochemically equivalent) pathway corresponds to motion from the center of the diagram to the right. Thus, 4N + 2 electron concerted photoreactions are forbidden.

These ideas are illustrated in Figure 6.15 for the electrocyclic reactions of cyclobutene-1,3-butadiene and 1,3-cyclohexadiene-1,3,5-hexatriene. For example, the disrotatory four electron ring closure of 1,3-butadiene to cyclobutene (and the reverse ring opening) is photochemically *allowed* and the analogous conrotatory electrocyclic reaction is photochemically *forbidden*.

These ideas are illustrated in Figure 6.15 for the electrocyclic reactions of cyclobutene-1,3-butadiene and 1,3-cyclohexadiene-1,3,5-hexatriene. For example, the disrotatory four electron ring closure of 1,3-butadiene to cyclobutene (and the reverse ring opening) is photochemically *allowed* and the analogous conrotatory electrocyclic reaction is photochemically *forbidden*. In contrast, the conrotatory six electron closure of 1,3,5-hexatriene to 1,3-cyclohexadiene is photochemically *allowed*.

In summary, concerted pericyclic reactions which are ground-state-forbidden are generally excited-state-allowed in S_1 because the surface topology of S_1 will generally possess a minimum which corresponds to a diradicaloid structure which possesses the geometry of the "antiaromatic" transition state on S_0. By contrast, pericyclic reactions which are ground-state-allowed will generally be forbidden on the S_1 surface because of the existence of a barrier to conversion to product structure and the lack of a suitable surface crossing to allow for the occurrence of a radiationless jump from S_1 to S_0.

6.11 Typical State Correlation Diagrams for Nonconcerted Photoreactions: Reactions Involving Intermediates (Diradicals and Zwitterions)[4,5]

The majority of known photoreactions of organic molecules are probably not *concerted* (*R → P) in nature. Rather, photochemical reactions tend to involve reactive intermediates along the reaction pathway (*R → I). The most common photochemical intermediates (I) are species which are not fully bonded, and possess two electrons in two orbitals of nearly comparable energy, i.e., the reactive intermediates correspond to diradicaloid structures (D, radical pairs and diradicals) and zwitterionic structures (Z, zwitterions). Figures 6.7 and 6.8 showed the surface topologies associated with the strecthing and breaking of a σ bond and the twisting and bending of a π bond, respectively. Figure 6.6 summarizes the relationships between these two fundamental surface topologies and the D and Z structures. For completeness, a strained molecule is included as a possible reactive intermediate, I, along the pathway to the D/Z structures. It is not uncommon for the representative point, while moving along an excited surface, to achieve, and temporarily maintain, a geometry similar to a "strained ground state molecule." Radiationless transitions to such structures may produce very strained species which are, nonetheless, stable to some extent on the ground state surface. Indeed, in Chapter 10 we shall see that photoreactions of ethylenes often produce strained ground state molecules as products.

We have characterized electronically excited states in terms of two characteristic half-filled SO orbitals (HO and LU of the ground state). We have seen (Figures 6.7 and 6.8) that motion along a reaction coordinate due to stretching a σ-bond or due to twisting a π-bond may bring the representative point to a geometry for which the two half-filled orbitals are nearly degenerate and which corresponds to a surface touching. In this geometry[5] the molecular structure is termed a "diradicaloid." As we have see such geometries which general two nearly degenerate orbital and generate four distinct electronic states: a diradical singlet ^1D; a diradical triplet ^3D; and two zwitterionic singlets, Z_1 and Z_2. The postulate that an electronically excited state corresponding to one of the topologies of Figures 6.7 and 6.8 tends toward a D

or Z primary product as a reaction proceeds is an exceedingly powerful device for interpreting the photoreactions of organic molecules of the type *R → I.

An Exemplar for the Photochemical Reactions of n,π* States

We shall use the hydrogen abstraction reaction of the n,π* state of ketones as an exemplar to derive prototypical orbital and state symmetry correlation diagrams for *R → I reactions which produce radical pair and diradical intermediates. This reaction may be initiated by a σ HO → n_OSO or π* SO → π*LU charge transfer orbital interaction (Figure 6.12). The results of the orbital and state correlation diagrams may be immediately applied to reactions involving n_N HO → n_O SO and $\pi_{C=C}$ → n_O SO interactions (electron abstraction and addition to π bonds).

The photoreaction of n,π* excited ketones with alcohols (Eq. 7.4) involves primary photochemical hydrogen abstraction which produces a radical pair intermediate as the primary photochemical product, I.[11] The radical pair undergoes radical-radical combination and disproportional reactions (eq. XX).

The state correlation diagram for the reaction of the n,π* state of a ketone is typical of a large class of photoreactions which involve radical pair and diradical intermediates and, as mentioned above, can be extended to all photochemical reactions that are initiated by the n_O orbital of the n,π* state. As a result this is an exemplar reaction and we shall discuss it in some detail. For most alkanones, such as acetone, S_1 = n,π* and T_1 = n,π*. Thus, our correlation diagram will seek to connect these states, and $S_0 = \pi^2n^2$ with the appropriate states of the product (D and Z states). We need to select a reaction coordinate in order to construct an orbital or state correlation diagram. What is a proper reaction coordinate for hydrogen abstraction by an n,π* state? To determine the most likely reaction coordinate, we must select the most favorable orbital interactions, search for elements of symmetry in the geometry of the reactants that lead to the most favorable orbital interactions, and then relate that symmetry element to establish a correlation along the reaction coordinate of the reactant to the primary product transformation.

For concreteness we shall analyze the reaction of formaldehyde with a hydrogen donor XH. Since a X-H bond of a hydrogen atom donor is being broken in the reaction and a HO bond is being made in the ketone, we select the charge transfer σ_{XH} HO → n_O SO orbital as the initiating interaction. Since the degree of positive overlap of these two orbitals changes only slightly with the specific degree of orientation of the two molecules involved in the reaction, we select the most symmetrical geometry for reaction in order to construct a state correlation diagram: this it is a geometry for which all of the atoms involved in the reaction are in the same plane (Figure 6.17, bottom).

We shall generate an orbital and state correlation diagram *assuming* that the strictly planar approach shown in Figure 6.17 represents the reaction coordinate. This assumption of an idealized coplanar reaction should provide a reasonable, qualitative Zero Order description of the surfaces. In general, the *plane* containing the pertinent reaction centers will be a *discriminating symmetry element* for selecting the reaction coordinates of n,π* states which lead to diradicaloid geometries. Let us now consider the consequences of this assumption in greater detail.

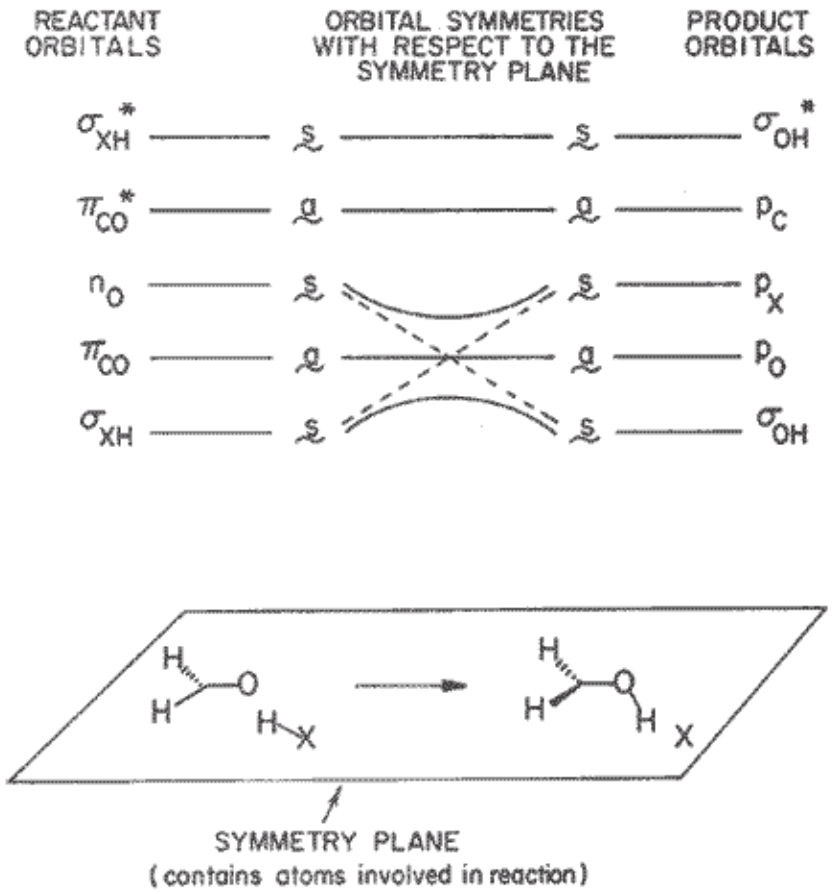

Figure 6.17 Orbital correlation diagram for coplanar hydrogen abstraction by formaldehyde.

The Symmetry Plane Assumption: Salem Diagrams[6]

An extension of the idealized symmetry plane shown in Figure 6.17 need only refer to a plane containing the nuclei *directly* involved in the electronic configuration approximation, i.e., the atoms in the C=O and HX bonds. In the case of $H_2C=O$ and XH, the pertinent atoms possess the orbitals associated with the charge transfer interactions that initiate the photochemical hydrogen abstraction. Under these assumptions the correlation between states of the same symmetry may be made by a simple electron classification and electron counting procedure. In turn, this classification and electron count may be simplified by using classical resonance structures for describing the electronic states involved (Figure 6.18). These resonance structures can only possess electrons in idealized orbitals which are either symmetric, **s** (do not change sign upon idealized reflection in the symmetry plane), or antisymmetric, **a** (change sign upon idealized reflection in the symmetry plane). The postulate of an idealized symmetry plane demands that orbitals possesses either **a** or **s** symmetry.

An Exemplar for n-Orbital Initiated Reactions of n,π* States: Hydrogen Abstraction

According to the principles of orbital interactions, the primary photochemical reactions of n,π* states are initiated by charge transfer to the electrophilic half filled n orbital or from the half filled π* orbital. Experimentally, the electrophilic n orbital dominates the initial interactions of n,π* states. For example, the four most important reactions of the n,π* states of ketones (hydrogen atom abstraction, electron abstraction, addition to double bonds and α-cleavage) are typically initiated (Figure 6.12) by

interaction of the half filled n orbital with a σ bond (hydrogen atom abstraction and α-cleavage), with a π bond (addition to double bonds) or with an unshared pair of electrons (electron abstraction). Each of these primary photochemical reactions can be described in terms of a similar orbital and state correlation diagram.

The pertinent orbitals for analysis of ***coplanar*** hydrogen abstraction are shown in Figure 6.17, top. This geometry is selected since it represents the best frontier orbital interaction between the n_o and σ_{XH} orbitals and because the assumption of a planar geometry allows a ready classification of the pertinent orbitals. The orbitals of the reactants are classified relative to the symmetry plane in a conventional notation. Any orbital which lies "in the plane" must be of **s** symmetry (i.e., the σ_{XH}, n_o, and σ^*_{XH} orbitals). Any orbital that exists "above and below" the plane must be of **a** symmetry (i.e., the π_{co} and π^*_{co}orbitals).

The pertinent product orbitals are σ_{OH} and σ^*_{OH} (both of **s** symmetry) and the p orbitals on carbon (p_c "above and below", **a**), the p orbital on X (p_x "in the plane," **s**) and the p orbital on O (p_o "above and below," **a**). From Figure 6.17, the initial (Zero Order) orbital correlations are maintained during reaction, except for the σ_{XH} p_X and n_0 σ_{OH} correlations which are *assumed to be avoided* (non-crossing rule for orbitals of the same symmetry). We shall return to this assumption later.

Remember that completely filled orbitals are always totally symmetric (**S**) with respect to a symmetry element (i.e., **A** x **A** = **S** and **S** x **S** = **S**), but half-filled orbitals may be **A** (i.e., **A** x **S** = **A**). Since the state symmetry of reactants by evaluating the product of the symmetry of appropriate reactant and primary product orbitals.

From Figure 6.17, the state symmetries of the reactants and products are easily deduced. For example, S_0 must be of **S** symmetry because it possess only doubly occupied orbitals. The symmetry of the n,π* state is **s** x **a** = **A**, the symmetry of the π,π* state is **a** x **a** = **S**, the symmetry of the D(p_c, p_x) state is **s** x **a** = **A**, and the symmetry of a Z state must be **S** because it possesses only doubly occupied orbitals.

We may now proceed to the Zero Order state correlation diagram or *Salem diagram* (Fig. 6.18) by connecting states of the same symmetry. We need consider only the number of states necessary to correlate S_1 and T_1 with product states. From Figure 6.18 we see that both S_1 and T_1 states correlate directly with the lowest states of the product, i.e., $S_1 = {}^1$n,π* correlates with ^{1}D and $T_1 = {}^3$n,π* correlates directly with ^{3}D. We say that coplanar hydrogen abstraction to form ketyl radicals from S_1(n,π*) or T_1(n,π*) is symmetry-allowed. By this we mean that in Zero Order, there is no electronic symmetry-imposed energy barrier on the surface connecting the initial excited state n,p* of a given spin and the lowest energy primary (diradical) product of the same spin.

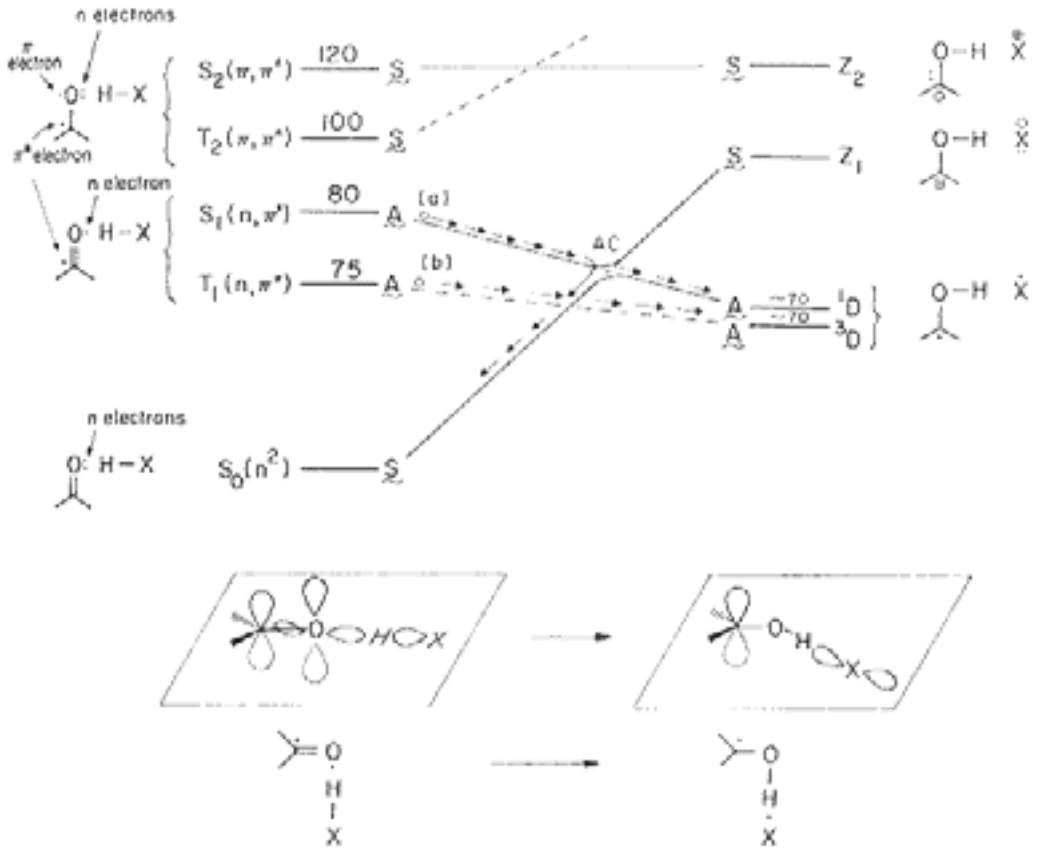

Figure 6.18 First Order correlation diagram for coplanar hydrogen abstraction. State energies in kcal/mole.

On the other hand, The S_2 and T_2 states (both π,π*) correlate with excited states of the zwitterion forms of the product. These excited zwitterionic states are expected to have very high energies relative to S_2 and T_2. As a result, if S_2 or T_2 were to attempt to participate in coplanar hydrogen abstraction, a symmetry-imposed energy barrier would have to be overcome. We say that coplanar hydrogen abstraction to form ketyl radicals is symmetry-forbidden from $S_2(\pi,\pi^*)$ or $T_2(\pi,\pi^*)$.

We may now propose how a First Order surface description of the hydrogen abstraction reaction may be derived from Figure 6.18. Destruction of the perfect coplanar geometry will result in a weakly avoided crossing between the $S_1 \rightarrow {}^1D$ and $S_0 \rightarrow$ Z surfaces. However, the $T_1 \rightarrow {}^3D$ and $S_0 \rightarrow$ Z crossing will remain, since the multiplicity (spin symmetry) of the crossing surfaces is still different. The result of the avoided crossing is to put a minimum along the S_1 surface. Since the symmetry of the two states crossings are different, the crossings are weakly avoided at best. This means that the situation is close to a real crossing and may correspond to a conical intersection. As a first approximation, we shall consider the consequences of the Zero Order crossing may be either a weakly avoided crossing or a conical intersection.

From Figure 6.18 we conclude that there are two low-energy pathways from n,π* states for the representative point in coplanar hydrogen abstraction reactions. These two pathways are:

1. From the ${}^1n,\pi^*$ state the representative point may proceed to decrease its energy until it reaches the geometry corresponding to the surface crossing. This crossing is either weakly avoided crossing (AC) or is a conical intersection (CI). What are the consequences of this AC or CI? We note that the occurrence of AC or CI has no effect on *reactivity*, i.e., the rate of reaction is determined by the energy barriers near the S_1 minimum. These small activation energies are not due to correlation effects and their possible origins will be discussed below in terms of natural correlation diagrams. However, the *efficiency* of

reaction from S_1 may be decreased since entry into the AC or CI allows partitioning from the excited surface to either S_0 of ^1D (by providing a "born-Oppenheimer hole" for radiationless transition from S_1 to S_0 or D_1), whereas in Zero Order only passage from S_1 to ^1D was allowed.

2. From the $^3n,\pi^*$ state the representative point may decrease its energy by moving directly to ^3D, i.e., proceeding through the crossing of T_1 and S_0 surfaces. Of importance is the fact that the reactivity and efficiency of T_1 are the same in both First and Second Order since the surface crossing involves a spin change and can be only weakly avoided at best.

Natural correlation diagrams.

The process of constructing state diagrams corresponding to adiabatic surfaces may proceed in two ways: (1) an intended or natural orbital correlation may be used first with interactions at the crossing points and then the resulting "adiabatic" correlations are used to construct the configuration and adiabatic state correlation diagrams or (2) an intended or natural orbital correlation may be made without interactions between orbitals, then the resulting "diabatic" correlations are used to construct the configuration diagram and finally the interactions are turned on to generate the adiabatic state correlation diagram. We shall now discuss how the second procedure is useful in producing insight to the presence of small barriers which are typical of many photochemical reactions, even those which are allowed by thermodynamic considerations and allowed according to the state energy diagram.

Because photochemical primary processes ($^*R \rightarrow$ I and $^*R \rightarrow$ P) must compete with relative fast photophysical processes ($^*R \rightarrow$ R), photochemical primary processes can only be efficient if small or zero energy barriers (energy maxima) exist along the pathways $^*R \rightarrow$ I and $^*R \rightarrow$ P. The qualitative adiabatic correlations at the *state* level fail to reveal the (often small) maxima that arise on potential energy surfaces as the result of avoided crossings at the *orbital* level. Orbitals tend to follow a "natural" change of shape allow a reaction coordinate, that is the wavefunctions which the orbitals represent have a natural tendency to converse their *local* phase relationships and *local* electronic distributions in addition to the conservation of overall state symmetry properties. Furthermore, in a natural correlation diagram two lines associated with the correlation of orbitals in the initial state ($^*R$) and final state (I or P) are always allowed to cross in order to emphasize the *intended* natural correlations of the orbitals, before any interactions are allow to "mix" the orbitals and produce the adiabatic correlation diagram. These crossings may provide insight to the source of small energy barriers (or energy minima which may result in either avoided crossings or conical intersections) because they indicate where the orbitals want to go naturally in the absence of mixing. Thus, is mixing is weak for any reason, the natural orbital correlation may be examined as the basis for barriers or minima. In a sense the natural correlation maxima or minima are "memories of avoided crossings" in the state correlation diagram.

The Natural Orbital Correlation Diagram for n-Orbital Initiated Reactions of n,π^* States: Hydrogen Abstraction by Ketones

As discussed above, the main orbitals that need to be considered in the initial state of hydrogen abstraction by a n,π^* state of a ketone are the σ_{CH} and σ_{CH}^* orbital of the hydrogen donor (assumed to involve abstraction of a CH bond), the n_O orbital on oxygen and the π_{CO} and π_{CO}^* of the CO chromophore. The main orbitals of the final product are the σ_{OH} and σ_{OH}^* orbitals of the OH bond of the ketyl radical, the n_C lone pair orbital of the carbon atom of the hydrogen donor and the π_{CO} and π_{CO}^* of the CO chromophore. The natural correlation diagram for hydrogen abstraction assume a reaction plane which includes the n_O orbital and the σ_{CH} bond, is shown in Figure 6.17. From this natural orbital correlation diagram, a state correlation diagram is readily constructed (Figure 6.18). The "natural orbital correlation" of the $^{1,3}(n,\pi^*)$ configuration is to a high energy σ_{OH}, π_{CO}^* configuration, not to the product which has a n_C, π_{CO}^* configuration. Thus, in contrast to the state correlation diagram, it would appear that in the orbital correlation approximation, hydrogen abstraction by a n,π^* state is "orbitally forbidden". The fact that the hydrogen abstraction is observed to occur experimentally with a small barrier, can be rationalized as the result an avoided crossing which "pushes down" the size of the energy barrier of the Zero Order surface crossing. Thus, an energy barrier exists in the direct correlation of states when there is some "work to be

done" is reorganizing the natural orbital pathways. We have seen that in quantum mechanics smooth transitions of wavefunctions are favored over transitions which require distortions during the transition. The orbital correlation diagram is faithful to the smooth transitions and minimum distortions of the wavefunctions of the local orbitals in going from initial to final states. The state correlation assumes that the wavefunction of the state can smoothly handle the orbital distortions. This will of course, only be true if the natural orbital distortions are small along the reaction pathway. When the natural orbital correlations require significant distortions, small barriers may along surfaces which have "direct overall" electronic correlations.

Extension of a Given State Correlation Diagram to New Situations

A combination of the methods of orbital interactions and state correlation diagrams allows us to generalize the correlation diagram for hydrogen abstraction to other reactions of n,π* state. At the orbital level, the key electronic features of hydrogen abstraction are the charge transfer from a H-X σ orbital to the half-filled n_O orbital (Figure 6.12). We may postulate that any reaction whose electronic mechanism is dominated by electrophilic attack by the n_O orbital will have the same surface topology as that deduced for hydrogen abstraction (Fig. 6.18).

For example, n,π* states of ketones are known to (a) abstract electrons from amines (and other electron donors), (b) add to electron-rich ethylenes, and (c) transfer energy to electron-rich unsaturated compounds. On the basis of orbital interactions, each of these reactions is expected to be dominated by electrophilic attack by the n_{oO} orbital of the n,π* state. In each case a radical pair or diradical intermediates is possible and the same generalizations and expectations as were made for hydrogen abstraction are possible. In other words, the topology of Figure 6.18 may be employed for the three reactions discussed above.

6.13 State Correlation Diagrams for α-Cleavage of Ketones[10]

A commonly observed fragmentation reaction of n,π* states of carbonyl compounds is the cleavage of a C-C σ bond which is α to the excited carbonyl group.[11] For example, the n,π* states of acetone undergoes α-cleavage to acyl and methyl radicals (eq. 6.11). This reaction is an analogue of the cleavage of a hydrogen molecule (Figure 6.7) and as the C-C bond is stretched a diradicaloid geometry is approached.

$$CH_3COCH_3 \rightarrow \underset{n,\pi^*}{CH_3COCH} \rightarrow CH_3CO^{\cdot} + {}^{\cdot}CH_3 \qquad (6.11)$$

The α-cleavage reaction is an exemplar for an interesting variation in the topologies for the surface correlations of n,π* states. The reaction coordinate in this case is essentially the distance separating the carbonyl carbon and methyl carbon atoms (some motion of the CH_3-CO moiety may also occur). The S_1 and T_1 states are both n,π* and both are **A** with respect to the characteristic symmetry plane associated with the reaction (Figure 6.19). However, in contrast to the situation for hydrogen abstraction, there are two diradicaloid geometries that can be produced at the acyl carbon atom by α-cleavage: (a) a geometry corresponding to a bent CH_3CO group, and (b) a geometry corresponding to a linear CH_3CO group. The two lowest energy electronic states of these structures have different electronic symmetries relative to the characteristic symmetry plane. This result occurs because the bent form of CH_3CO will be sp^2 hybridized at the carbonyl carbon, whereas the linear CH_3CO will be *sp* hybridized at the carbonyl carbon (Fig. Figure 6.19). The bent acyl radical site (sp^2 orbital) generated in the bent acyl group remains in the symmetry plane, and is therefore **s** with respect to coplanar cleavage. The important new feature of the linear acyl radical is that two π orbitals are generates when the system approaches the linear geometry.

The linear acyl group possesses a $\pi_{\mathbf{s}}$ orbital which is in the symmetry plane and a second $\pi_{\mathbf{a}}$ orbital which is perpendicular to the symmetry plane. Thus, the π_s orbital is **s** and the $\pi_{\mathbf{a}}$ orbital is **a** with respect to coplanar cleavage. Thus, ***two degenerate electronic states correspond to the linear acyl-methyl radical pair***. One state ($\pi_{\mathbf{s}}$, p) is **S** and the other state ($\pi_{\mathbf{A}}$,p) is **A** with respect to the symmetry plane. The number

of distinct radical sites developed during a reaction is termed the reaction ***topicity***.[6] Since α-cleavage to produce a bent acyl radical and alkyl radical produces two distinct radical sites, it is said to have a topicity equal to two. On the other hand, α-cleavage to produce a linear acyl radical and alkyl radical produces three distinct radical sites and is said to have a topicity of three. In the latter case, an odd electron may be in the π_s or π_a orbital, leading to two different diradical pairs.

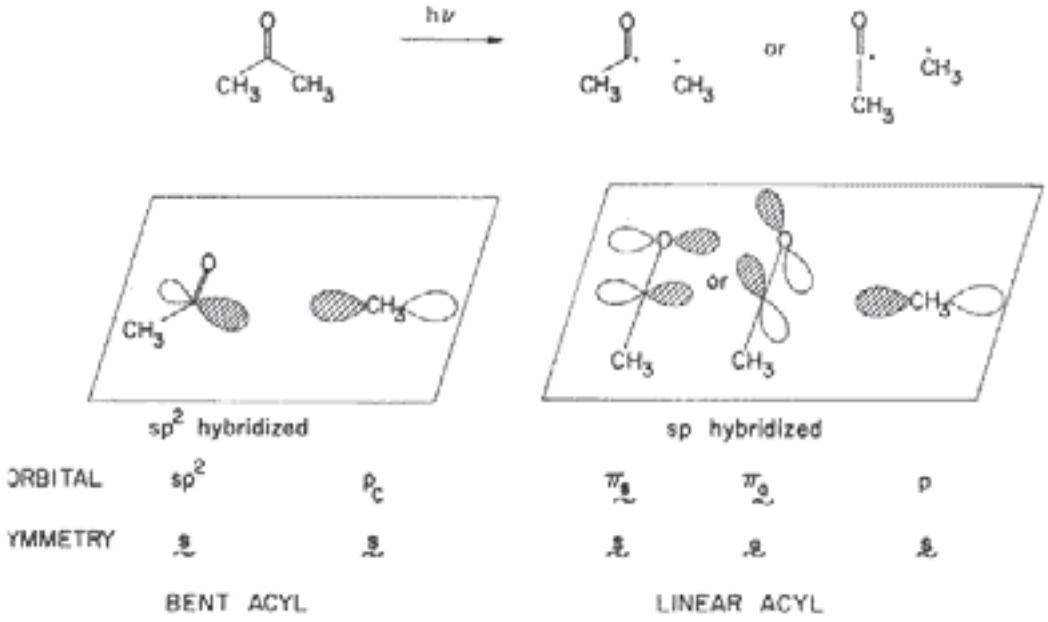

Figure 6.19 ***α-cleavage of acetone. Either a bent acyl or a linear acyl fragment may be formed.***

Topicity can have a major influence on the topology of a correlation diagram. Let us construct the correlation diagram for α-cleavage by proceeding in the usual manner. First we identify the symmetry of the key orbitals involved in the transformation. The orbital correlation is given in Figure 6.20. Notice that the half-filled orbital on CH_3 is assumed to be a p orbital contained by the discriminating reaction plane, i.e., this orbital is of **s** symmetry.

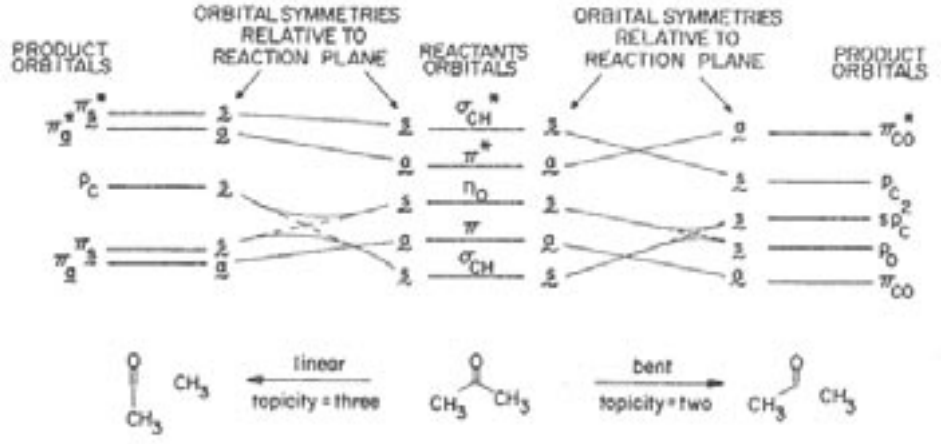

Figure 6.20 ***Orbital correlation diagrams for bent (right) and linear (left) α-cleavage of acetone.***

We may now construct the Zero Order state correlation diagram (Fig. 6.21). In the case of cleavage to form a linear acyl fragment, the lowest excited states $S_1(n,\pi^*)$ and $T_1(n,\pi^*)$ correlate directly to low-lying $^1D(\pi_a,\pi_c)$ and $^3D(\pi_a,p_c)$ states. However, for the cleavage to form bent acyl, $S_1(n,\pi^*)$ and $T_1(n,\pi^*)$ correlate with excited forms of D, namely $D^*(sp^2, \pi^*_{co})$. As a result, the initial slope of the surface for cleavage from an n,π* state to a bent acyl rises steeply as this state tries to correlate with D*, ***and excited state of the diradical***.

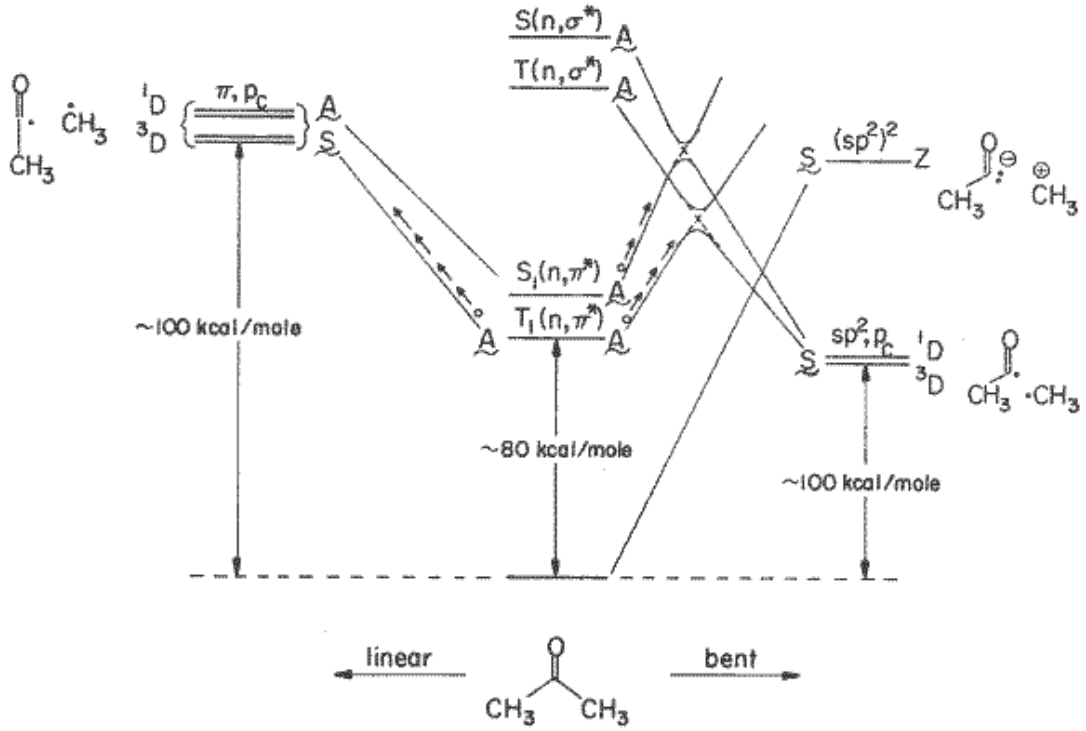

Figure 6.21 Zero Order state correlation diagram for bent (right) and linear (left) α-cleavage. Circled crossings are weakly avoided.

From the Zero Order diagram (Fig. 6.20) we deduce that α-cleavage of n,π* states to yield a linear acyl fragment is symmetry-allowed, but that α-cleavage of n,π* states to yield a bent acyl fragment is symmetry-forbidden.[12] Thus, the pathway of higher topicity is allowed, whereas the pathway of lower topicity is forbidden.

Now let us consider a more realistic First Order correlation diagram (Fig. 6.21) which depicts α-cleavage for acetone. The state and diradical energies are also shown. The situation for cleavage to the linear fragment is essentially the same. However, weakly avoided crossings occur along the surfaces for cleavage to the bent acyl fragment (circled in the Zero Order diagram, Fig. 6.21). Notice, however, that the $T_1(n,\pi^*)$ surface is subject to a First Order crossing at an earlier point than $S_1(n,\pi^*)$. This earlier crossing may lead to a lower energy symmetry-imposed energy barrier for cleavage of $T_1(n,\pi^*)$ relative to $S_1(n,\pi^*)$.

Figure 6.22 First Order correlation diagram for α-cleavage.

6.14 A Standard Set of Plausible Primary Photoreactions for π,π* and n,π* States

We have noted that the most commonly encountered lowest-energy excited states of organic molecules may be classified as $S_1(\pi,\pi^*)$, $T_1(\pi,\pi^*)$, $S_1(n,\pi^*)$ or $T_1(n,\pi^*)$. In this chapter we have seen how

theory can lead (a) to a prediction of the possible (i.e., low-energy) primary photochemical processes via the consideration of orbital interactions, and (b) to the generation of the network of surface (reaction) pathways via the maps which result from state correlation diagrams. Now we can create a list of ***all of the expected plausible primary photoreactions of S_1 and T_1*** based on the above theoretical considerations.

The Characteristic Primary Photochemistry Processes of π,π* States

From the above discussion of orbital interactions and potential energy surfaces, we expect $S_1(\pi,\pi^*)$ states to undergo concerted pericyclic photoreactions according to the Woodward-Hoffmann rules. The favored stereochemical pathways of these reactions can be predicted by considering orbital interactions, and the prototype surface topology for such reactions will be analogous to Figures 6.15 and 6.16.

Since $S_1(\pi,\pi^*)$ states will often possess a substantial zwitterionic character, and this zwitterionic character is enhanced as the double bond twists and mixing with $S_2(\pi^*)^2$ occurs. As a result, the formation of radical pairs and/or of diradicals is not expected when *R is $S_1(\pi,\pi^*)$. The $S_1(\pi,\pi^*)$ excited state is expected to behave as a zwitterion, i.e., a carbonium ion/carbanion. Thus, the plausible set of reactions are proton or electron transfer reactions, nucleophilic or electrophilic additions, or carbonium or carbanion rearrangements to produce intermediates which will then proceed to isolated products.

Finally, $S_1(\pi,\pi^*)$ of ethylenes and polyenes will often possess an inherent tendency to twist its double bonds, which is a process that leads to twisted zwitterionic intermediates and/or cis-trans isomerization.

Thus we may now tabulate the list of plausible primary photochemical reactions that are initiated in $S_1(\pi,\pi^*)$:

1. Concerted pericyclic reactions (electrocyclic rearrangements, Cylcoadditions, Cycloeliminations, Sigmatropic rearrangements, etc.).

2. Reactions characteristic of carbonium ions (carbonium ion rearrangements, addition of nucleophiles, etc.) and of carbonanions (addition to electrophilic sites, protonation, etc.)

3. Cis-trans isomerization.

Granted that $S_1(\pi,\pi^*)$ has the possibility of the above set of characteristic reactions, the rate of any one of these reactions will depend on the reactant structure and the reaction conditions. The probability of any reaction from $S_1(\pi,\pi^*)$ will depend on a competition between the rate of reaction and the rate of other photophysical or photochemical pathways from $S_1(\pi,\pi^*)$.

$T_1(\pi,\pi^*)$ is not expected to undergo concerted pericyclic reactions (unless the product can be produced in a triplet state or if a good spin-orbit coupling mechanism is available along the reaction coordinate, both of which are improbable). Thus a concerted pericyclic reaction is not considered as a member of the plausible set of reactions from $T_1(\pi,\pi^*)$. Indeed the reactions of $T_1(\pi,\pi^*)$ should be typical of those of a carbon radical, and the major pathway of reaction of $T_1(\pi,\pi^*)$ is expected to be formation of a triplet radical pair or triplet diradical, i.e., $T_1(\pi,\pi^*) \rightarrow {}^3D$. The ***typical reactions of a carbon centered radical are identical to the reactions of an oxygen centered radical***. Of course, the rates of the reactions for the two types of radicals may differ dramatically, but the types of reactions are identical. Using the n_O as a model for an oxygen radical leads to the following plausible set of primary photochemical reactions initiated from the $T_1(\pi,\pi^*)$:

1. Hydrogen atom or electron abstractions.

2. Addition to unsaturated bonds.

3. Homolytic fragmentations.

4. Rearrangement to a more stable carbon centered radical.

In addition, $T_1(\pi,\pi^*)$ will generally possess an inherent driving force to twist about double bonds, a process that could lead to cis-trans isomerization or twisted diradical intermediates, which in turn can undergo transition to a strained twisted ground state.

The Characteristic Primary Photochemical Processes of n,π* States

The photochemistry of n,π* states can be expected to contrast with that for π,π* states in two major respects: (a) the photochemistry of $S_1(n,\pi^*)$ and $T_1(n,\pi^*)$ for a given molecule should be qualitatively identical and differ only quantitatively in terms of rates. On the other hand, reactions expected from $S_1(\pi,\pi^*)$ and $T_1(\pi,\pi^*)$ differ qualitatively, i.e., zwitterionic and/or concerted versus diradicaloid and non-concerted, respectively; and (b) the photochemistry of n,π* states is completely diradicaloid to a good approximation, i.e., $n,\pi^* \rightarrow$ D processes are typical.

Based on an orbital interaction analysis (Fig. 6.12), and the postulate that all n,π* reactions proceed preferentially via D states (Fig. 6.14), we can conclude that the primary photochemical processes of n,π* will produce radicals and that the overall photoreactions will mimic radical chemistry. Let us consider that the plausible primary processes expected from a theoretical standpoint are:

n-Orbital Initiated	**π*-Orbital Initiated**
Atom abstraction	Atom abstraction
Radical addition	Radical addition
Electron abstraction	Electron donation
α-Cleavage	β-Cleavage

Although both atom abstraction and radical addition are expected in theory to be initiated by either the n or by the π* orbitals, the former will exhibit *electrophilic* and the latter will exhibit *nucleophilic* characteristics. The reactions initiated by the n orbital will be analogous to those of an alkoxy radical (RO) and the reactions initiated by the π* orbital will be analogous to those of a ketyl radical (R_2COR). Furthermore, the stereoelectronic dispositions of the reactions will differ, depending on which orbital dominates the electronic interactions with the substrate. For example, if the n orbital initiates the interaction, the reaction will be sensitive to steric factors influencing the approach of the substrate in the plane of the molecule and near the "edges" of the carbonyl oxygen. On the other hand, if the π* orbital initiates the reaction, the reaction will be sensitive to steric factors which influence the approach of the substrate above and below the "faces" of the carbonyl function. Convincing experimental support for these predictions is given in Chapter 9.

Since the π* orbital is delocalized, attack may be initiated predominantly at the carbon atom or at the oxygen atom. Ignoring the specifics of the substrate (which is either an atom donor or an electron abstractor), we note that if the reaction is initiated by the π* electron, only the addition to carbon produces a low-energy diradical state. Attack of the π* orbital to produce a bond to oxygen produces an electronically excited diradical and will therefore encounter a symmetry-imposed energy barrier. Convincing experimental support for these predictions is given in Chapter 9.

6.15 Intersystem Crossing in Radical Pairs and Diradicals.

The theory of photochemical reactions of organic molecules presented in this chapter reveals that a majority of primary photochemical processes ($^*R \rightarrow I$) will produce a reactive intermediate, I, that can be characterized as a radical pair or a diradical. If the primary process involves a $S_1 \rightarrow {}^1I$ process, there is no spin prohibition to the elementary step $^1I \rightarrow P$. Thus, only ***singlet*** radical pairs or ***singlet*** diradicals are produced as reactive intermediates from S_1. Such species are expected to undergo one of two extremely rapid reaction involving the radical centers: recombination or disproportionation (Chapter 8). The rates of these radical-radical reactions are often faster than diffusional separation of the fragments of the radical pair or faster than stereochemical change of conformation due to rotation about C-C single bonds. Thus,

even though S_1 may produce a radical pair or a diradical, the reactions of these species may be stereospecific.

However, if the primary photochemical process involves a $T_1 \rightarrow {}^3I$ process, there is a spin prohibition to the elementary step of ${}^3I \rightarrow P$. Thus, there will be a delay imposed on product formation until intersystem crossing, ${}^3I \rightarrow {}^1I$ occurs. If the rate of intersystem crossing for the triplet radical pair is slow relative to diffusional separation of the fragments of the radical pair, the two fragments will separate with high efficiency and free radical formation will result. All of the products formed will proceed through free radicals and the pathway $T_1 \rightarrow {}^3I \rightarrow {}^1I \rightarrow P$. If the rate of intersystem crossing for a diradical is slow relative to the rates of rotation about C-C bonds, loss of stereochemistry will occur in any intramolecular reactions of the diradical.

We has seen in Chapter 4 that spin orbit coupling is the dominant mechanism for intersystem crossing from S_1 to T_1 and T_1 to S_0 in organic molecules. However, in radical pairs and diradicals this may not be the case. Under certain circumstances spin-orbit coupling is "quenched", i.e., made inefficient. When this is the case, in addition to spin-orbit interactions, very weak magnetic interactions with nuclear spins and laboratory magnetic fields, which are completely negligible for organic molecules, may determine the rate of intersystem crossing. This situation is common for triplet reactions for n,π^* ketones. We shall use the α-cleavage reaction of triplet ketones as an exemplar to explore the theory of intersystem crossing for radical pairs and diradicals.

6.16 Magnetic Energy Diagrams Including the Electron Exchange Interaction.

As discussed in Chapter 2 (Section 2.37), it was noted that the electron exchange interaction, J, between two electrons, results in a Coulombic (non-magnetic) splitting of the energy of the singlet state (S) from the triplet state (T). As a result, the magnetic energy diagrams of radical pairs and diradicals had to take into account the extent of electron exchange. When the value of J is very small and comparable to the strength of magnetic interactions which cause spin flips and spin rephasing, external magnetic fields from nuclear spins and applied laboratory magnetic fields can influence the rate of intersystem crossing of the radical pair or diradical. The term low field refers to situation for which the splitting between the magnetic sublevels (in a doublet, D, or a triplet, T) are small relative to the value of J. The term high field refers to situation for which the splitting between the magnetic sublevels (in a doublet, D, or a triplet, T) are large relative to the value of J. There are four important conditions which are commonly encountered in photochemical systems, two corresponding to zero of low field and two corresponding to high field (Figure 6.23). The first is the condition for which J = 0 in the presence of a zero (or low) magnetic field. Condition I is typical of solvent separated spin correlated geminate pairs and extended biradicals. The second condition is in the presence of zero (or low) magnet field with a finite value of J. Condition II is typical of molecular triplets, spin correlated pairs in a solvent cage and small biradicals. Condition III occurs at high field for values of J which 0 or are comparable to the Zeeman splitting (i.e., $J = 0$ or $J \sim g\mu_e H$) and condition IV occurs for values of J which are much larger than the Zeeman splitting (i.e., $J >> g\mu_e H$). these situations will be analyzed in detail in the following sections with a "case history" example.

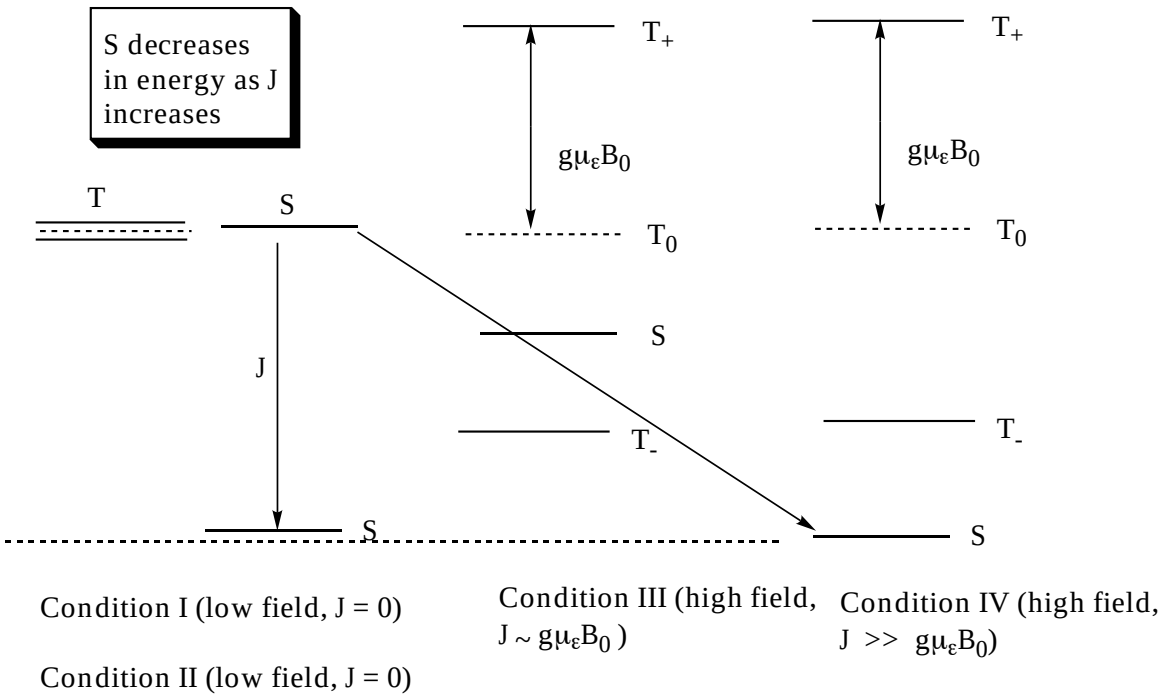

Figure 6.23. Three important situations of Zeeman splitting and exchange splitting. See text for discussion.

6.17 Magnetic Interactions and Magnetic Couplings

Transitions between the magnetic energy levels discussed in the previous section can be visualized as occurring through the result of magnetic torques exerted on the magnetic moment vectors of an electron spin, or equivalently, as the result of coupling of spin angular momentum to another angular momentum. Spin-orbit coupling is one such interaction in which the magnetic moment is generated by the orbital motion of the electron. Coupling of this spin-orbit induced magnetic moment with the spin magnetic moment provides a mechanism for spin flips and spin rephasing the leads to intersystem crossing. In addition to the magnetic moment due to spin-orbit coupling (which is the major mechanism for intersystem crossing in molecules), two other magnetic couplings are important for intersystem crossing in radical pairs and diradicals: the magnetic coupling of an electron spin to the magnetic moment due to a nuclear spin (termed electron-nuclear hyperfine coupling) and the coupling of an electron spin to the magnetic moment of a laboratory magnetic field (termed Zeeman coupling). We now need to review the two major magnetic interactions which induce intersystem crossing.

Dipolar and Contact Magnetic Interactions

A magnetic moment is a magnetic dipole, i.e., the magnetic moment gives rise to a magnetic field in its vicinity and can be considered to have a “north” and “south” pole. Whatever the source of the magnetic moment (orbital motion of an electron, the spin moment of an electron or nucleus or an applied laboratory magnetic field), the interaction of the magnetic moment with an electron spin may be treated as an interaction with one of two mathematical forms: as a ***dipole-dipole interaction*** between the magnetic moment of the electron spin and the second magnetic moment or as a ***contact interaction*** between the electron spin and some other spin (nuclear or electronic). We shall investigate the mathematical forms of the two interactions in order to obtain some intuition concerning the magnitude of the interactions as a function of molecular structure.

Dipole-dipole Interaction

Insight to the nature of the magnetic dipole-dipole interaction is available from consideration of the mathematical formulation of the interaction and its interpretation in terms of the vector model. The beauty of the formulation is that its representation provides an identical basis to consider all forms of dipole-dipole interactions. These may be due to electric dipoles interacting (two electric dipoles, an electric dipole and a nuclear dipole or two nuclear dipoles) or to magnetic dipoles interacting (two electron spins, an electron spin and a nuclear spin, two nuclear spins, a spin and a magnetic field, a spin and an orbital magnetic dipole, etc.). This mathematical formalism is the same whether one is discussion interactions between the transition dipoles of electrons or the magnetic dipoles of electronic or nuclear spins. For example, we shall see this interaction again in Chapter 7 as one that triggers energy transfer between electronically excited states.

Classically, the dipole-dipole interaction energy depends on the relative orientation of the magnetic moments (consider two bar magnets). To obtain some concrete insight to the dipolar interaction consider the case for which the two magnetic dipoles, μ_1 and μ_2, are held parallel to one another (this is the case for two interacting magnetic dipoles in a strong magnetic field (Figure 6.24). We can obtain an intuitive feeling for the nature of the dipole-dipole interaction by considering the terms of the dipole-dipole interaction in eq. 6.12. In general, the strength of the interaction is proportional to several factors: (1) the magnitudes of the individual interacting dipoles, $\mu_1\mu_2$; (2) the distance separating the interacting dipoles, r,; (3) the orientation of the dipoles relative to one another, $3\cos^2\theta - 1$; and (4) the spectral “overlap integral" of resonances that satisfy the conservation of angular momentum and energy. In fact, eq. 6.12 strictly speaking refers to the interaction of two "point" dipoles (if r is large relative to the dipole length, the dipole may be considered a "point" dipole).

Dipole-dipole interaction α $[(\mu_1\mu_2)/r^3](3\cos^2\theta - 1)$(overlap integral) (6.12)

The ***rate*** of a process involving an interaction of a given strength is typically proportional to the ***square*** of the strength of the interaction. Thus, strength of the dipole-dipole interaction has a distance dependence which falls off as $1/r^3$ but the rate of a process driven by dipolar interactions falls off as $1/r^6$.

The term involving the $3\cos^2\theta - 1$ (Figure 6.24) is particularly important because of two of its features: (1) for a fixed value of r and integrating magnetic moments, this term causes the interaction energy to be highly dependent on the angle θ that the vector r makes with the z axis and (2) the value of this term averages to zero, if all angles are represented, i.e., the average value of $\cos^2\theta$ over all space is 1/3. A plot of a dimensionless parameter, $y = 3\cos^2\theta - 1$, is shown at the bottom of Figure 6.24. It is seen that the values of y are symmetrical about $\alpha = 90^o$. It is interesting to note that for values of $\alpha = 54^o$ and 144^o, the value of y = 0, i.e., for these particular angles, the dipolar interaction disappears even when the

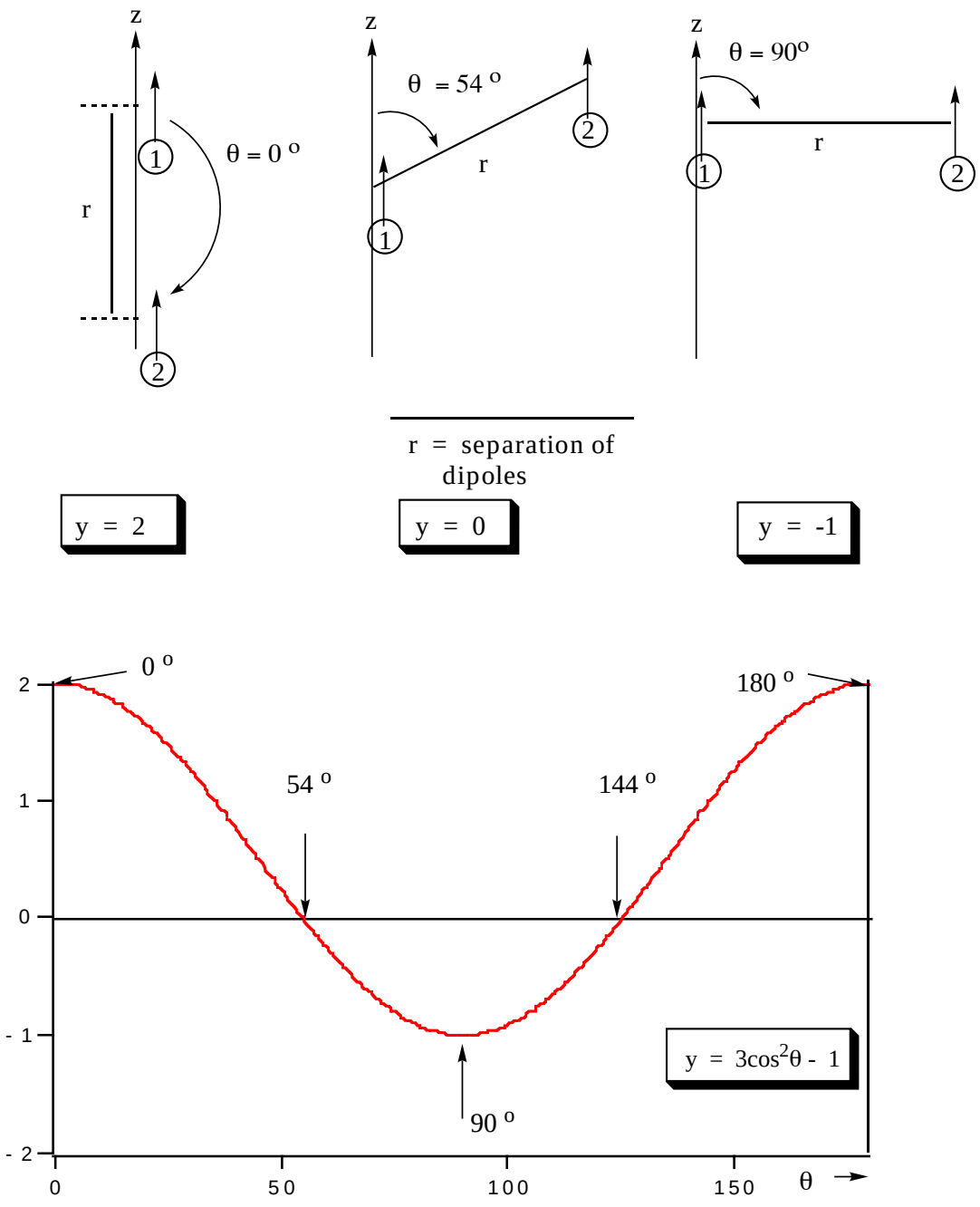

Figure 6.24. Dipole-dipole interactions of parallel magnetic moments. Top: vector representation of dipoles interacting at a fixed separation, r, and various orientations relative to a z axis. Bottom: plot of the value of $3\cos^2\theta - 1$ as a function of θ.

spins are close in space! This is the familiar "magic angle" employed to spin samples in the magnetic field of an NMR spectrometer for removing chemical shifts due to dipolar interactions. It is important to note that certain values of y are positive (magnetic energy raising) and certain values of y are negative (magnetic energy decreasing).

The Contact Interaction

A so called contact interaction arises when the wave functions for two objects overlap in space. The most important cases are (1) the overlap of the electronic wave functions of a spin with the electronic wave function of another spin and (2) the overlap of the electronic wave function of a spin with the electronic wave function of a nucleus. For two electrons in the triplet state the two unpaired electrons are forbidden from "making contact" by the Pauli principle (overlap leads to a triplet singlet splitting, however). Because the nucleus has a finite size, it is also possible that the electron approaches the nucleus so closely that the two particles are effectively in contact. A magnetic interaction (completely different from the dipole-dipole interaction) results when the wave function of an electron and nucleus occupy the same reason of space. This sort of interaction between an electron and a nucleus is termed a ***hyperfine interaction*** between the electron spin and the nuclear spin.

Magnetic interactions can often be well approximated by the dipolar interaction of eq. 6.12. However, this approximation breaks down when the interacting spins approach and the point dipole approximation is no longer valid. In particular, an electron in an orbital possessing s character has a finite probability of approaching and entering a magnetic nucleus (of, say, a proton). As the electron approaches the nucleus, it brings with it a magnetic moment and discovers that the magnetic field very close to the nucleus is no longer purely dipolar. The interaction of the magnetic moment of the nucleus and the electron spin within the "contact" zone of the nucleus is quite different from the dipolar interaction of the magnetic nucleus and the electron spin when the electron is outside the nucleus. The non-dipolar interaction of an electron spin and the nucleus is termed the ***Fermi contact interaction*****.** The strength of this interaction is readily obtained from EPR spectra (Chapter 8). For the 1s orbital of a proton, the contact interaction, a, corresponds to an average magnetic field of ca 510 G (ca 1400 x 10^6 Hz) acting on the electron spin. From this simple analysis, we expect that the greater the amount of s character, the larger the value of a, so that there should be a correlation between the value of a and molecular structure. The magnitude of the contact interaction depends on the magnitude of the magnetic moment of the electron, μ_e, and the magnetic moment of the nucleus, μ_p, and the probability of finding the electron at the nucleus, $|\Psi(0)|^2$ (eq. 6.13).

$$\text{contact interaction} \propto \mu_e\mu_p|\Psi(0)|^2 \qquad (6.13)$$

For an electron is a 2s orbital of a F atom the contact interaction is very substantial (17,000 G or ca 50,000 x 10^6 Hz). For “heavy atoms” for which electrons can approach large nuclei of high positive charge, the contact interaction can approach 10^6 G.

Figure 6.25b shows schematically the dipolar interaction between the electron and the nucleus (left) and the contact interaction between the electron and the nucleus (right).

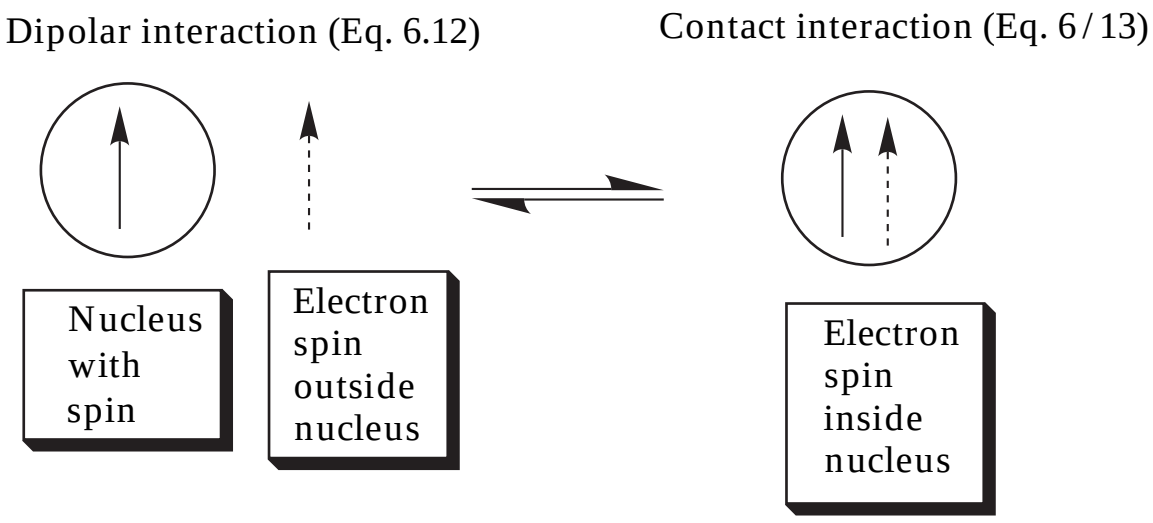

Figure 6.25b. Schematic representation of the dipolar and contact interactions between electron and nuclear spins responsible for hyperfine coupling.

Because s orbitals are spherically symmetric, the contact interaction does not average to zero as the result of molecular motion, as is the case for the dipolar interaction This effect is absent for all other orbitals, because p, d, etc. orbitals possess nodes at the nucleus, so the effectively an electron cannot penetrate the nucleus when it is in any but an s orbital. It is also interesting to note that the ideas behind the electron nuclear hyperfine interactions are employed to explain the basis of nuclear spin-nuclear spin coupling in NMR in addition to the basis of nuclear spin-electron spin hyperfine coupling in ESR.

Couplings of an electron spin with external and internal magnetic fields

The term **external** magnetic coupling refers to applied **laboratory static** or **oscillating** magnetic fields whose strengths and directions can be controlled by the experimenter. These fields contrast to the **internal** magnetic fields, such as those arising from dipolar and contact interactions between spins. The external static magnetic fields are those produced by ordinary laboratory magnets. The strengths of the static fields of conveniently available laboratory magnets may be varied from 0 gauss (0 Tesla) to over 500,000 gauss (50 Tesla). The external oscillating magnetic fields are those produced by oscillating magnetic field associated with electromagnetic radiation (Chapter 4). Such oscillating magnetic fields, in contrast to static magnetic fields, are only effective in interacting with electron spins when the frequency of oscillation is close to, or identical to, the frequency corresponding to the energy gap between two magnetic levels for which a transition is allowed ($h\nu = \hbar\omega = \Delta E$, where $\hbar = h/2\pi$). The strengths, i.e., the intensities (photons/s), of the external oscillating fields may be varied over many orders of magnitude. The frequency of the external oscillating fields may be varied continuously. However, coupling with the magnetic moments only occurs when the energy matching condition is met.

The term **internal** magnetic couplings refers to **microscopic static or oscillating** fields whose strengths and directions are due to the electronic and nuclear structures in the vicinity of the electron spin. Whether these couplings are considered static or oscillating depends on the motion and direction magnetic moments in the vicinity of the electron spin. The strengths and frequencies of oscillations of these microscopic fields may vary over many orders of magnitude and are related to the molecular structure and motion of the molecule containing the electron spin and to the molecular structure and motion of the solvent surrounding the electron spin. The most important microscopic magnetic couplings may be classified in terms of the molecular structure in the vicinity of the electron spin as (1) **electron spin-electron orbit** or **spin-orbit** couplings, by which the electron spin experiences magnetic coupling with its own orbital motion (in general the magnetic couplings due to the orbital motion of other electrons is negligible); (2) **electron spin-nuclear spin** or **hyperfine** couplings, by which the electron spin

experiences magnetic coupling resulting from nuclear spins; (3) **electron spin-lattice** couplings, by which the electron spin experiences magnetic coupling resulting from the surrounding molecules in the solvent (termed the "lattice" because the origin of the theory of spin-lattice couplings referred to crystal lattices); (4) **electron spin-electron spin** or **electron exchange** couplings, by which an electron spin experiences magnetic coupling resulting from another electron spin.

Magnetic Coupling Mechanisms

In quantum mechanics, a convenient means of classifying the magnetic coupling mechanism of an electron spin with other magnetic moments involves the so-called **spin Hamiltonian operator**. This Hamiltonian is a mathematical expression which contains representations of all of the important magnetic couplings that will influence the energy and therefore the precessional frequency of the electron spin. These couplings of an electron spin vector, $\mathbf{S_1}$, with other magnetic moments are typically of a certain mathematical form given in the following discussion. These forms have been simplified for the purposes of clarity and are only of qualitative significance. Each may, however, be readily interpreted in terms of the vector model.

(1) ***The Zeeman Coupling.*** The **external** magnetic coupling of the electron spin to the magnetic moment of an applied laboratory field is termed the Zeeman coupling, H_Z. Its mathematical representation in the spin Hamitonian has the form $H_Z = g\mu_e \mathbf{H_z}\cdot\mathbf{S_1}$, where g is the so called "g factor" (dimensionless units) of the electron, μ_e is the magnetic moment of the electron, H_0 is the strength of the applied laboratory magnetic field and S_z is the value of the spin angular momentum in the direction of the applied field.. This coupling has the same form if the source is an internal field applied along the z axis.

(2) ***Dipole-dipole Coupling.*** The **internal** magnetic coupling of the electron spin to the magnetic moment of another electron spin, $\mathbf{S_2}$ is called the **spin-spin dipolar** coupling. Its mathematical representation in the spin Hamiltonian has the form $H_{DP} = D_e\mathbf{S_1}\cdot\mathbf{S_2}$. The dipolar interaction, as discussed above, averages to zero if the spin system tumbles rapidly because all dipolar interactions averages to 0 for rapidly tumbling systems (eq. 6.X and figure 6.X).

(3) ***Hyperfine Coupling.*** The **internal** magnetic coupling of the electron spin to the magnetic moment of a nuclear spin, **I** is termed the **spin-nuclear hyperfine** coupling. Its mathematical representation in the spin Hamiltonian has the form $H_{HF} = a\mathbf{S_1}\cdot\mathbf{I}$. There may be a dipolar contribution or contact interaction leading to hyperfine coupling, but in solution the dipolar interaction usually averages to 0 because of rapid tumbling. The major contribution to a for radicals in solution is usually the Fermi contact interaction (eq. 6.X), which depends on the amount of s character in the orbital containing the unpaired electron. This interaction is distance independent, since the electron and nucleus are in the same radical.

(4) ***Spin-orbit Coupling.*** The **internal** magnetic coupling of the electron spin to the magnetic moment due to orbital motion of the electron, **L** is called **spin-orbit** coupling. As we have seen in earlier Chapters, its mathematical representation in the spin Hamiltonian has the form $H_{SO} = \zeta\mathbf{S_1}\cdot\mathbf{L}$. This coupling depends on overlap of the orbital involving the unpaired spin with other orbitals and is distance dependent for radical pairs and biradicals, but distance independent for molecular triplets and individual radicals.

We note that each term in the Hamiltonian has the mathematical form $H_B = k\mathbf{S_1}\cdot\mathbf{X}$, where k represents a constant which is a measure of the strengths of the magnetic couplings and $\mathbf{S_1}\cdot\mathbf{X}$ represents the vector coupling of the magnetic moments.

In addition to these magnetic interactions, the electron spin can also experience a magnetic coupling to the oscillating internal magnetic fields resulting from molecular motions of the environment. This coupling is called **spin-lattice coupling** and its contribution to the Hamiltonian is mainly in causing transitions between spin states rather than modifying the energies of the spin states. Spin-lattice coupling

may be viewed as the magnetic coupling of the electron spin to the fluctuating magnetic moments due to to random motion of molecules in the vicinity of $\mathbf{S_1}$. The frequency of these fluctuations and the intensity of the fluctuation at any given frequency determine the extent of the coupling. Spin-lattice coupling is not strictly expressible in an analogous form to the other internal couplings. However, to a rough approximation this term can be expressed as $H_{SL} = \mathbf{S_1}\cdot\boldsymbol{\rho}_L$, where $\boldsymbol{\rho}_L$ is the "spectral density" of frequencies in the environment (lattice) that are at the Larmor frequency of $\mathbf{S_1}$ and therefore capable of coupling to the spin.

Finally, the electron spin is influenced by the oscillating magnetic field associated with an electromagnetic field and is termed **spin-photon coupling**. This coupling is responsible for radiative transitions between magnetic states. To a rough approximation this coupling can be expressed as $H_{h\nu} = \mathbf{S_1}\cdot\boldsymbol{\rho}_{h\nu}$

The Electron Exchange Interaction.

The exchange of electrons is a non-classical effect resulting in a splitting of singlet and triplet states as discussed in the previous section as responsible for splitting the singlet state from triplet states. The form of J in a spin Hamiltonian is given by eq. 6.14. The splitting energy is defined as 2J (a splitting of J above and below the energy corresponding to no exchange). The sign of J may be positive or negative, but in most cases of interest it is negative. In these cases, the singlet state is lower in energy than the triplet.

$$H_{ex} = J\mathbf{S}_1\cdot\mathbf{S}_2. \qquad (6.14)$$

Although electron exchange is a Coulombic (electrostatic) effect and not a magnetic effect, it influences magnetic couplings in two important ways: (1) the exchange interaction causes the singlet and triplet states to be different in energy; and (2) for the two electrons in a strong exchange situation the spins are tightly electrostatically coupled to each other. When the energy gap, J, is much larger than available magnetic energy, singlet triplet interconversions are said to be "quenched" by J. In addition, since exchange electrostatically correlates the motions of electrons and electron spins, this tight coupling makes it difficult for magnetic couplings to operate on either of the spins and cause intersystem crossing. In this case we view the two spin vectors to be precessing about each other to produce a resultant and it is not longer meaningful to think of the individual spins as components!

The magnitude of J depends on the "contact" region of orbital overlap of the electron spins. This overlap region of two orbitals is usually well approximated as an exponential function such as eq. 6.15, where J_0 is a parameter which depends on the orbitals and R is the separation of the orbitals in space.

$$J = J_0 e^{-R} \qquad (6.15)$$

6.18 Coupling Involving Two Correlated Spins. $T_+ \rightarrow S$ and $T_- \rightarrow S$ Transitions.

The visualization of a single spin coupled to a second spin (or any other generalized magnetic moment) is readily extended in Figure 6.26 to the visualization of two correlated spins coupled to a third spin (or any other generalized magnetic moment). In Figure 6.26 (upper left) two electron spins, $\mathbf{S_1}$ and $\mathbf{S_2}$ are shown as correlated in the T_+ state (the correlation is indicated by showing the resultant vector produced by coupling and precession about the resultant). Now we suppose that a third spin, either an electron spin or a nuclear spin (represented as $\mathbf{H_i}$ in the Figure) is capable of coupling specifically to the spin $\mathbf{S_2}$ (shown in the middle top of Figure 6.26in terms of a new resultant and precession about the resultant). As for the single coupled spin in Figure 6.26, the coupling of $\mathbf{S_2}$ to $\mathbf{H_i}$ causes $\mathbf{S_2}$ to precess about

the x or y axis and the α and β orientations. From the vector diagram it is readily seen that this oscillation produced by coupling of $\mathbf{S_2}$ and $\mathbf{H_i}$ causes triplet (T_+) to singlet (S) intersystem crossing.

At zero field the three T sublevels are usually strongly mixed by dipolar interactions between electron spins. Thus, radiationless $T_+ \rightarrow$ S ISC is plausible and will depend on the strength of the coupling between $\mathbf{S_2}$ and $\mathbf{H_i}$ and the strength of the exchange interaction. For simplicity, in Figure 6.26 (bottom) we assume that J = 0. There is no radiative transitions between T and S possible at zero field because there is no energy gap between the states.

At high field the $T_+ \rightarrow$ S ISC transition is not plausible by a radiationless pathways. The radiationless pathway is inefficient because it requires some source of magnetic energy conservation by coupling with the lattice. The plausibility of a radiative $T_+ \rightarrow$ S transition depends on the relative coupling of the electron spins to one another (value of J) and to the radiative field. If the value of J is very small, the individual spins behave more or less independently so that radiative transitions of each spin ("doublet" transitions) become plausible. The vector diagram for the $T_- \rightarrow$ S transition is readily constructed from the symmetry relationships of the T_- vector representation to that of the T_+ vector representation.

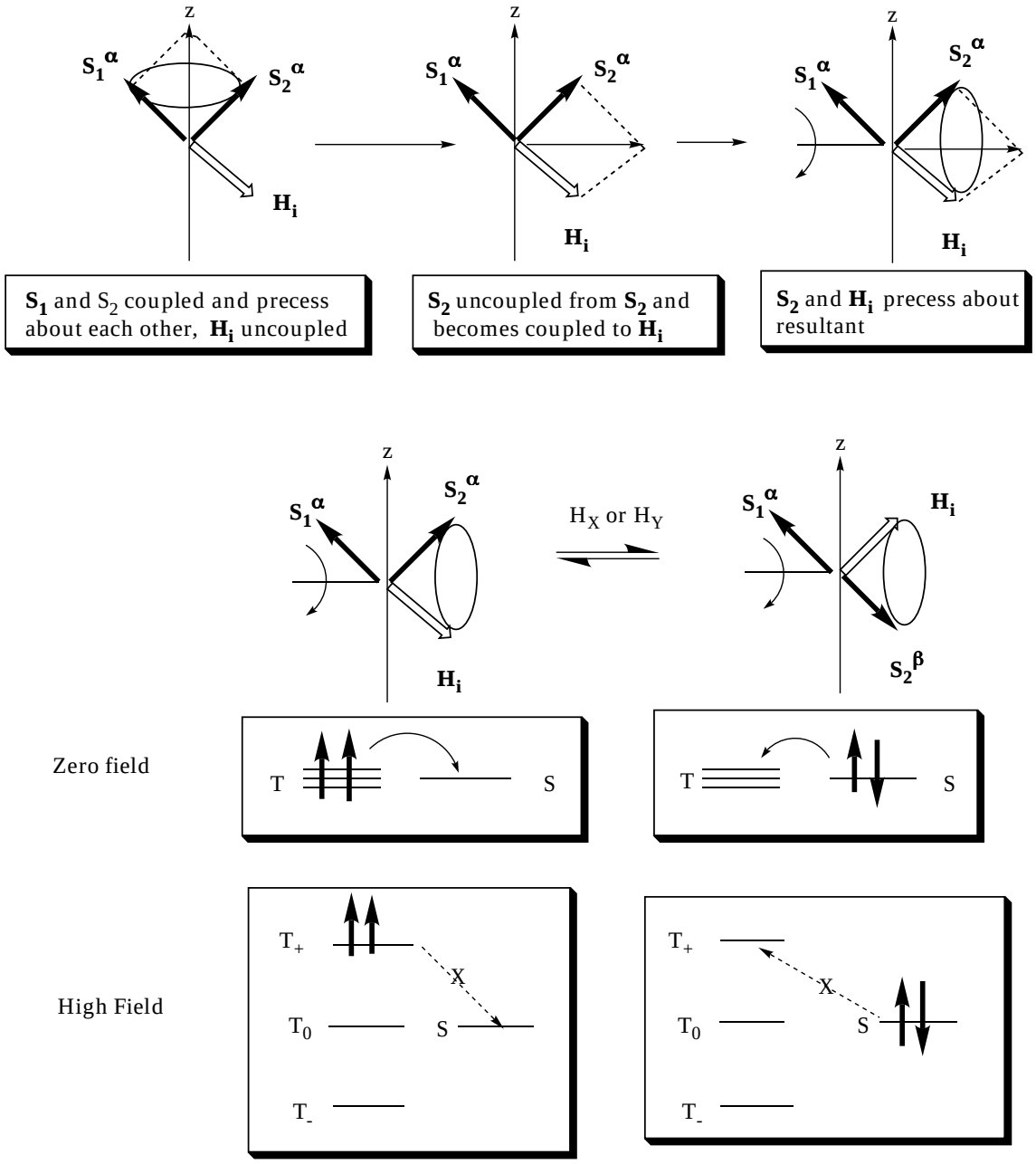

Figure 6.26. Vector representation of coupling of two correlated spins with a third spin along the x or y axis. See text for discussion.

Coupling Involving Two Correlated Spins. $T_0 \rightarrow S$ Transitions.

As for a single spin, it is also possible for $\mathbf{H_i}$ to operate on correlated electron spins along the z axis. This situation is shown in Figure 6.27 for an initial T_0 state. Again under the assumption that J = 0, rephasing along the z axis occurs is if $\mathbf{H_i}$ is coupled selectively to one of the electron spins (say, $\mathbf{S_1}$). This rephasing causes $T_0 \rightarrow S$ ISC at low field or at high field if J = 0.

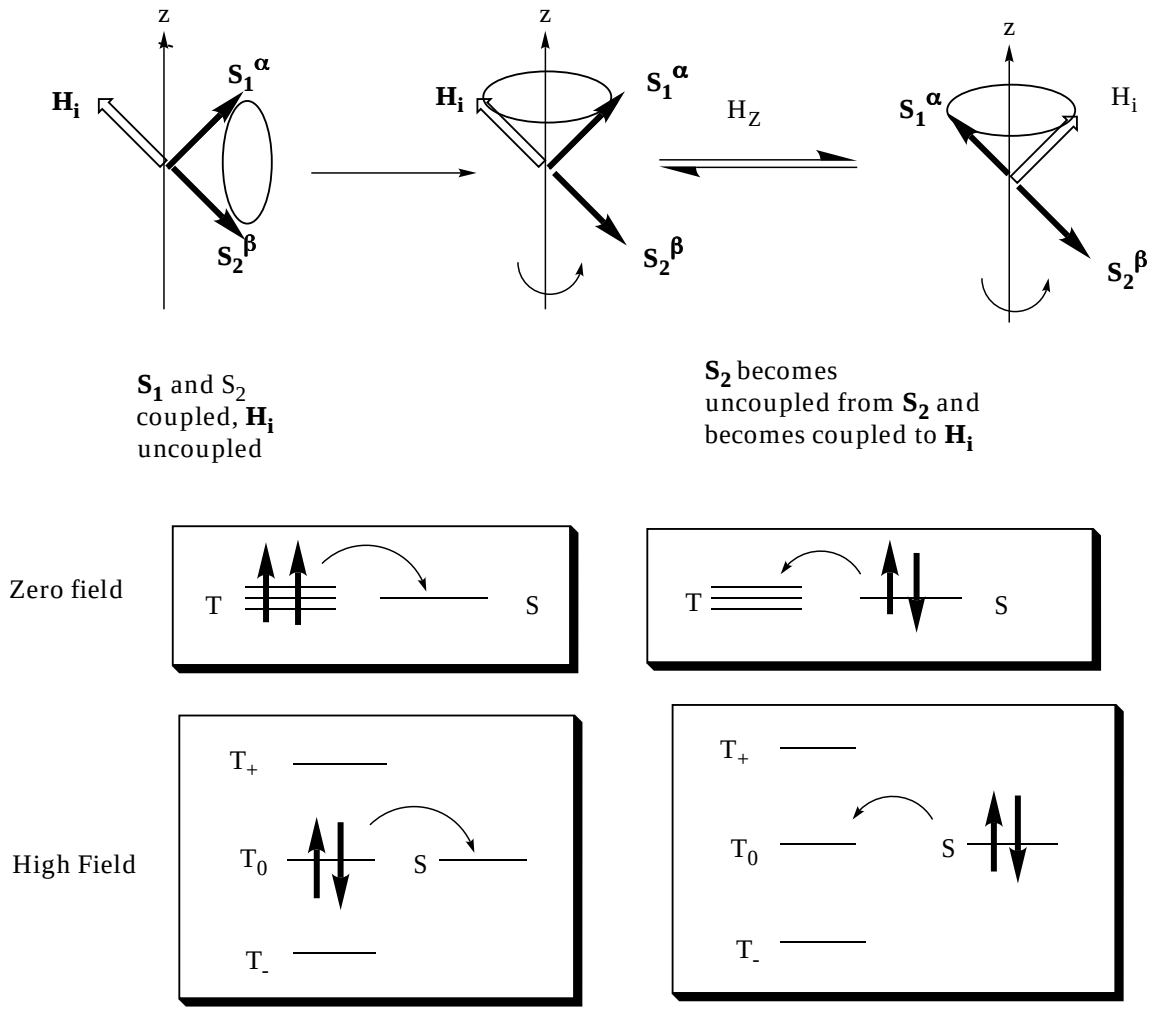

Figure 6.27. Vector representation of two correlated spins in a T_0 state coupled to a third spin along the z axis. See text for discussion.

6.19 Intersystem Crossing in Radical Pairs and Diradicals. Exemplar Systems.

As we have seen in section XX, the paradigm given in Figures 6.28 represents organic photochemical reactions involve photochemical primary processes initiated in the lowest nπ* triplet state, T_1, to produce a radical pair (^{3}RP) or diradical intermediate (^{3}D) which then proceeds to products in secondary thermal reactions. Figure 26 reviews the key intermediates in such a paradigm.

The paradigm we shall develop will be analogous for weakly coupled radical pairs and weakly coupled flexible biradicals. For the sake of simplicity, the discussion will mainly refer only to radical pairs first and then the special features introduced by the diradical structure will be considered. One should keep in mind that in nearly all of the discussion the word "flexible biradical" can be substituted for "radical pair".

$$R \xrightarrow{h\nu} {}^1{*R} \longrightarrow {}^{3*}R \longrightarrow {}^3I \longrightarrow {}^1I \longrightarrow P$$

$$S_0 \longrightarrow S_1 \xrightarrow{1} T_1 \xrightarrow{2} {}^3RP \xrightarrow{3} {}^1RP \xrightarrow{4} P$$

Figure 6.28. Simplified paradigm of a photochemical process proceeding through a nπ* triplet electronically excited state, T_1.

Regions of Chemical Space and Spin Space Explored During a Photochemical Reaction.

We have seen that electronic surface energy diagram are extremely useful in visualizing the electronic features of photochemical reactions. We shall now combine the "chemical space" of electronic energy surfaces and "spin space" of the vector model to examine a case history of a photochemical reaction. It will be shown that the intersystem crossing step, $S_1 \rightarrow T_1$ occurs "vertically" in a region of the energy surface for which the exchange interaction is very large. Thus, this step can be treated in terms of a vertical jump (spectroscopic) of a representative point between energy surfaces described for radiative and radiationless transitions. The remaining steps, $T_1 \rightarrow {}^3RP \rightarrow {}^1RP \rightarrow P$, involve bond breaking, separation and reencounters of radical pairs and bond formation so that ${}^3RP$ and ${}^1RP$ constitute a **dynamic radical pair**. These processes involve both horizontal and vertical motion of the representative point on energy surfaces separated by various values of J. We shall see that the variation of J strongly influences the magnetic resonance spectroscopy and the spin chemistry of the dynamic radical pair.

Photochemical α-Cleavage of Ketones as an Exemplar for Intersystem Crossing in Radical Pairs and Diradicals

We shall now use as an exemplar the α-cleavage reaction of a ketone in its triplet state, to bring together the principles of the vector model to understand the mechanisms of intersystem crossing in radical pairs and diradicals. Figure 6.29 shows the four steps 1-4 of the general paradigm of Figure 26 expressed in terms of a ketone, ACOB. We shall examine each of these steps to develop a working paradigm for photochemical reactions proceeding through triplet states of organic molecules.

We shall examine the elementary step of bond breaking (step 2) in zero field and in high field. We shall employ a “dynamic radical pair” model to analyze the systems. Again a flexible diradical can be considered a “dynamic diradical” differing form the dynamic radical pair mainly in the constraints that a flexible chain imposes on the distance of separation and dynamics of encounters of the ends of the chain.

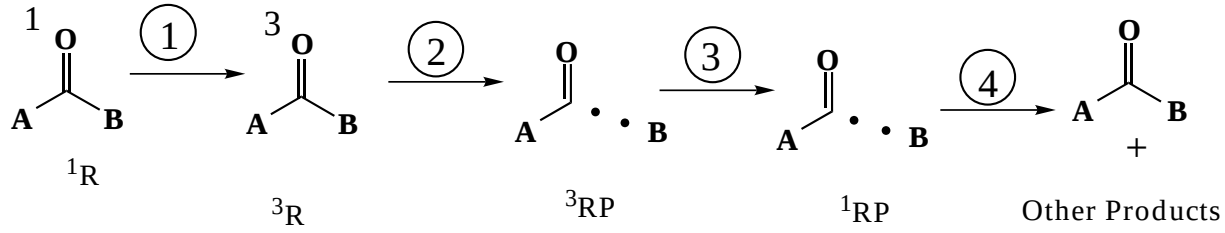

Figure 6.29. Paradigm for the α-cleavage reaction of ketones.

The Dynamic Radical Pair

The triplet geminate radical pair produced in the primary photochemical step 2 of Figure 6.29 is not a static structure but, because of its diffusional and rotational dynamics, constitutes a **dynamic** system and therefore is termed a **dymanic radical pair**. We need to analyze the dynamics of the pair at three levels: (1) the level of molecular dynamics whereby the partners of the pairs may be collision partners in a solvent cage or be separated by one or more solvent molecules and may interconvert between these situations; (2) the level of spin dynamics whereby intersystem crossing and rephasing of spin occur; (3) the level of chemical dynamics whereby the partners of the pair undergo chemical reactions through bond formation, scavenging or radical pair rearrangements or fragmentations. In order to keep this riot of molecular dynamic activity organized in our minds in physical space, spin space and time, we result to a combination of energy surfaces, the vector model and conventional molecular structures. Effectively in

exploring with our imaginations we need the same tools as when we explore an unfamiliar territory: a map, a clock and a compass. The map is the energy surface (molecular structures are the geographical identifiers on the map), the clock is the time scale on which the interactive dynamics occur and the compass is the magnetic field that tell us about spin orientation.

Electronic Energy Surfaces and Molecular Dynamics.

We need to keep track of the several interacting dynamic events that are occurring simultaneously in the primary photochemical step of Figure 6.29, i.e., the ^{3}ACO-B (^{3}R) → ^{3}ACO· ·B (^{3}I) primary photochemical process. We start by considering an energy surface description of the process (Figure 6.30) which employs the exemplar of the stretching and breaking of a C-C single bond (Figure 6.7). In accord with this exemplar, the triplet surface is shown as decreasing in energy and the singlet surface as increasing in energy as the carbon-carbon bond stretches and then breaks. The energy gap between the triplet and the ground singlet state is considered to be due mainly to the exchange interaction, J. When the bond is completely broken and the partners of the pair separate by a solvent molecule or two, the exchange interaction is decreases to negligibly small values (J ~ 0), so that the singlet and triplet surfaces are effectively degenerate and "touching". Beyond this point the singlet-triplet energy gap, $\Delta E = 0$ and is independent of further separation of the radical partners. In Figure 6.30, a representative point is shown moving down the surface.

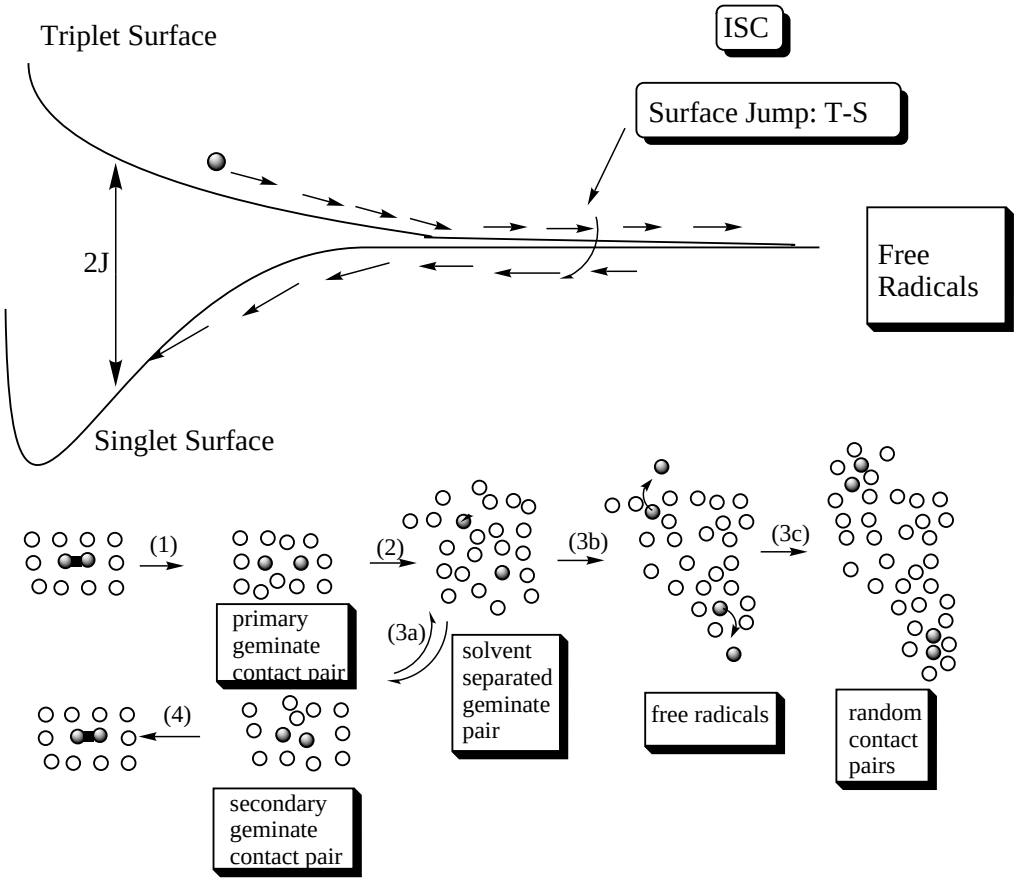

Figure 6.30. Surface energy diagram displaying the spin and molecular dynamic features of a dynamic radical pair.

Definition of Terms for Radical Pairs

In order to understand the behavior of the representative point we must consider its molecular, spin and chemical dynamics as it moves alontgthe triplet surface. Let us consider each of these dynamics

separately and start with the molecular dynamics which are represented schematically at the bottom of Figure 6.30. We shall employ the following terms to describe the molecular dynamics and structures of the pair.

1. **Geminate radical pairs.** A radical pair whose fragments are "born together" and share the parentage of a common precursor molecule, e.g., step 2 of figure 6.29.

2. **Free radicals or random radicals.** Radicals which have separated to a distance for which non-geminate reaction with radicals has a higher probability than geminate reaction.

3. **Random (or free radical) pairs.** A radical pair formed by an encounter of two free or random radicals. As one tracks the representative point as it makes an excursion down a dissociative triplet surface starting from the parent triplet excited state (^{3}*R) all the way to a separation of radicals that is so large that the pair becomes statistically distributed in space with radicals from other dissociations (right of Figure 6.30). Such a radical "pair" no longer is geminate in the sense that it becomes more probable that reencounters will occur with radicals from other dissociations than with the original geminate partner. At this point each partner of the original geminate pair is considered a "free radical" or a "random radical".

4. **Solvent cage**. The first shell of solvent molecules which surround a molecule or a radical pair (geminate or random). A pair in a solvent cage undergoes repeated collisions before one of the partners can find a "hole" in the cage wall and become separated by a solvent molecule.

4. **Contact radical pair.** A radical pair (geminate or random) whose partners are in a solvent cage without a solvent molecule between them, i.e., the pair is in contact through repeated collisions. A contact pair is able to react to form molecules through combination reactions directly if it is in the singlet state and the partners of the pair can achieve the appropriate geometry and energy required for reaction. A contact pair in the triplet state is inert to combination reactions because of Wigner's spin conservation rule for elementary chemical reactions.

5. **Solvent separated radical pair.** A radical pair (geminate or random) whose partners are separated by one or more solvent molecules.

Visualization of the Primary Photochemical Step: ^{3}ACO-B → ^{3}ACO· ·B in Zero Field. The Dynamic Radical Pair.

Imagine the behavior of the representative point during the primary photochemical bond cleavage, ^{3}ACO-B → ^{3}ACO· ·B, in zero field. The point begins to move along the triplet surface as the bond stretched and eventually breaks (Figure 31). Immediately after the bond has broken, the radical pair is produced as colliding neighbors that are born together in a solvent cage (termed the **primary, geminate collisional pair**, step (1) bottom of Figure 6.30). As the result of random thermally induced motions (the molecular dynamics), the partners of the pair eventually diffuse apart out of the solvent cage (producing a **geminate, solvent separated pair**, step (2) Figure 6.30, bottom). The solvent separated pairs make random excursions in space and time. Some of the excursions (step 3a in Figure 6.30, bottom) cause the geminate pair to return to the contact state in a solvent cage (such excursions are termed **reencounters** and such pairs are termed **secondary, geminate collisional pairs**). Some of the excursions lead to separation of the partners of the pair to distances so large (step 3b in Figure 6.30) that further diffusional trajectories (step 4 in Figure 6.30 are more likely to have each partner randomly encounter radicals other than the geminate partner (pair that encounter to form contact pair from such excursions are termed **random, collisional pairs**).

The importance of the dynamic model of a radical pair to spin chemistry derives readily from consideration of the behavior of the triplet electronic energy surface on which the radical pair is created and the singlet electronic energy surface which the pair must reach in order to become reactive as a pair. As is

shown in the top half of Figure 6.30, the energy separating the triplet and singlet surface is a strong function of the distance of separation of the pair in physical space. This is due to the fact that the exchange interaction, J, which is the most important contributor to the energy gap between the S and T surfaces, falls off exponentially as the electrons in the bond being cleaved are separated in physical space. **When J is large compared to available magnetic couplings, it controls the correlated precessional motion of the two odd electron spins of the pair in spin space.** Under these conditions only a strong interaction, which is only possible through spin-orbit coupling for organic radicals, can induce intersystem crossing.

It is only during the trajectories when the dynamic pair is not in contact that intersystem crossing is important, because only under these circumstance can the electron spin experience torques that are effective enough to cause a rephasing ($T_0 \rightarrow S$) or spin flip ($T_{\pm} \rightarrow S$), i.e., it is essentially only during the excursions out of the collisional state in the solvent cage that ISC can be induced by the weak magnetic interactions available to induce reorientation or rephasing of the electron spins of the pair, because only for large excursions does the value of J decrease to values close to zero.

Regions of Magnetic Interactions for a Triplet Electronic Excited State and a Triplet Radical Pair in Zero Field

Consider the breaking of a carbon-carbon bond in an α-cleavage reaction of a triplet ketone. Figure 6.31 depicts a representative point moving down the triplet surface as the bond breaks. What are the regions for which the point can "jump" from the triplet surface to the singlet surface? Let us consider four regions along the energy surface at which the ISC might occur: (1) a region for which the bond is strongly stretched, but not quite broken; (2) a region for which the bond is completely broken and a contact, collisional pair in a solvent cage is produced; (3) a region for which the pair has separated by at least one solvent molecules; and (4) a region for which the pair is separated to such large distances that the geminate character is lost, i.e., the probability of reaction of random pairs is much greater than the probability of reaction of geminate pairs.

Visualization the Spin Dynamics. Intersystem Crossing in Geminate Radical Pairs in Zero Field.

In the previous sections we have considered the simultaneous visualization of the motion of the representative point along energy surfaces and the molecular dynamics of the diffusional motion of the radical pair after the bond breaks. We now seek to visualize, in zero field, the spin dynamics simultaneous with conventional chemical structures of the pair, which are shown at the bottom of Figure 6.31. A vector model representation of the triplet is shown on the upper surface and a possible T_+-S ISC is shown (in principle any one of the triplet sublevels might be populated, although in general selective population of one of the sublevels is favored). The vector representation shows initial strong coupling of the two individual spin vectors in T_+. This representation means that the two spins are phase and orientation correlated and precess precisely in step. The chemical structure corresponding to this vector representation has the orbitals of the two radicals of the pair overlapping strongly and because of the overlap, strong electron exchange (large J) occurs.

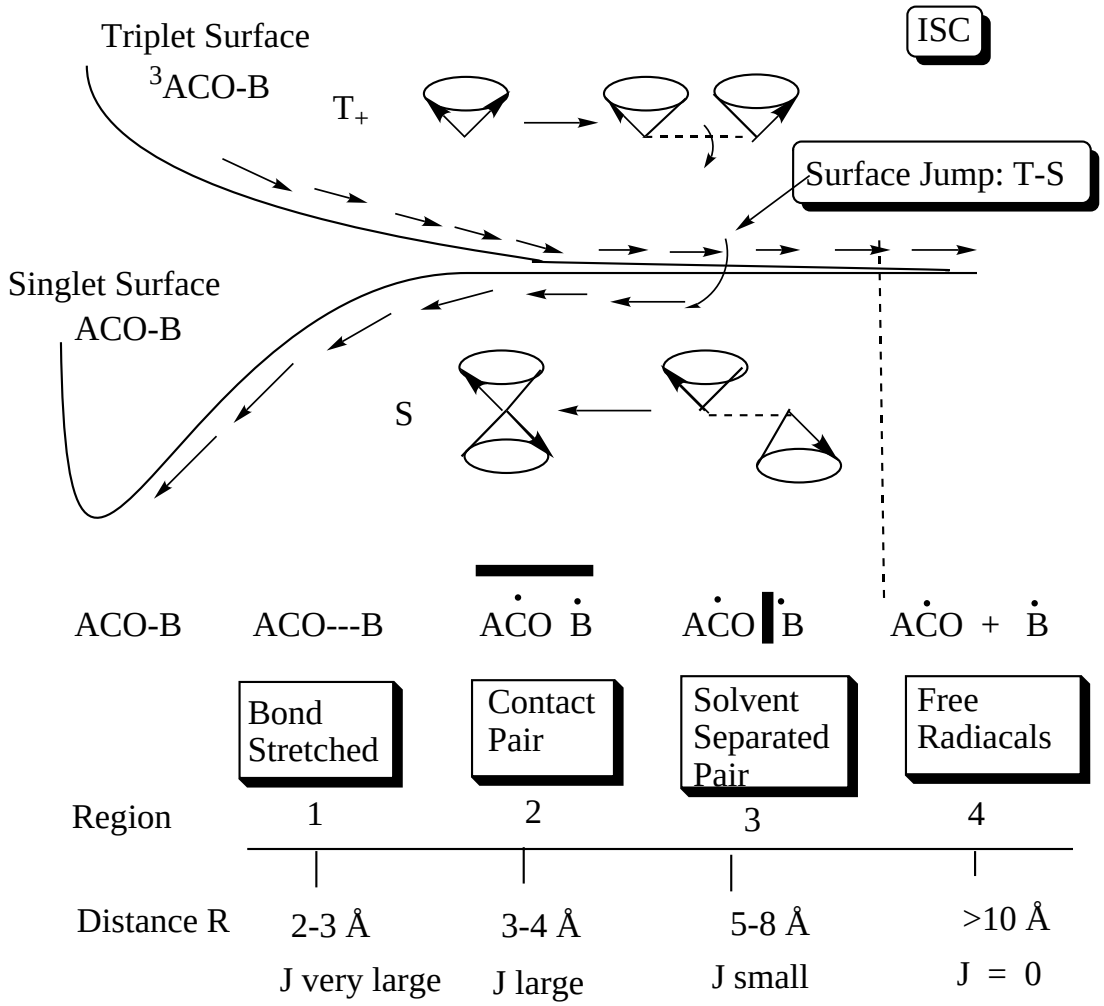

Figure 6.31. Distance dependence of spin correlated radical pairs. See text for discussion.

The Bond Breaking Step. $T_+ \rightarrow {}^3RP$

In the primary cleavage step, $T_+ \rightarrow {}^3RP$ to form ACO· ·B (**region 1**, Figure 6.31, ca < 3Å separation of the partners of the pair), the carbon-carbon bond is stretched and then eventually broken. Is ISC plausible during the bond breaking step? The answer is, generally it is not plausible because the act of bond breaking (the time it takes the representative point to "fly through" region 1) takes of the order of a vibrational time period (10^{-13} s) whereas the rate of spin precession in organic molecules is of the order of 10^{-10} s. Thus, the spin vectors are "frozen" in spin space during the time period in which the bond is broken, i.e., the orientation and phase of the spin vectors are identical as the representative point passes through region 1. This conclusion is equivalent to **Wigner's spin selection rule which says that in any elementary step of bond making or bond breaking, the spin state of the reactant and product must be identical.** This situation may be viewed as a "horizontal" Franck-Condon selection rule for the spin vector: horizontal displacements on a dissociative energy surface occur faster than changes in the angular displacement of the spin vectors, thus, spin orientation is preserved when a bond breaks on a dissociative surface. Just as the Franck-Condon Principle is based on inability of nuclei motion to follow electronic reorganization when an electronic transition occurs, the Wigner Principle is based on the inability of spin motion to follow electronic reorganization when a bond is made or broken. As in the conventional Franck-Condon Principle, for which nuclear configuration is preserved upon rapid vertical jumps of the representative point, Wigner version, spin configuration (orientation or phase) is concerved upon rapid horizontal jumps of the representative point.

In addition to the kinetic problem associated with ISC in region 1, these is a second problem associated with coupling magnetic moments of the spins to induce ISC. The value of J is expected to be much larger than any available magnetic interaction for the pair, so that the coupling required for ISC is implausible. Thus, from both the kinetic standpoint and the coupling standpoint, *ISC is considered as implausible in region 1* and this conclusion is incorporated into our working paradigm of the dynamic radical pair.

Trajectories of the Dynamic Radical Pair.

Figure 32 schematically displays three regions of importance (regions 2, 3 and 4 of Figure 32) to the dynamic radical pair. In **region 2** (ca < 4Å separation), the value of J is still expected to be much larger than any available magnetic interaction for the pair, so that ISC will be inhibited. Thus, contact radical pairs experience large values of J compared to magnetic interactions because the single and triplet are split in energy and do not mix; the pair behaves as a spin 1 system, and ISC is difficult. We say that in the contact state the electron spins are strongly correlated. Although we conclude that ISC is implausible when the pair is in the contact state, the kinetic problem of rapid and irreversible passage through region 1 is not present. As a result, if the contact state is particulary long lived or if an exceptionally strong magnetic mixing is avaliable to the pair, ISC may result. However, as a rule in a non-viscous solvent for typical organic radicals, *the paradigm assumes that ISC is implausible in the contact pair. (region 2)*

The solvent separated radical pair experiences a rapidly diminishing exchange interaction, which is expected to falloff exponentially (Eq. 22) in value with separation of the spins. In **region 3** (ca 5-8 Å separation) the value of J is expected to be comparable to the available magnetic interactions for the pair, so that ISC is plausible. We say that for the solvent separated pair the electron spins are weakly correlated. By weakly correlated we mean that the two electron spins, although correlated, begin to behave as if there were independent doublets. If the pair jumps from the T surface to the S surface, the molecular dynamics may either carry the singlet solvent separated pair toward a reencounter (3a in Figure 32) or toward the formation of random radicals (3b → 4) in Figure 32. Thus, depending on the trajectory followed, either a geminate cage reaction or free radical formation will occur.

In **region 4** the electron correlation is 0 (J = 0) because of the large separation between the unpaired electrons. In Figure 6.31 the spins are shown as correlated up to a certain point (dotted vertical line) and beyond this distance the pair is separated so far that the exchange interaction can be considered to be zero. Thus, beyond this point the magnetic interactions are so weak that the pair is considered as uncorrected. Hypothetically, if there were no different magnetic interactions experienced by either spin, then the phase and orientation features of the initial triplet would be preserved even at infinite distances of separation! However, it is more likely that weak magnetic interactions which are not dependent on the separation of the radicals, such as electron spin-lattice coupling, electron spin orbital coupling and electron spin-nuclear hyperfine coupling, will cause the spins to lose the phase and orientational correlation imposed by the exchange interaction. In this region the pair is not well represented as a singlet or triplet, but as a pair of doublets, i.e., neither the phase nor the orientation of the spin on one center influences the phase or orientation of the spin at the other center.

Order of Magnitude Estimates of ISC.

We can obtain some insight to the magnitude required for magnetic effects to uncouple the exchange interaction and allow ISC by considering the relationship between the precessional rate, ω (in units of rad/s), and the exchange energy, J (in units of gauss, G). The rate of precessional motion of the electron spins that are coupled by the exchange coupling is given by eq. 30, which is analogous in form to Eqs. 12 and 13.

$$\omega_{ex} = 2J/\hbar \qquad (6.17)$$

From various modeling of organic radical pairs the value of J falls off roughly exponentially as a function of separation of the radical pairs. An approximate expression for this function is $J \sim 10^{10}10^{-R}$, where the units of separation are Å and the units of J are in G. This, means that the following relationships hold for the four regions of Figure 6.31: Region 1, $J \sim 10^{12}$ G; region 2, $J \sim 10^{8-9}$ G; region 3, $J \sim 10^{2}$ G; region 4, J ~ 0 G. We can compare these values of J to the magnitude of hyperfine couplings of typical organic radicals (100 G) and it is clear that only in region 3 is ISC plausible, unless some exceptionally strong coupling or very long lifetime is available in region 2. We can also compare these estimates to the value of a the magnetic field of 1,000 G (of the order of typical ESR spectrometers). We note that the applied field will control the spin motion of solvent separated (weakly correlate) geminate pairs and free radicals, but not contact pairs. Let us now consider the influence of application of a high field on spin chemistry and then consider the magnetic resonance spectroscopy of the pair in the three regions of the energy surface.

Intersystem Crossing in Diradicals. Influence of Chain Length

For a flexible diradical, Figure 31 can also be used as an exemplar. The major important difference is that the largest separation of the two radical centers is limited by the maximum extension that is possible for the extended chain (Figure XX). If the diradical chain is relatively short (say n = 3-7) at maximum extension the separation is ca 3-10 Å. For the shorter chains J is much larger than the magnetic interactions. For the longer chains J is beginning to be or the order of the stronger available magnetic interactions. When the chain increases in size to n > 9 or so, in the most extended conformations, the value of J is close to zero and magnetic interactions from nuclear spins (mainly proton spins) can begin to determine the rate of intersystem crossing. We thus expect a diradical chain length dependence on intersystem crossing.

Figure XX. Diradical chain length (to be added).

6.20 Conclusion: Energy Surfaces as Reaction Maps or Graphs

Orbital interactions and state correlation diagrams provide the basic elements of a qualitative theory of photoreactions. The *possible* products of a photoreaction which starts from a particular state may be deduced from state correlation diagram maps. The *probable* products may also be deduced from consideration of (a) symmetry-imposed barriers, and (b) minima which facilitate pathways from an excited surface to the ground state.

The difficulties in establishing a quantitative theory of photoreactions are substantial. Photoreactions are at once blessed with richness of chemistry and cursed by the profound complexity which results from the multidimensionality of excited-state surfaces. The omnipresent competition between photochemical and photophysical processes requires a knowledge of the dynamics of both electronic relaxation routes before a quantitative theoretical prediction cay be made. Furthermore, the role of Franck-Condon factors ($f\nu$) and spin-orbit coupling (f_S) must be considered in any quantitative formulation of photoreactivity and/or efficiency.

Despite the formidable difficulties demanded by a quantitative theory, the qualitative factors discussed in this chapter serve as a useful systematizing, unifying framework in the consideration of photoreactions.

The state correlation diagram may be viewed as a *reaction graph* which displays the possible pathways for interconverting reactants to products. The vertices of the reaction graph correspond to structures corresponding to maxima or minima on the various energy surfaces. A major goal of mechanistic organic photochemistry is to provide experimental support for the occurrence or nonoccurrence of "transition structures" (maxima or minima) along the reaction pathway. Once the structures along a reaction pathway have been established, the dynamics of the reaction (rate constants for conversion of one structure into a second structure) can be determined. The theoretical reaction graph given by energy surfaces provide mechanistic photochemistry with a framework for thinking about experiments, i.e., transition structures are suggested and are subject to experimental verification. Chapter 7 discusses the experimental methods available to test the mechanisms suggested by state correlation diagrams.

References

1. For reviews and discussions of the theory of orbital interactions, see:
(a) Fukui, K., *Topics in Current Chemistry*, *15*, 1 (1970); *Acc. Chem. Res.*, *4*, 57 (1971).
(b) Hudson R.F., *Angew. Chem. Intern. Ed. Eng.*, *12*, 36 (1973).
(c) Epiotis, N.D., *ibid.*, *13*, 751 (1974).
(d) Dewar, N.J.S., *ibid.*, *10*, 761 (1971).
(e) Salem, L., *J. Am. Chem. Soc.*, *90*, 3251-3255 (1968).

2. (a) For discussions of symmetry in chemistry, see Pearson, R.G., *Symmetry Rules for Chemical Reactions*, New York: John Wiley, 1976.
(b) For an elementary discussion of commonly encountered symmetry operations, see Cotton, F.A., *Chemical Applications of Group Theory*, New York: John Wiley, 1971.

3. For reviews of orbital symmetry control of chemical reactions, see:
(a) Woodward, R.B., and Hoffmann, R., *The Conservation of Orbital Symmetry*, New York: Academic Press, 1970.
(b) Zimmerman, H.E., *Acc. Chem. Research*, *4*, 272 (1971).
(c) Dewar, M.J.S., *Angew. Chem. Int. Ed. Eng.*, *10*, 761 (1971).

4. For reviews of the role of diradicals and zwitterions in photoreactions, see Salem, L., and Rowland, C., *Angew. Chem. Int. Ed. Eng.*, *11*, 92 (1971); Salem, L., *Pure Appl. Chem.*, *33*, 317 (1973).

5. Michl, J., *Molec. Photochem.*, *4*, 243, 257, 287 (1972); *Topics in Current Chemistry*, *46*, 1 (1974).

6. (a) Salem, L., *J. Am. Chem. Soc.*, *96*, 3486 (1974).
(b) Dauben, W.G., Salem, L., and Turro, N.J., *Acc. Chem. Res.*, *8*, 41 (1975) and references therein.

7. Devaquet, A., *Topics in Current Chemistry*, *54*, 1 (1975); *Pure Appl. Chem.*, *41*, 535 (1975).

8. Longuet-Higgins, H.C., and Abrahamson, E.W., *J. Am. Chem. Soc.*, *87*, 2046 (1965).

9. Van der Lugt, W.T.A.M., and Oosterhoff, L.J., *J. Am. Chem. Soc.*, *91*, 6042 (1969).

10. Carr, R.W., and Walters, W.D., *J. Phys. Chem.*, *69*, 1073 (1965).

11. For a discussion, see Turro, N.J., et al., *Acc. Chem. Research*, *5*, 92 (1972) and references therein.

12. Turro, N.J., Farneth, W.E., and Devaquet, A., *J. Am. Chem. Soc.*, *98*, 7425 (1976).